Performance Analysis and Algorithm Enhancement of Feature-Aided-Tracker (FAT) Simulation Software using 1-D High-Range-Resolution (HRR) Radar Signature Profiles

by

Michael J. O'Brien

B.S., Systems Engineering (2003)

United States Naval Academy

Submitted to the Department of Mechanical Engineering
in Partial Fulfillment of the Requirements for the Degree of
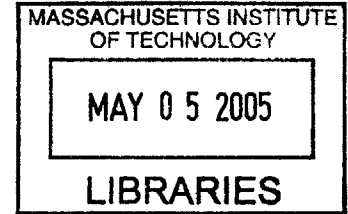Master of Science in Mechanical Engineering

at the

Massachusetts Institute of Technology

[February 2005]
January 2005

Signature of Author..

......

Department of Mechanical Engineering
December 17, 2004

Certified by..

....

Derek Rowell
Professor of Mechanical Engineering
Thesis Supervisor

Accepted by...

Lallit Anand
Chairman, Department Committee on Graduate Students

Performance Analysis and Algorithm Enhancement of Feature-Aided-Tracker (FAT) Simulation Software using 1-D High-Range-Resolution (HRR) Radar Signature Profiles

by

Michael J. O'Brien

Submitted to the Department of Mechanical Engineering
on December 17, 2004 in Partial Fulfillment of the
Requirements for the Degree of Master of Science in
Mechanical Engineering

ABSTRACT

The current Lincoln Laboratory (LL) MATLAB Feature-Aided-Tracker (FAT) software was adjusted and appended to provide a robust ground-target radar tracking simulation tool. It utilizes algorithms from the LL UAV Radar Moving Target Tracker (1991) and the LL FAT Tracking Software (2002). One-dimensional High-Range-Resolution (HRR) radar signature target profiles were used to assist in track-to-report data association through classification-aided and signature-aided tracking (CAT and SAT) algorithms. Profiles were obtained from the DARPA-sponsored Moving Target Feature Phenomenology (MTFP) program.

Performance Analysis of this simulation tool reinforced the hypothesis that target aspect angle error estimation (state estimation) drives the performance of CAT, SAT, and Kinematic Tracking (KT) algorithms. A decaying exponential relationship exists between the Kalman filter estimate of target speed and expected aspect angle error. This relationship was exploited to optimize the allocation of computational resources while enlarging the database aspect angle search in CAT to improve performance. Vehicle classification accuracy is improved by 70% and data association accuracy is improved by 12% in kinematically ambiguous situations such as when target intersections occur. SAT was improved 3% using this knowledge.

Additionally, the target report HRR profile from each scan was used to generate an "On-The-Fly" SAT HRR profile database. This algorithm tests the similarity between the current target report HRR profile and the database HRR profiles. If there is sufficient resemblance, the report HRR is added to the database; if not, the database is reset. This information can be employed to provide up to a 9% performance improvement over the previous version of SAT in a best-case scenario. In realistic situations, a 6% performance improvement is still attainable. If a large, accurate database exists, near-perfect data association is achieved.

Overall, the above technique adjustments provide an improvement of 6.3% (13.6% in realistic, GPS-generated scenarios) in data association accuracy over the initial FAT algorithm and a corresponding 28.8% improvement over the results of the KT itself.

Thesis Supervisor: Derek Rowell
Title: Professor of Mechanical Engineering

TABLE OF CONTENTS

4

ACKNOWLEDGEMENTS

LIST OF TABLES

LIST OF FIGURES

CHAPTER 1.

BACKGROUND/INTRODUCTION

Tracking, as it will be used below, can be defined as the estimation of the condition of a moving target. It is correct to assume that 'estimation of condition' in this sense explains the outcome of a number of statistical tests and decisions. Three specific types of 'estimation' apply to the FAT algorithm discussed in this report:

1) State Estimation
2) Target Class/Identification Estimation
3) Radar Signature Estimation

The expected 'condition' of each target will depend upon this estimation, and a decision will ultimately be made assigning all target reports to particular tracks, or histories.

The goal of any military target-tracking system is to use the accumulated target history to estimate the future condition of a vehicle. This study will specifically focus on high value ground vehicles. Today's tracking systems are equipped with the capability to identify a target as being under a specific track given sufficient evidence accrual. However, the ability to simultaneously track and identify targets can be impeded by dense traffic, low target speeds, unfavorable geometry, and noisy target detections. These situations lead to inevitable mistakes made by simple kinematic tracking systems that depend solely on state (position and velocity) estimation. It has recently been proven that the possibility exists to correct most of these mistakes through incorporation of the capability to identify targets during kinematic tracking. This presents the opportunity to ensure that evidence is amassed and associated with the correct track history.

Currently, one-dimensional high-resolution target range profiles (HRR profiles) can be used to aid and rectify this data association problem. Combined with a filtered kinematic estimate, the expectation of target class and radar signature can be utilized to prevent future "missasociations" (incorrect report-to-track history association). Figure 1 represents a situation in which a target report is assigned to the wrong track using a kinematic tracker alone.
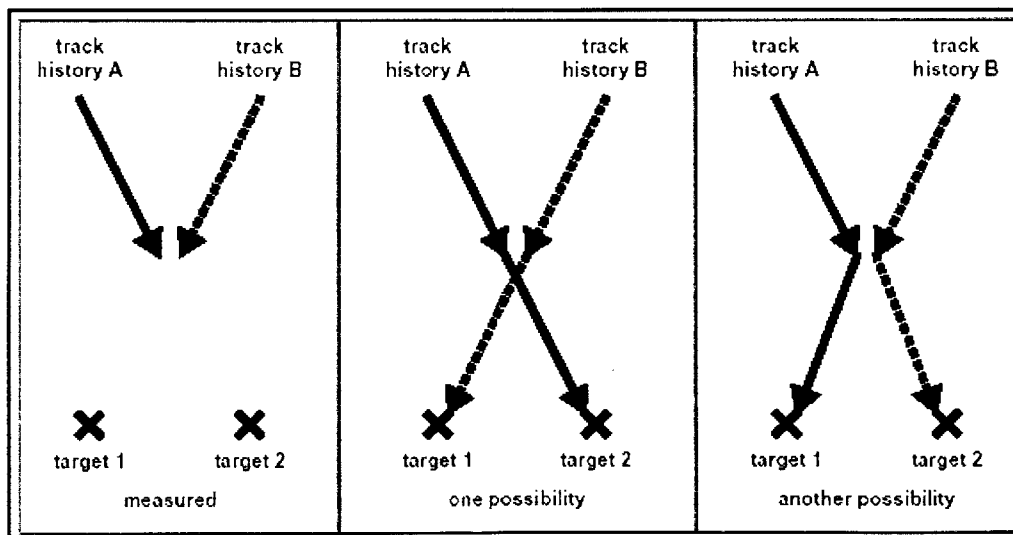
Figure 1. Typical kinematic misassociation.

This report will attempt to build upon past research and algorithm developments involving Feature-Aided-Tracking at Lincoln Laboratory. Nguyen et al. [1] has completed significant work to include FAT/Automatic-Target-Recognition (ATR) algorithm development and signal processing used in the generation of 1-D HRR profiles. This FAT system is used as an addition to a simple kinematic tracker developed by Keith Sisterson [2]. Additionally, Nguyen has demonstrated that 2-D SAR and ISAR target imaging can also be exploited to vastly improve ATR algorithms. The work below, however, will focus solely on FAT algorithm performance evaluation and technique enhancement while solely utilizing the less-complex one-dimensional HRR information. The form of signal processing used to develop the profiles is kept constant in an attempt to better control and understand the trends and performance of the algorithm itself.

1.1 High-Level-Description of LL FAT Application

Figure 2 gives a general overview of the functional operations within the Lincoln Lab Feature-Aided-Tracker Software.
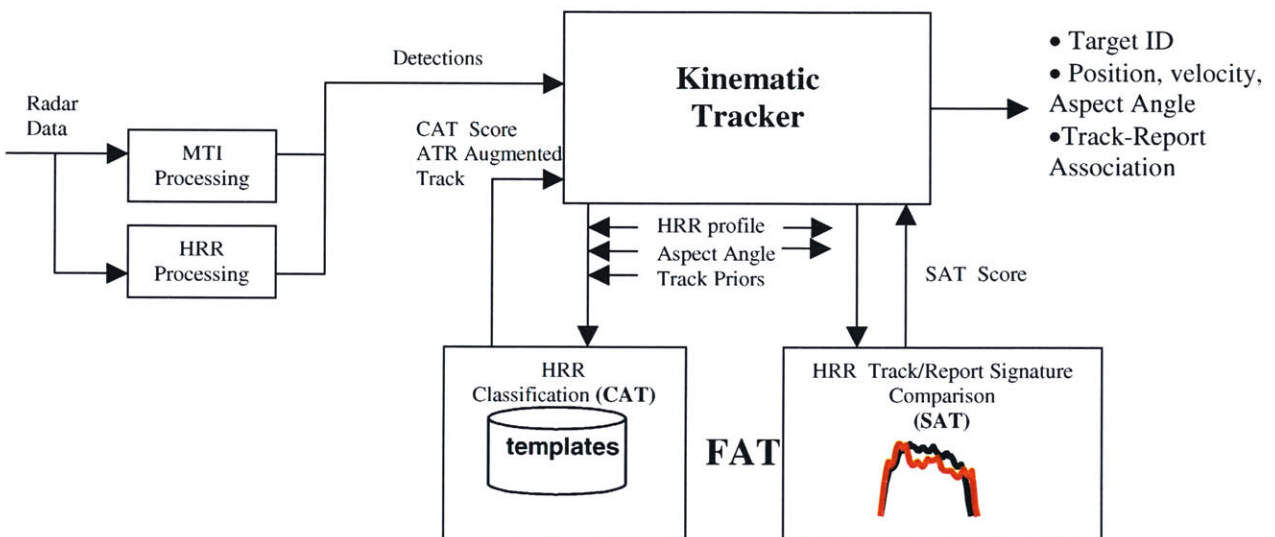
Figure 2. Overview of FAT

As shown above, there are three main components within this tracking system: the Kinematic Tracker (KT), CAT, and SAT. KT uses HRR-augmented GMTI target detections as its input. A single detection consists of the target range, azimuth, Doppler (range rate), and HRR profile [simply referred to as HRR below] in addition to clutter Doppler and the position and velocity of the radar platform. The HRR and associated track-report aspect angle is sent to CAT where the target identification is hypothesized and an adjoining confidence score is generated.* The HRR and aspect angle is also sent to SAT where another confidence score is generated to represent the probability that the current report HRR and the previous track history HRR originate from the same target. This information

---

* Target aspect angle is the angle between the heading of the target and the line of sight from the radar to the target

12

from CAT and SAT is fused to provide a final "best estimate" of a track-report pairs and the track history is thus updated.

1.2 Data Selection/Generation

1.2.1 HRR profiles

High Range Resolution target radar signatures form the foundation of current ground-moving-target classification algorithms. There were few options in obtaining HRR profile data to be used in this analysis. The continuing issues remain availability, releasability, usability, and completeness of the data. Three options existed if real target radar data was to be obtained, two of which are unclassified (MSTAR and MTFP). Usability refers to the ease in which fully signal processed HRR target data can be uploaded and used by the MATLAB FAT application. Signal processing software was developed by Nguyen [1] to transform stationary target SAR images from the aforementioned data sets into Range profile data (HRR). Additional limitations include the number of available targets and, more importantly, aspect angle coverage; 360 degrees of data is desired.

1.2.1.1 MSTAR

The MSTAR HRR profiles used in this study were formed from SAR imagery provided to Lincoln Laboratory by Wright Laboratories, Wright-Patterson Air Force Base, Dayton, OH. This data was collected in 1995 and 1996 by the Sandia National Laboratory X-band (9.6 GHz) HH-polarization SAR sensor in support of the DARPA-sponsored MSTAR program [1].

The data set received via Group 104 contained SAR images of 12 military vehicles images in spotlight mode at 15 and 17 degree depression angles over 360 degrees of aspect angle. Images of three variants each of the BMP2 armored personnel carrier, the M2 Bradley fighting vehicle, and the T72 Russian tank. This data set also included images of the M109 self-propelled howitzer, the BTR60 and BTR 70 armored personnel carriers, the HMMWV (Humvee), M1 tank, M110 gun, M113 transport vehicle, M35 transport truck, and the M548 transport vehicle. Figure 3 shows ground photographs for some of these vehicles.

| M2 | BTR60 | BTR70 | M548 |

M35 HMMWV

Figure 3. Photographs of vehicles used in study

1.2.1.2 MTFP (Moving Target Feature Phenomenology)

Veridian Engineering of Dayton, OH, provided the MTFP data used to form HRR Range profiles. It was collected in 2000 by the Data Collection Sensor (DCS) X-band (9.6 GHz) HH and VV-polarization sensor in support of the DARPA-sponsored MTFP program. This data contains SAR images of nine military vehicles that have been imaged in spotlight HH and VV

13

polarization mode at 17, 10, and 8 degree depression angles. Unfortunately, the data that was received did not have 360-degree aspect angle coverage. Most targets had between 180 and 300 degrees of aspect angle coverage, presenting the FAT simulator with a difficult situation. Only two targets had sufficient aspect angle coverage; thus limiting the number (2) of target classes used. The MTFP data set also contained moving-target ISAR images available for use. The familiar HRR generation software could only be used on the SAR images, however. The targets used from this data set include the BTR80 transport vehicle, the M2 tank, the ZIL transport truck, the Russian T72 tank, the TEL missile launcher, the ZSU tank, and the 2S1 mobile gun.

1.2.1.3 HRR Profile Generation

As mentioned above, the HRR target range profiles used in the CAT template database were obtained by uploading the raw data files and performing signal/image processing operations to create 1-D templates from the 2-D complex SAR (non-moving) images. This was done with the aid of pre-existing MATLAB software developed by Duy Nguyen. Prior to signal processing and HRR "extraction", the raw complex image of the target must be cropped to a filtered 80 x 80 pixel image containing the entire target. Figure 4 below gives a visual example of this process.
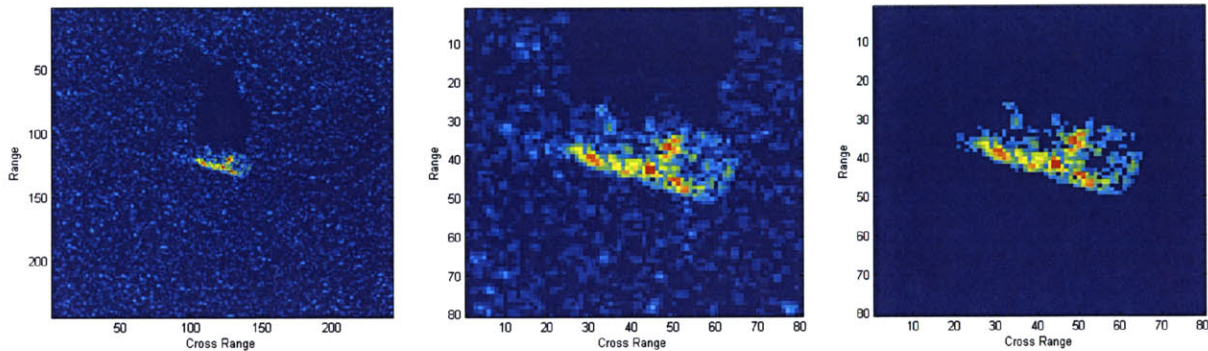
Figure 4. Cropping and filtering of a raw MTFP SAR image of a T-72 Tank. The first image is a 243x243 image of the target; the second image is an 80x80 cropped image of the target; the third image is the filtered cropped image

It was discovered when interacting with the MTFP data set that the software did not properly perform this task. It would center the cropped image on the maximum intensity cell. For larger targets, or in very noisy situations, this estimated center was far from the true center of the target. This is shown below as the first image in Figure 5.
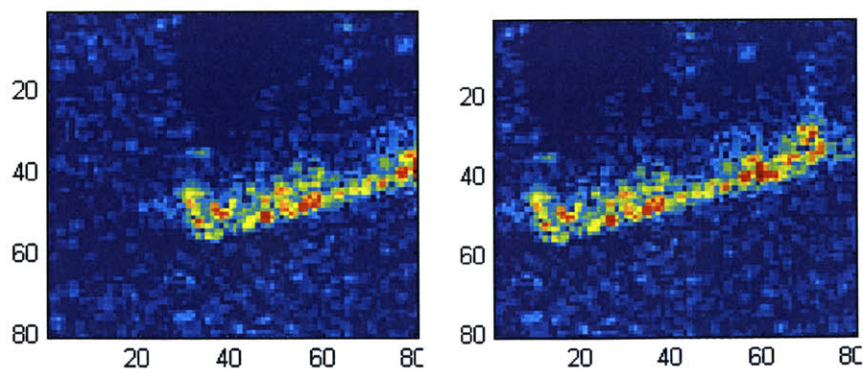
Figure 5. Cropped images of Scud Launcher to demonstrate improper extraction

14

The code was then adjusted to estimate the center of the target using image thresholding through a histogram and an averaging filter. An example of the improved result is shown above as the second image in Figure 5 (both images are of the same target).

Much of the following is a summary of information presented in [1]. The template generation software forms three 1-degree HRR templates by dividing each complex SAR image into three contiguous non-overlapping subsets; each subset contains HRR profiles collected over a continuous 1-degree aspect angle look. There were approximately 350 images used to construct approximately 1000 distinct HRR profiles for each target over aspect angles between 0 and 360 degrees.

More specifically, an HRR profile is the phasor sum of the time returns from different scatterers on the target located within a range resolution cell. Its profile represents the projection of the apparent target scattering centers onto the range axis. Figure 6 gives a highly simplified visual graphical example of this: Basically, the average intensity returns across each of the red lines is processed to form a 1-D image with the same number of data points as there are "horizontal red lines" below (54 data points with MTFP profiles).
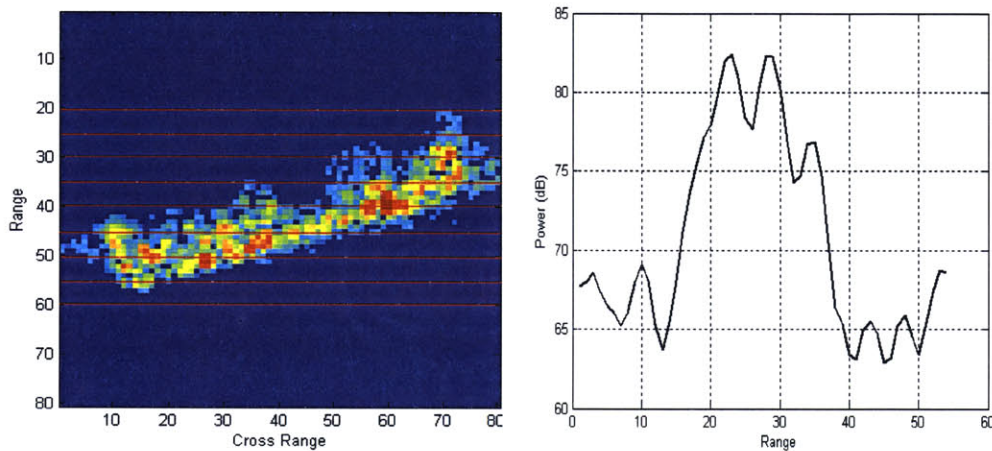
Figure 6. 2-D SAR image and corresponding 1-D HRR profile (20 dB SNR, 1 m resolution)

1-D HRR profiles are not as distinctive as SAR or ISAR images, however, they still provide valuable information about both moving and non-moving targets. In practice, a profile is formed by illuminating a target with a high-resolution waveform, for a series of pulses known as a CPI (coherent processing interval). By Fourier transforming the pulse stream, and correcting for target range rate, the signature will be contained in a single Doppler bin for relatively short pulse streams. A single CPI HRR is obtained by extracting information from the bin containing the target. Multiple CPI's can be use to average out speckle noise and provide a more accurate HRR profile. The range resolution of the HRR depends on radar quality (bandwidth) while SNR and the number of CPIs used depends on the MTI (Moving Target Indicator) radar dwell time. As you increase the number of CPI's used, there is a reduction in noise yet an increase in dwell time thus straining radar resources. Specifically, a decreased revisit frequency (increased dwell time) degrades the performance of the tracker.

In the past, super-resolution techniques (data-adaptive image formation methods) were used by Nguyen et al. in [1] to improve the features of the HRR profiles given limited radar resources. These methods include Beamspace High Definition Imaging (BHDI) among others

and are more effective in reducing noise relative to the conventional weighted-FFT technique. The HRR template profiles in this study were formed using the baseline weighted FFT technique to obtain 20 dB SNR, 1-meter range resolution profiles using 5 CPI's. This simulates performance using minimally effective HRR profiles thus providing results that can easily be improved upon using super-resolution techniques. The method used was simple yet effective.

1.2.1.4 Pattern Matching

All HRR pattern-matching operations in FAT use a weighted Mean Squared Error (MSE) metric. Comparing the input test profile against the template profiles at every pixel of interest and computing the sum of the mean squared errors[*] leads to an effective measure of similarity:

$$\text{Weighted MSE} = \frac{\displaystyle\sum_{k=1}^{HRRPixels} w_k (t_k - h_k)^2}{\displaystyle\sum_{k=1}^{HRRPixels} w_k} \qquad (1)$$

t_k is the magnitude of the kth pixel in the track HRR profile,
h_k is the magnitude of the kth pixel in the report (measurement) HRR profile,
and w_k is the weight for the kth pixel calculated as

$$w_k = 1 - pr_k \times pt_k$$

where

$$pr_k = \begin{cases} 1 & t_k \le 2\eta \\ 0 & otherwise \end{cases}$$

$$pt_k = \frac{1}{8} e^{-2t_k / \eta}$$

with η as the clutter power level (mean noise power)

Due to sensor parameter differences, the range samples and the gain of the test and template profiles might be misaligned. The ideal values for both range shift and power gain may be found through brute force. The MSE metric forms a parabolic function of shift and gain, so the optimum values are found by first shifting in range then in gain [1] (see Figure 7 and 8 below).
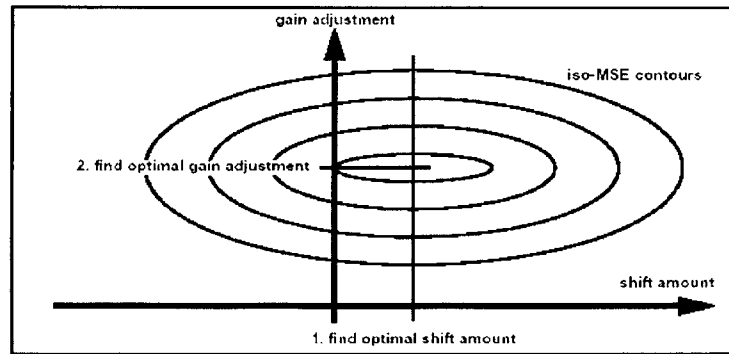
Figure 7. two step method for finding minimum MSE score

---

[*] The log of the MSE score is used in all FAT calculations to ease computational analysis.

16

| Original HRR profiles | Shifted (Range Aligned) | Scaled (Gain Aligned) |
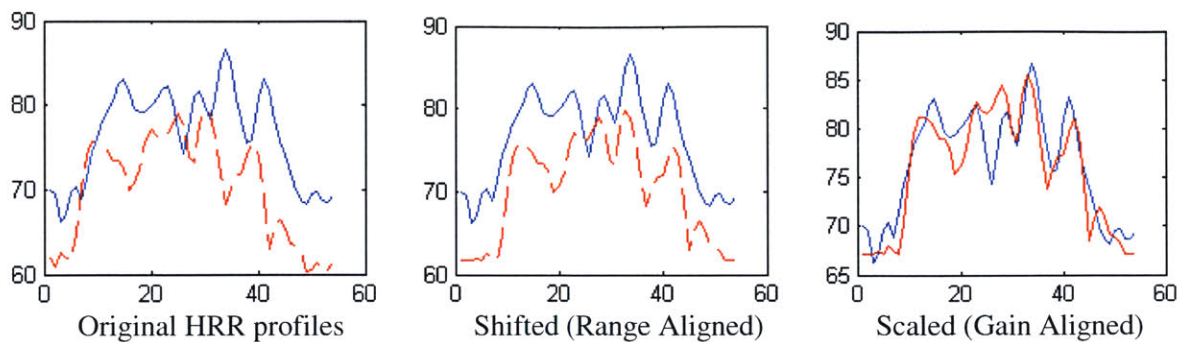
Figure 8. Scaling and Shifting for HRR matching MSE operations

1.2.2 GPS data

Ground truth in the form of GPS data (position and velocity) for most test scenarios was generated using Lincoln Laboratory's ModSAF/VMAP military vehicle traffic simulator. This software overlays a set of high-value targets on a series of pre-set roads and paths. VMAP is a collection of map and road data taken from multiple cities and countries. ModSAF places high value targets among background targets on these roads and simulates vehicle movements as desired. The road and terrain model used in this study originates in the vicinity of San Diego, CA. The data is returned to the user in the form of a text file that specifies time, target ID#, longitude, latitude, longitudinal velocity (m/s) and latitudinal velocity (m/s). A MATLAB function was developed to convert the information in this text file to a form expected by the tracker. The following are ModSAF scenarios that represent difficult target tracking environments:

1) Simple Linear Acceleration/Deceleration or Constant Velocity – State estimation is severely degraded during extreme deceleration and near-stop situations

Cartesian coordinate plane: x (meters) and y (meters)
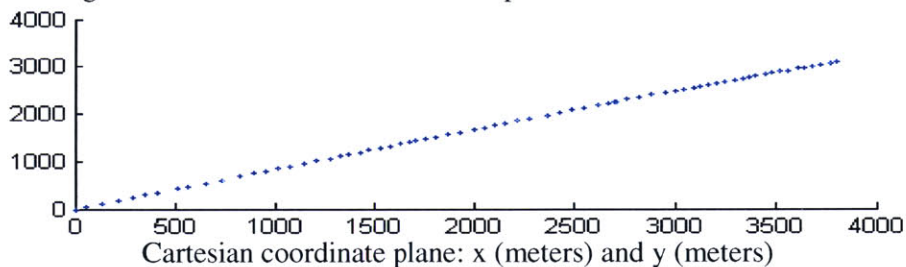
2) Curve/Sharp Turn – This scenario includes target maneuvers that are extremely difficult to track consisting of change-of-direction and arc-of-turn maneuvers. Acceleration and deceleration through turns is accurately simulated simulated.

Cartesian coordinate plane: x (meters) and y (meters)

17
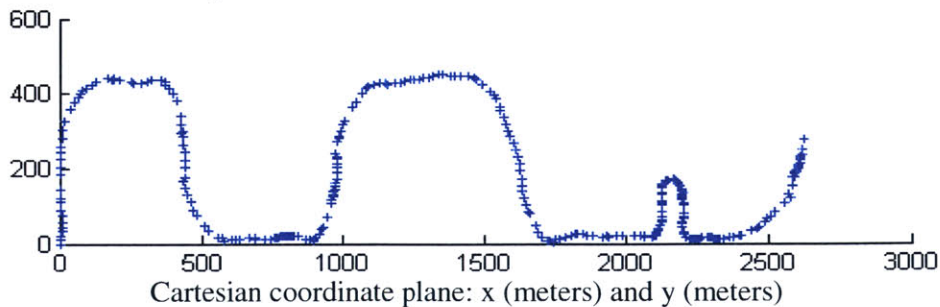
3) X Non-Crossing - Targets (red and blue) approach in a crossing situation but do not actually cross. Similar to Figure 1, this is recognized as the typical example in which the use of a kinematic tracker alone will fail.
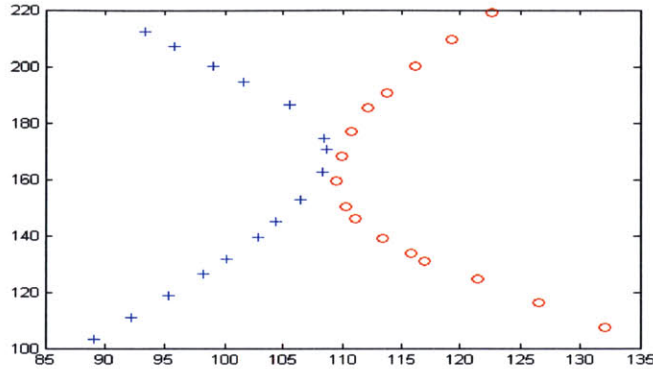
Cartesian coordinate plane: x (meters) and y (meters)

1.3 Kinematic Tracking/LL UAV Tracker

The Kinematic Tracker component of FAT used in this study is a version of the Lincoln Lab UAV tracker created in 1991 by Keith Sisterson [2]. It was designed to support a small, lightweight radar payload flown on a UAV. Generally, it is a software module that runs in a ground data processing system. It receives measurements/reports that include the location of both the target and UAV. The tracker uses stored and filtered positions and velocities to either associate incoming target reports with stored kinematic track histories or to initialize a new track when no association is hypothesized. Much of the following is a summary of information contained in [1], [2], and [3].

1.3.1 Measurement Data Processing

The tracker receives measurements (reports) that include the range, Doppler (range rate), and azimuth angle of the target as well as the velocity and position of the radar in 3-dimensional Cartesian coordinates (x, y, z). Azimuth angle is measured clockwise from North. This data is received in discrete "bursts", or scans. Typically, during each scan, a radar system will use clutter Doppler, absolute target Doppler, and radar velocity to determine the target Doppler with respect to the radar. The MTI (Moving Target Indicator) radar simulator used in this study performs this function. The range, azimuth angle, grazing (or depression) angle, and position of the radar are also used to determine target position in Cartesian coordinates. The coordinate plane contains a 2-dimensional "flat" section of the earth, the origin of which is at a parameterized latitude and longitude. The origin changes with the location of each scenario. This tracker uses a square grid system based upon this plane in order to eliminate unnecessary calculations; specifically, it only performs computations on reports when track histories are in the same or adjacent grid squares.

The tracker performs all calculations within this 2-dimensional plane. Therefore, the target "Doppler" used in the tracker is computed using the grazing angle to project the 3-D Doppler (relative to the radar) velocity onto this 2-D horizontal plane. Finally, the target reports reach the tracker and include the position of the target and the 2-D "Doppler" velocity.

$$z = [x \ y \ d]^T$$

The Doppler speed from the first scan is used to initialize track velocity. Subsequently, the KT uses the Doppler measurement in data association and track filtering to improve track accuracy and filter performance. Incoming measurements are then analyzed relative to existing track histories whose state vectors have the form (over-dot is used to indicate time derivative):

$$x = [x \ \dot{x} \ y \ \dot{y}]^T$$

1.3.2 Data Association

1.3.2.1 Track Initiation

The tracking process can be broken down into two phases: data association and track filtering/updating. Track initiation must take place before this can occur. If measurements exist that are not associated with a pre-existing track, a new track is initialized. There is very little information at this point, but a velocity vector and covariance matrix can still be calculated. This is done for all possible velocity values, taking Doppler aliasing/ambiguity into account. Doppler ambiguity is defined as when the PRF (pulse repetition frequency) is less than the maximum Doppler frequency that may be encountered thus the true Doppler frequency may equal the indicated frequency plus or minus some integer multiple of the PRF [4]. Simply put, two targets that differ in Doppler frequency by an integer multiple of the radar PRF will be seen as having the same frequency. Subsequent scans are then used to affirm the validity of indicated Doppler velocity*: The maximum speed forms a circle of possible velocity values for the track. The Doppler value constrains the possible velocity to lie along a line that is a chord of the circle of maximum speed and perpendicular to the line of sight between the UAV and the target. Because of aliasing, there can be several chords and several possibilities. The velocity represented by the Doppler velocity itself is chose as the initial track velocity. The resulting covariance matrix can be found in [2].

1.3.2.2 Hypothesis Testing

A tracker must consider all possible track/report association pairs and maneuvers before a data association decision is made. On each subsequent scan, association hypothesis testing will determine what type of maneuver each specific target-report pair is likely to be undergoing. The tracker tests successive statistical hypotheses to both determine the most likely track-report pairs and choose the appropriate measurement filtering parameters for each maneuver. Pairing a track and report means that the current report is considered to be the next part of the track. The details of hypothesis testing depend upon a track's status:

a) *New* – one measurement
b) *Novice* – 2-6 measurements; Doppler ambiguity not resolved
c) *Established* – 2+ measurements; ambiguity resolved

---

* Doppler "velocity" and frequency are related by $v = \left(\dfrac{PRF}{2 \times CenterFrequency} \right) \times c$

New and Novice tracks use the velocity possibilities (velocity windows) to determine if any new measurements should be associated with the track in question. There is a limit computed on the distance between the measurement and extrapolated track position corresponding to nine times the variances from all sources of error plus the distance the target would move if it accelerated with the parameterized maximum permissible.[*] If the track-report pair is determined to be kinematically possible, a χ^2-like quantity is calculated and used in the data association matrix to resolve conflicts.

Established tracks have at least two measurements and enough data to have initialized the Kalman filter; its resulting matrices and equations and are subject to more complex hypothesis testing. There are four movement models tested and used with this tracker. The maneuver associated with a track is used mainly to increase or decrease the expectation of noise in the Kalman filter. Before filtering is addressed, hypothesis testing must be understood:

1.3.2.2.1 Unmodeled Maneuver Hypothesis

A limit is computed on the distance between the measurement and extrapolated position of the track using the past Kalman filter state. This limit is the same limit mentioned above. If the difference is within this limit, a χ^2-like quantity is stored for possible use later on. If this test fails, the association is deemed 'impossible' as processing continues with the next possible track-report association. If it succeeds, the constant velocity hypothesis is tested next.

1.3.2.2.2 Constant Velocity Hypothesis

This is the most constrained hypothesis. However, most targets will result in measurements that fit this hypothesis due to either large expected measurement error and/or slow changes in speed and direction that are unrecognizable with smaller scan update times.

The plant noise matrix (Q), used in the Kalman filter (discussed below in Section 1.3.3), is computed using the parameterized constant $cvsq$ when this hypothesis is chosen. The χ^2 score used in the data association matrix is computed for the difference between the measurement and extrapolated track position. The track position has a covariance matrix of:

$$ R = \begin{pmatrix} \sigma^2_{x_t} & \sigma_{x_t}\sigma_{y_t} \\ \sigma_{x_t}\sigma_{y_t} & \sigma^2_{y_t} \end{pmatrix} \tag{2} $$

The terms in this matrix are obtained from the extrapolated track covariance matrix, which includes terms from the final covariance update in the track's Kalman filter history, the measurement covariance matrix, and the plant noise covariance matrix, Q. The variance of the distance r between (x_m, y_m) and (x_t, y_t) is (m and t denote measurement/report and track, respectively):

$$ \sigma_r^2 = \frac{(x_m-x_t)^2(\sigma_x^2+\sigma_{xt}^2)+(y_m-y_t)^2(\sigma_y^2+\sigma_{yt}^2)+2(x_m-x_t)(y_m-y_t)(\sigma_{xy}+\sigma_{xtyt})}{r^2} \tag{3} $$

---

[*] 9 times the variance is the same as 3 times the standard deviation, which by definition should include 99% of all measurement errors

An actual χ^2 score is calculated using

$$\chi^2 = \frac{r^2}{\sigma_r^2} + \frac{(d_m - d_t)^2}{\sigma_d^2 + \sigma_{dt}^2} \qquad (4)$$

where d is a Doppler value with corresponding track variance $\sigma^2{}_{dt}$ computed along the radar line of sight. (4) results in a χ^2 value with 2 degrees of freedom. If the errors are normally distributed, as assumed, tables can be used to select the parameterized confidence limit. If the resulting χ^2 score is within this limit, the test succeeds and there are no more tests. If it fails, subsequent tests follow:

1.3.2.2.3 Linear Accelerating Track Hypothesis

The target is allowed to be accelerating along the line of the track. A track/report association passes this test if the acceleration computed from a least squares fit of the measurement to the track is below the maximum permissible value and the χ^2-value (obtained from the position differences (r) and Doppler expectation) is within the confidence limit. The projected measurements and χ^2 are calculated as:

$$x_t = x_p + \dot{x}t + \frac{\ddot{x}t^2}{2} \qquad (5)$$

$$y_t = y_p + \dot{y}t + \frac{\ddot{y}t^2}{2\dot{x}} \qquad (6)$$

$$\chi^2 = \frac{\left((\dot{x} + \ddot{x})\sin a + (\dot{y} + \frac{\ddot{y}t}{x})\cos a - d_m \right)^2}{\sigma_d^2 + \sigma_{dt}^2} + \frac{r^2}{\sigma_r^2} \qquad (7)$$

where r^2 and $\sigma^2{}_r$ are calculated as in Section 1.3.2.2.2. This χ^2 value has one degree of freedom and is tested against a parameterized limit. If the test succeeds there are no more tests. If it fails, one more test follows:

1.3.2.2.4 Constant Speed Arc-of-Circle Track Hypothesis

The extrapolated arc-of-circle position is constructed from the track position and heading at the last track update and the current measurement. A χ^2 value with one degree of freedom is computed from the difference between the predicted and measured Doppler and the difference between the predicted and measured track length:

$$\chi^2 = \frac{(x_t \sin a + y_t \cos a - d_m)^2}{\sigma_d^2 + \sigma_{dt}^2} + \frac{(vt - s)^2}{t^2 \sigma_v^2 + \sigma_s^2} \qquad (8)$$

where target speed $v = \sqrt{\dot{x}^2 + \dot{y}^2}$, s = distance along the arc of circle, $\sigma^2{}_v$ is the variance of v, and $\sigma^2{}_s$ is the variance of s. If the resulting χ^2 score is within a specified limit, the test succeeds and the χ^2 score aids in data association. If not, the maneuver is considered "Unmodeled" and the initial unmodeled χ^2 score is used. For unmodeled hypothesis, there is an additional value

21

of 10 is added to the original χ^2 score to ensure that at an association undergoing an 'unmodeled' maneuver is never chosen over an association with a hypothesized modeled maneuver.

1.3.2.3 Association Assignment

An assignment matrix is formed to aid in the association of target reports to track histories. The matrix contains the aforementioned final χ^2 scores for every possible track/report pair. If one track/report association is found to be impossible, an exceptionally high score is given to that cell in the matrix (specifically, 'invalid' χ^2 = 1000). Below is an example of what one of these association matrices would look like in a two-target, two-report case:

$$\chi^2 matrix = Track \begin{array}{c} \\ 1 \\ 2 \end{array} \begin{bmatrix} .687 & 2.459 \\ 3.982 & 1.324 \end{bmatrix}$$

Measurement
1   2

However, depending on the maneuver associated with each pair, certain χ^2 scores may be associated with differing degrees of freedom. Therefore, they must be normalized to equivalent values with two degrees of freedom using the χ^2 distribution curves shown below.
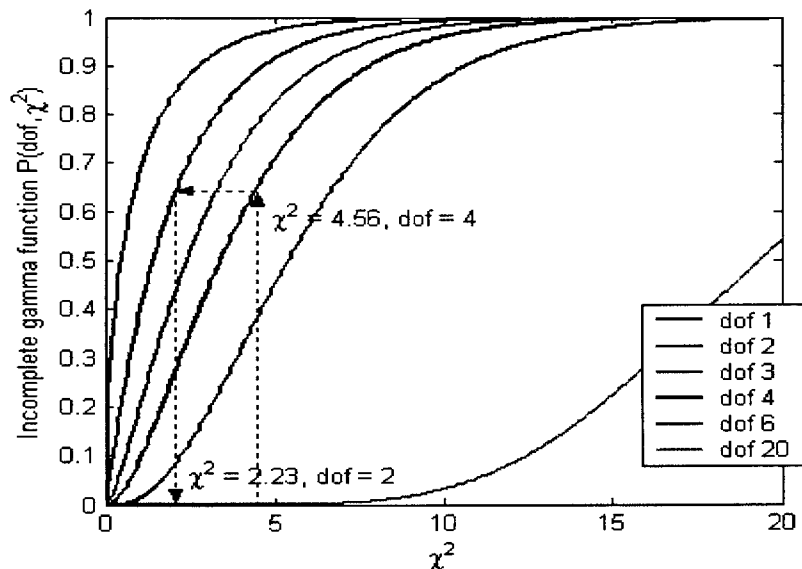
Figure 9. Normalizing χ^2 scores to 2 degrees-of-freedom (dof)

An example is given to explain the conversion of a χ^2 score of 4.56 with 4 degrees-of-freedom to an equivalent χ^2 score with 2 degrees-of-freedom (i.e. find χ^2 such that P(χ^2,2) = P(4.56, 4)). This normalization procedure is used again within FAT. The χ^2 distribution P(χ^2,dof) is given by the incomplete gamma function:

$$P\left(\chi^2 \middle| dof\right) = Q\left(\frac{dof}{2}, \frac{\chi^2}{2}\right) \qquad (9)$$

such that

$$Q(a, x) = \frac{1}{\Gamma(a)} \int_0^x e^{-\tau} \tau^{a-1} d\tau \qquad (a > 0) \qquad (10)$$

After the association matrix is correctly normalized, the extended Munkres algorithm is used to determine optimal track/report association [5]. The smaller the χ^2 score, the more likely it is that the tested track/report pair is correct. The output of the Munkres algorithm is a set of paired assignments (e.g. Track1 to Report 2, Track 3 to Report 1, etc.). It is also noted if no measurement is assigned to a particular track, or vice versa. Therefore, the maximum number of possible pairs will be $t + m^*$, while the minimum number of pairs will be $\max(t,m)$. Once the optimal track/report pair assignments are made, the track histories are updated. If a track exists without an associated measurement, the time and number of scans since the last association is compared against a parameterized constant to determine if the track should be kept.

1.3.3 Kalman Filtering/State Estimation

The Kalman filter is a well-established technique used to provide state estimates when measurements are under the influence of noise. Its advantages stem from its adaptability for use with digital systems and processes involving gaussian noise. The target model used in this tracker (straight line, constant velocity) assumes measurement noise to be normally distributed with a mean of zero. An estimation of the target state and covariance matrix is all that is required to define the probability density function (PDF) associated with the target positions in state space [6]. As mentioned earlier, the tracker works with objects in a horizontal plane. A two state system[**] is used with a measurement having three components: x, y, and a 2-D Doppler value computed using 3-dimensional geometry. When this kinematic tracker was created, computational resources were tremendously limited. Specifically, requirements were minimized because the need to invert a 3x3 matrix was eliminated by splitting the filter into two separate sections (essentially two filters). The first section uses only position information while the second performs analysis only on the Doppler measurement. The filter used is a constant-velocity Kalman filter with maneuvers modeled as acceleration noise in the plant state covariance matrix.

The Kalman filter is used only with Established tracks. New tracks, however, are used to initialize the covariance matrices and store relevant initial information. The actual process of computing the measurement covariance matrix is discussed in Section 2.2. If a track has Novice status, the tracker checks to see whether the Doppler ambiguity can be resolved. The measurement is saved, and once ambiguity is resolved, the Kalman filter is recursively run on all previously saved target reports in addition to the current one. Kalman filtering will be performed on all subsequent scans for an Established track. The following steps (1-10) describe this

---

[*] t is # of tracks and m is # of measurements
[**] recall that the target state in this case is $\mathbf{x} = [x \ \dot{x} \ y \ \dot{y}]^T$

23

particular Kalman filter. The true current state is (k indicates current scan and k-1 indicates previous scan):

$$x_k = \phi_{k-1} x_{k-1} + noise \qquad (11)$$

ϕ_{k-1} is the state transition matrix:

$$\phi_{k-1} = \begin{bmatrix} 1 & t & 0 & 0 \\ 0 & 1 & 0 & 0 \\ 0 & 0 & 1 & t \\ 0 & 0 & 0 & 1 \end{bmatrix}$$

x is the state vector:

$$x_k, x_k^{-}, \text{or } x_k^{+} : \begin{bmatrix} x \\ \overset{\&}{} \\ y \\ \overset{\&}{} \end{bmatrix}$$

1) The current target report can be represented by

$$z_k = H_k x_k + noise \qquad (12)$$

z is the measurement vector (x, y are position, d is Doppler):

$$z_k = \begin{bmatrix} x \\ y \\ d \end{bmatrix}$$

and H is the observation matrix (converts the measurement to position; a is azimuth angle):

$$H_k = \begin{bmatrix} 1 & 0 & 0 & 0 \\ 0 & 0 & 1 & 0 \\ 0 & \sin a & 0 & \cos a \end{bmatrix}$$

2) The initially extrapolated next state for the track is (- indicates extrapolation, ^ indicates estimation):

$$\overline{x}_k = \phi_{k-1} \hat{x}_{k-1} \qquad (13)$$

3) The error covariance matrix for the initially extrapolated next state is:

$$\overline{P}_k = \phi_{k-1} \hat{P}_{k-1} \phi^T{}_{k-1} + Q_{k-1} \qquad (14)$$

Q is the process noise covariance matrix. "t" is time update rate, q is a constant parameter that changes with hypothesized maneuver (i.e. $cvsq = 9.83$ for constant velocity, $arcsq$ and $latsq = 7.82$ for linear accelerating, arc-of-circle, and unmodeled hypothesis):

$$Q_{k-1} = \begin{bmatrix} \frac{qt^3}{3} & \frac{qt^2}{2} & 0 & 0 \\ \frac{qt^2}{2} & qt & 0 & 0 \\ 0 & 0 & \frac{qt^3}{3} & \frac{qt^2}{2} \\ 0 & 0 & \frac{qt^2}{2} & 0 \end{bmatrix}$$

P is a covariance matrix for the updated states generated by the Kalman filter:

24

$$P_k^- \text{ or } P_k^+ : \begin{bmatrix} P_1 & P_2 & P_3 & P_4 \\ P_2 & P_5 & P_6 & P_7 \\ P_3 & P_6 & P_8 & P_9 \\ P_4 & P_7 & P_9 & P_{10} \end{bmatrix}$$

4) The Kalman gain stage 1 (only involving measurements x, y):

$$^1 K_k = \overline{P}_k H^T{}_k [H_k \overline{P}_k H^T{}_k + R_k]^{-1} \qquad (15)$$

For stage 1,

$$H_k = \begin{bmatrix} 1 & 0 & 0 & 0 \\ 0 & 0 & 1 & 0 \end{bmatrix}$$

R is the measurement covariance matrix calculated using parameterized variances

$$R_k : \begin{bmatrix} R_1 & R_2 \\ R_2 & R_3 \end{bmatrix}$$

$^1 K$ is the Kalman gain matrix for stage 1

$$^1 K_k : \begin{bmatrix} K_1 & K_2 \\ K_3 & K_4 \\ K_5 & K_6 \\ K_7 & K_8 \end{bmatrix}$$

5) The error covariance matrix is then updated:

$$\hat{P}_k = [I -^1 K_k H_k] \overline{P}_k \qquad (16)$$

6) The extrapolated track covariance matrix is set to the updated track covariance matrix:

$$\overline{P}_k = \hat{P}_k \qquad (17)$$

7) The Kalman gain stage 2 (only involving measurement d - Doppler):

$$^2 K_k = \overline{P}_k H^T{}_k [H_k \overline{P}_k H^T{}_k + \sigma^2{}_d]^{-1} \qquad (18)$$

For stage 2,

$$H_k = \begin{bmatrix} 0 & \sin a & 0 & \cos a \end{bmatrix}$$

and $\sigma^2{}_d$ is the Doppler variance

$^2 K$ is the Kalman gain matrix for Stage 2: $\quad ^2 K_k : \begin{bmatrix} K_9 \\ K_{10} \\ K_{11} \\ K_{12} \end{bmatrix}$

8) The final error covariance update is: $\quad \hat{P}_k = [I -^2 K_k H_k] * \overline{P}_k \qquad (19)$

9) The final state estimate update is:

$$\hat{x}_k = \overline{x}_k + K_k [[I - BK_k X][z_k - H_k \overline{x}_k]] \qquad (20)$$

H_k is as originally constructed,

25

B and X originate from H_k,

$$B = \begin{bmatrix} 0 & 0 & 0 & 0 \\ 0 & 0 & 0 & 0 \\ 0 & \sin a & 0 & \cos a \end{bmatrix}, \text{ and } X = \begin{bmatrix} 1 & 0 & 0 \\ 0 & 1 & 0 \\ 0 & 0 & 0 \end{bmatrix}$$

and K_k is the fused Kalman gain matrix,

$$K_k = \begin{bmatrix} {}^1K_k & {}^2K_k \end{bmatrix}$$

The above equations update the state of the track by "smoothing" the noise from each measurement. Only x, $\dot{x}$, y, $\dot{y}$, and P are updated by the above equations. Tracks are later fully updated with information retrieved during FAT.

1.4 Classification-Aided-Tracking (CAT)

Classification-Aided-Tracking is a method of using an ATR (automatic target recognition) classifier to aid in data association by measuring class continuity from scan to scan. Consider the following two-class example below where a Scud launcher (blue) and ZSU troop carrier (red) are approaching an intersection. The detection positions from the next scan appear in black. Under these circumstances, the targets will either continue along their respective roads, or choose to follow another road. The kinematic tracker will always make an incorrect association in situations where target A follows the expected path of target B and vice versa. Figure 10 shows that if the detections are augmented with HRR profiles, then a classifier may be used to correctly determine which detections belong to which track (the track histories contain knowledge of track target class). CAT is extremely valuable in these scenarios.
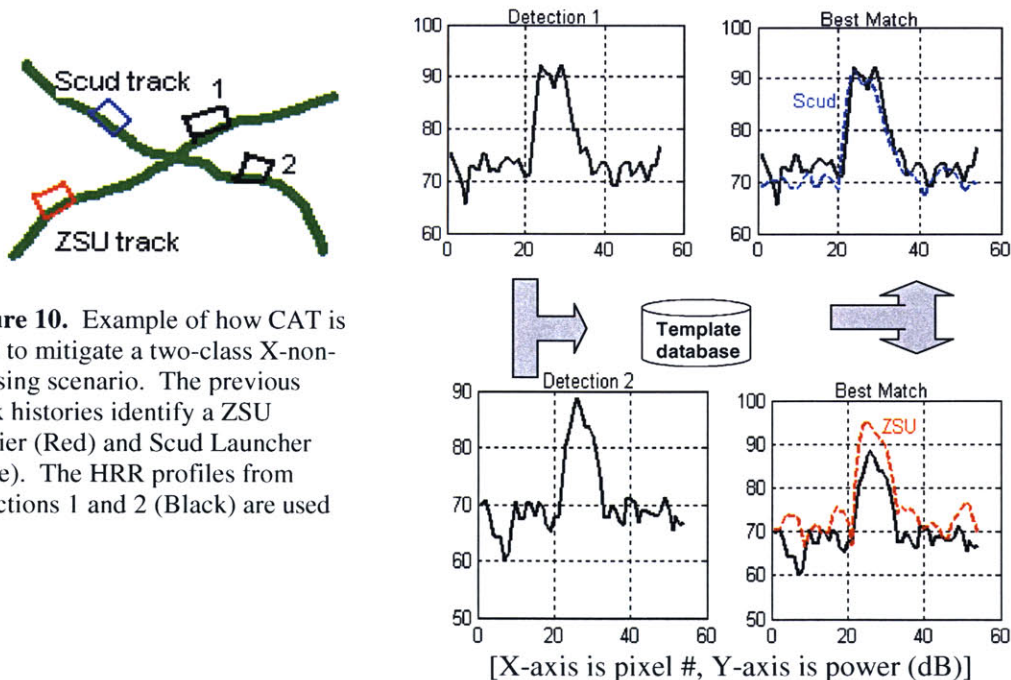
Figure 10. Example of how CAT is used to mitigate a two-class X-non-crossing scenario. The previous track histories identify a ZSU Carrier (Red) and Scud Launcher (Blue). The HRR profiles from detections 1 and 2 (Black) are used

[X-axis is pixel #, Y-axis is power (dB)]

CAT is used when a multi-class database of HRR profiles is available *a priori*. This database typically contains non-moving-target HRR profiles. The moving-target profiles should be noisy or "smeared" versions of the former. If a template database is available, each report

26

(using its moving-target HRR profile) can be assigned a probability or likelihood that it is a member of a specific target class. CAT is particularly helpful in situations where the high-value target is of a known class that has template HRR profiles readily available. Depending upon their radar signature characteristics, CAT may or may not help resolve data association conflict when targets are of an unknown class. Another shortcoming of CAT is that, in contrast to KT or SAT, an appreciably large amount of computational resources are required. It may also not be helpful in all kinematic situations (Section 4.2.1.1).

1.4.1 Bayesian Classifier

A Bayesian classifier is used to generate the likelihood that a report is of a particular target class. This likelihood is a function of both the ATR result and the previous track identification. First, a vector of MSE scores is generated for each track/report pair under analysis. This vector consists of the minimum MSE score from the comparison of the report HRR against a group of template database HRR profiles from each target class in the database. The size of the MSE vector is therefore 1 x [# of classes in database]. The aforementioned "group" of template HRR's is collected by taking all profiles from aspect angles within ten degrees of the estimated (via Kalman filter) track/report association aspect angle.[*] This aspect angle "error window" of ten degrees is included because there is an assumed error inherent in aspect angle estimation due to the measurement noise that accompanies radar detections.

It is also assumed, and can be shown, that the collection of minimum MSE scores used to populate each cell of the MSE vector resemble a normal distribution with mean MSE μ and variance σ^2. Using HRR profiles from the *a priori* database templates, the expected value of each cell (mean and variance) in the MSE vector is generated for future use. Because the HRR profiles and thus MSE scores are highly distinct across all aspect angles, statistics are generated by aspect angle sector (0-30°, 30-60°, ...to 180°). There are no statistics generated above 180° because of hemispherical symmetry; the HRR profile for a target at an aspect angle 180° from its true aspect angle will mirror itself and therefore the MSE statistics will be similar. The FAT software ensures that statistics from the appropriate sector are used for all target aspect angles between 0-360°.

These statistics can be used to estimate the probability that a particular report HRR profile either originates from a particular known target class or has the characteristics of an unknown target class. A "classification" vector is formed where N is the number of target classes in the database such that $\mathbf{P_{class}} = [p_1, p_2, ..., p_{N+1}]$ where p_k is the probability that the track is of type k and p_{N+1} is the probability that the track is of type *"other"* while $\sum_{i=1}^{N+1} p_i = 1$. Type *"other"* is assigned when a match in HRR is not found within the template database for the report HRR profile in question. Expected MSE statistics for the *"other"* class are formed by comparing class "1" HRR profiles against a set of profiles from multiple dissimilar target classes (class 2...N). $\mathbf{P_{pdf}}$, a vector of PDF likelihood values used to calculate the posterior probabilities in $\mathbf{P_{class}}$, is obtained using the MSE vector and pre-generated statistics in:

---

[*] this aspect angle is estimated using the velocity component of the Kalman filter output given the track-report pair in question

27

$$\mathbf{P_{pdf}} = P_{pdf}(MSEVec \mid Class_k) = \frac{e^{-\frac{1}{2} \bullet \Delta x_k \bullet Cov_k^{-1} \bullet \Delta x_k^T}}{\sqrt{(2\pi)^\wedge \# classes \times \det(Cov_k)}} \quad (21)$$

where $k = 1...N + 1$, Δx_i is the difference between the given MSE vector and mean MSE vector for class k, Cov_k is the pre-generated statistical covariance matrix for MSE vectors observed from class k, and det refers to the determinant.

Bayes' decision rule for this specific set of events (such as a target being of a particular class) leads to the calculation of the classification vector:

$$\mathbf{P_{class}} = P(Class_i \mid MSEVec) = \frac{P(Class_i)P_{pdf}(MSEVec \mid Class_i)}{\sum_{k=1}^{N-1} P(Class_k)P_{pdf}(MSEVec \mid Class_k)} \quad (22)$$

where $P(Class_k)$ for $k = 1...N + 1$ ($i = k$ at some point), are the track priors ($\mathbf{P_{priors}}$; prior probability that track is of class k). This is simply the classification vector of size $1 \times [N +1]$ generated using the current report HRR and the hypothesized associated track's information from the previous scan. With a new or novice track, the values in this vector are equal with $\sum_{i=1}^{N+1} p_i = 1$.

The vector $\mathbf{P_{class}} = P(Class_i \mid MSEVec)$ is a conditional probability reading "the probability that the report is of target class i given the specified MSE vector" for $i = $ class $1.. N$, and $other$. Additionally, we can use the above information to generate a Bayes' likelihood value that a given report is associated with one particular track:

$$P(\text{track } x \leftarrow \text{report } y) = \mathbf{P_{priors}} \text{ (from track x)} \bullet \mathbf{P_{pdf}} \text{(from report y)} \quad (23)$$

1.4.2 χ^2 Adjustment

The posterior probability ($\mathbf{P_{class}}$) aids in data association by contributing an additional χ^2 score to the association matrix. CAT adds a χ^2_{CAT} score to the initially calculated kinematic χ^2 score. χ^2_{CAT} is non a true χ^2 score, but a χ^2-like quantity generated using the track/report association probability calculated in (23). Specifically,

$$\chi^2_{CAT} = \text{-log } [P(\text{track } x \leftarrow \text{report } y)] \quad (24)$$

, leading to the following translation of $P(\text{track } x \leftarrow \text{report } y)$ into a χ^2_{CAT} score:
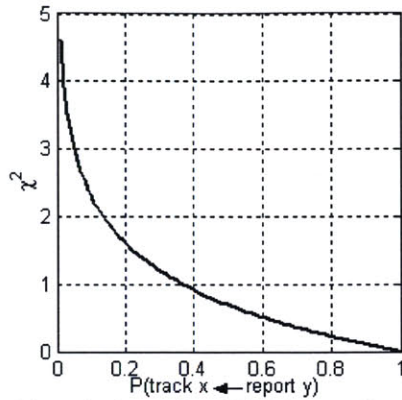
Figure 11. Translation of an MSE score into a χ^2_{CAT} score

If the kinematic tracker makes an incorrect association, the difference between the incorrect track-report association kinematic χ^2 and χ^2_{CAT} must exceed the difference between the correct association kinematic χ^2 and χ^2_{CAT} for CAT to be effective. When this χ^2_{CAT} score is added to the initial χ^2, an additional degree of freedom exists, requiring further normalization of the final, fused χ^2 score (χ^2_{fused}). This modification did not exist in the code that was used in this study and was subsequently added.

1.5 Signature-Aided-Tracking (SAT)

Signature-Aided-Tracking also utilizes HRR pattern matching to aid data association. Consider a two-target scenario where target A is closely following target B on a parallel track. The next scan indicates that the two targets appear to have merged and are headed in the same direction. This is a considered a kinematically ambiguous situation because either detection can be associated with either track. To mitigate this problem, we compare the stored track HRR profiles from the last scan (A and B) to the HRR profiles from the current detections (1 and 2) to measure HRR continuity and subsequently determine the most likely set of track/report pairs:
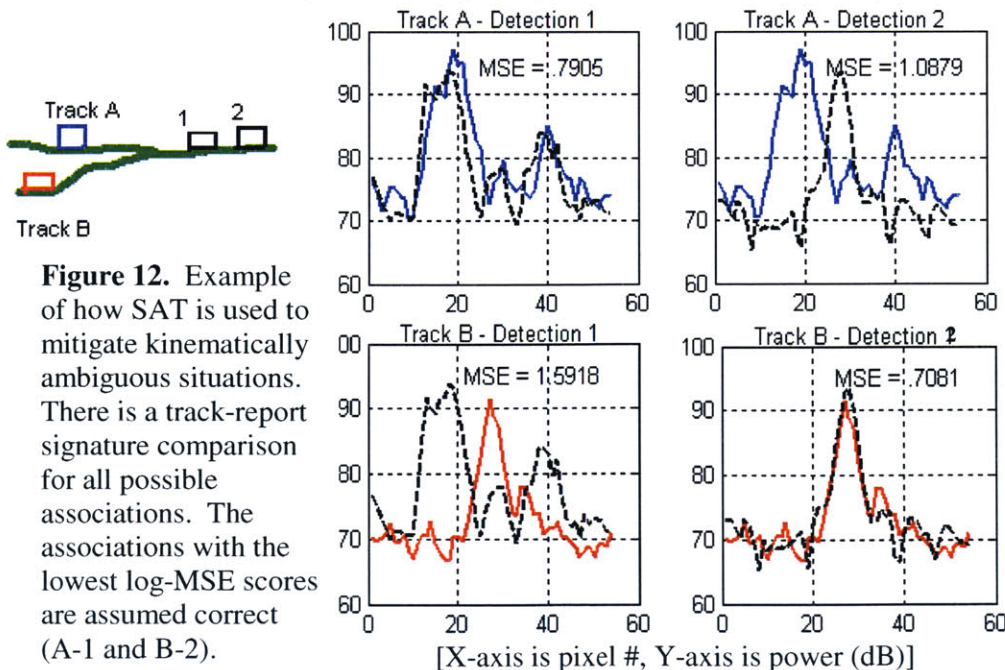
Figure 12. Example of how SAT is used to mitigate kinematically ambiguous situations. There is a track-report signature comparison for all possible associations. The associations with the lowest log-MSE scores are assumed correct (A-1 and B-2).

[X-axis is pixel #, Y-axis is power (dB)]

29

SAT requires no prior knowledge of target class and is thus extremely helpful in situations where the target class/type is unknown. SAT provides an MSE value for every possible track/report association and contributes a supplementary adjustment to the association matrix. Additionally, it should be noted that HRR profiles for one target distinct across all aspect angles. Recall that a 1-D HRR profile is a projection of the object in range towards the radar. When a target turns, various features might not be observable. Consequently, when there a large change in aspect angle exists from one scan to the next, SAT provides little assistance.

1.5.1 Statistics

As mentioned earlier, the kinematic tracker is used to generate an assignment matrix of χ^2 scores for every possible track/report association. SAT assumes that every report is augmented with a moving-target HRR profile. After the Munkres algorithm assigns a report to a given track, the track then stores both the estimated aspect angle and HRR profile from that report. During the ensuing scan, the Kalman filter is again used to estimate the aspect angle for each track/report pair. If the difference between the current report's estimated aspect angle and the track's stored aspect angle is less than a desired threshold (typically ten degrees), then a signature comparison is made. Otherwise, the signature information is ignored and only kinematic information is used.

A weighted log-MSE score is calculated for each hypothesized pair. This MSE score is then measured against the expected MSE scores for both matching[*] and mismatching targets. Similar to CAT, this type of comparison is expected to yield a Normal distribution of MSE scores. Statistics representing the Match and Mismatch means and variances (μ_{match}, $\mu_{mismatch}$, σ^2_{match}, $\sigma^2_{mismatch}$) are pre-generated using HRR profiles from the non-moving template database. Again, the template profiles can be used because moving profiles should simply resemble noisy versions of non-moving profiles. A set of HRR profiles from one target class is evaluated against a set of profiles from the same (Match statistics) and differing (Mismatch statistics) target classes within the specified aspect angle threshold. This comparison is repeated multiple times for multiple target classes.

If an MSE score comes from comparing two profiles of the same class, it is expected to lie near the center of the match PDF (blue); if not, it should lie near the center of the mismatch PDF (red):
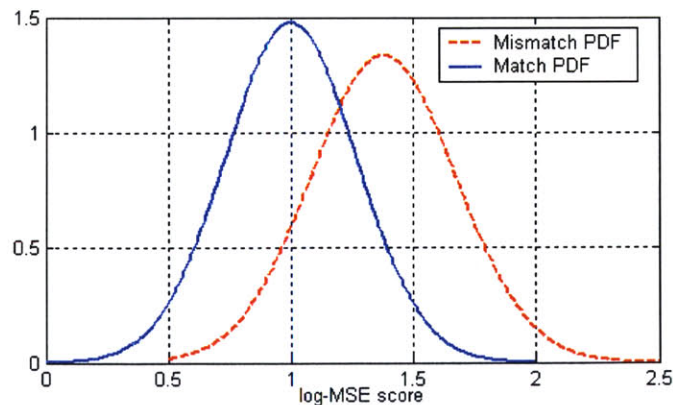
Figure 13. Match/Mismatch PDF's for SAT calculations

---

[*] target and report are of the same class

The statistical likelihood (probability density value) of receiving a given log-MSE score from a matching and mismatching target is then calculated using these curves:

$$MatchPDF = \frac{e^{-\frac{1}{2}\cdot\frac{(MSE-\mu_{match})^2}{\sigma^2_{match}}}}{\sqrt{2\pi\sigma^2_{match}}} \tag{25}$$

and

$$MismatchPDF = \frac{e^{-\frac{1}{2}\cdot\frac{(MSE-\mu_{mismatch})^2}{\sigma^2_{mismatch}}}}{\sqrt{2\pi\sigma^2_{mismatch}}} \tag{26}$$

1.5.2 χ^2 Adjustment

A χ^2-like quantity is computed using these values as a negative log-likelihood:

$$\chi^2{}_{SAT} = -\log(MatchPDF / MismatchPDF) \tag{27}$$

Figure 14 shows how, using the above PDF's, an MSE score will be translated into a χ^2 score:
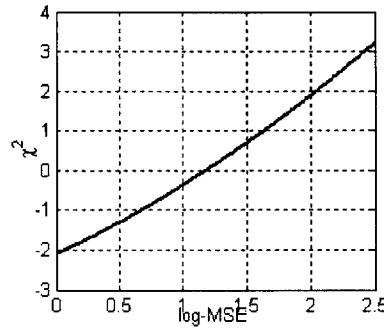
Figure 14. Translation of an MSE score into a $\chi^2{}_{SAT}$ score

Similar to CAT, $\chi^2{}_{SAT}$ is added to the initial kinematic χ^2 calculated for this track/report pair and adds another degree of freedom to the sum, known as $\chi^2{}_{fused}$. Normalization to two degrees of freedom must again take place (Section 1.3.2.3.). Another modification is necessary if any of these χ^2 -like scores force cells in the final fused association matrix to be less than zero. If this occurs, the entire association matrix is simply offset so that the minimum cell value (χ^2 score) in this matrix not less than zero. This normalization and offset was added to the software. If the kinematic tracker makes an incorrect association, the difference between the incorrect association's kinematic χ^2 and $\chi^2{}_{SAT}$ must exceed the difference between the correct association's kinematic χ^2 and $\chi^2{}_{SAT}$ for SAT to be effective.

Similarly, if both CAT and SAT are used, $\chi^2{}_{fused} = \chi^2{}_{CAT} + \chi^2{}_{SAT} + \chi^2$, two more degrees of freedom are added to the initial kinematic χ^2 score. Therefore, as above, if the kinematic tracker makes an incorrect association, the difference between the incorrect association's kinematic χ^2

31

and ($\chi^2_{CAT} + \chi^2_{SAT}$) must exceed the difference between the correct association's kinematic χ^2 and ($\chi^2_{CAT} + \chi^2_{SAT}$) for FAT to be effective.*

1.6 Aspect Angle Estimation

Recall that the aspect angle is the angle between a target's heading and the line of sight between the radar and the target. For all possible track/report associations, a target's heading is computed using the velocity vector output of the Kalman filter. The filter necessitates current detection information in addition to a track's Kalman filter. What requires emphasis here is not the specific calculations leading to this estimation, but the extraordinary dependence of both aspects of FAT (CAT and SAT) upon accurate aspect angle estimation.

During each scan, CAT uses *a priori* HRR information to analyze the probability that a given report is associated with a particular track. Every possible track-report pair provides CAT with an estimate of the current aspect angle of the target given the associated track history. Profiles are then retrieved from all classes in the database from aspect angles within the aforementioned ten-degree error "window". The assumption is made that a "match" in HRR will be found among the collection of profiles and the report will be classified correctly if the hypothesized track-report association is true. Consider a correct track/report pair with an aspect angle of 50°. When CAT compares this report HRR against a profile from the same target class at 50°, a "match" will be found and the correct classification will occur. However, noisy measurements lead to a radar report position approximately 10 meters from the true target position and the Kalman filter consequently estimates the aspect angle at 61°. CAT will then only analyze template profiles between 51° and 71° of aspect angle. Since the true profile originates from a target at a 50° aspect angle, the "matching" profile will not be found. We must then rely on a result where the minimum MSE score obtained in this manner is less than the minimum MSE score obtained by comparing the report HRR against numerous profiles from all other target classes. This will most likely not occur for more extreme cases of aspect angle estimation error. Research will show for targets undergoing maneuvers (turning; not constant velocity straight line), the aspect angle error is typically greater than ten degrees. If true, the performance of the previously described version of CAT is severely degraded, leading to an increased rate of incorrect associations.

SAT is similarly dependent upon accurate aspect angle estimation. At the end of each scan, a report HRR profile is stored in the associated track's history with the corresponding estimated aspect angle. During the following scan, an estimate of the aspect angle is generated for all possible track/report pairs. If the difference between this estimate and the track aspect angle is less than ten degrees, SAT is allowed to proceed. If not, the signature information is thrown aside and full dependence on the kinematic tracker exists. Consider a case where one target is traveling in a straight line and the true aspect angle remains approximately 30° for the duration of the scenario. Due to noisy radar detections, the current report position is 20 meters from the track's last stored position. If the stored estimated aspect angle is 26° and the new estimated angle is 36.1°, SAT is not used in spite of a truly constant aspect angle. If the generation of a database containing SAT moving-target HRR profiles were desired, the profiles would be stored and extracted according to aspect angle. If the estimated aspect angle error is

---

* further work with SAT has been accomplished by Duy Nguyen using pattern matching techniques with SAR and ISAR images in [1]. Due to ease of implementation and data limitations, this report focuses solely on the use of 1-D HRR profiles with both SAT and CAT

above a given threshold (assumed ten degree error), the profiles will be stored incorrectly and computations will be performed on incorrectly extracted profiles.

It is hypothesized and will be proven that aspect angle error is the single most significant inhibitor for this feature-aided-tracking system. It is an obvious but necessary statement that the aforementioned error and the effects of this error are dependent upon the level of noise associated with radar detections (which also depend on target range). Accurate tracking in the face of noisy radar measurements will occur only if:

(1) Aspect Angle error is minimized, and
(2) Aspect Angle error is quantified and understood.

This report will seek to achieve the above.

1.7 Research Goals

This section will serve to explain the contents of the remainder of this report. The motivation of this research is dual-faceted:

I) My first task is to assist Lincoln Lab in achieving a higher level of understanding concerning the current Lincoln Laboratory Feature-Aided-Tracking code. A robust simulation tool should be developed that is able to easily ingest and utilize a variety of target and radar information. The code should be well documented, intuitive, and easily operated. Simulations occurring within this code should be based upon know radar and tracking principles making for a realistic operating environment. Basically, my goal was to create an inter-operable testbed for FAT, possibly to be used within a greater testbed (Space-based radar program). Overall, the main task was to **modify pre-existing Lincoln Lab MATLAB FAT simulation software and create a robust, accurate, and intuitive simulation tool**.

II) The second, more flexible set of goals has more of an academic motivation. It hinges upon accurate and full comprehension of the FAT system and software. Mainly, this research strives to analyze and enhance the performance of the existing FAT software in the three aforementioned influential areas:

1) **Kinematic Tracking**
   – Analyze the use of a constant velocity, two-state, "2-D" Kalman filter and explore other options.
   – Improve State and Aspect Angle estimation through possibilities such as curve fitting
   – Analyze and improve maneuver detection.
   – Quantify expected aspect angle estimation error
2) **SAT**
   – Analyze the performance of the current SAT algorithm
   – Explore the use of an On-The-Fly SAT HRR Template Database
   – Ideally utilize real or simulated moving-target HRR profiles
3) **CAT**
   – Analyze the performance of the current CAT algorithm
   – Explore the ramifications of increasing the aspect angle error "window"
   – Ideally utilize real or simulated moving-target HRR profiles

CHAPTER 2.

SOFTWARE ADJUSTMENTS/UTILIZATION

2.1 Initial Code Review – LL Integrated-Radar-Tracker (IRT) Application Code

The software received, analyzed, and adjusted throughout research is an appended version of the original Lincoln Lab UAV tracker developed and tested in 1991 by Keith Sisterson [2]. This code was verified through testing in simulated and realistic environments. Error distributions from the realistic test data were found to be close to normal, validating the use of the χ^2 testing technique and Kalman filter to smooth the noise inherent to measurement detections. This code was written and developed using "C".

Duy Nguyen appended this original kinematic tracker from 1999-2002 with his own feature-aided-tracker software [1] described above. This code was also originally written in "C" with select functions written in MATLAB. Initially, the code was strictly designed for use with 1-D HRR profiles. This version of the FAT code is the one that is utilized and analyzed in this report. [1] states that SAT, in the above form, cannot provide valuable assistance to the data association problem using only HRR profiles. Accordingly, SAR (synthetic aperture array) and ISAR (inverse SAR) imaging technology have been shown to improve the performance of SAT. SAR and ISAR are less sensitive to aspect angle change, thus mitigating the problem of aspect angle dependence. A move-stop-move scenario can exploit SAR technology when it is detected that the target has stopped, leading to more accurate data association. Specifically, a SAR image is taken when targets are stopped, and can further be used to compare a 2-D radar image against future 1-D HRR profiles whose aspect separation exceeds the HRR aspect angle threshold through simple rotation and projection procedures. The match and mismatch PDF's from such comparisons exhibit a higher degree of separation than those mentioned above from comparisons involving 1-D HRR profiles leading to more valuable comparisons. These images can be used to dynamically generate and utilize HRR profiles throughout a tracking scenario. However, the prediction of ISAR opportunities depends upon knowledge of the terrain and road patterns. Moreover, at 20 dB SNR (the SNR for the HRR profiles) the separation between the PDF's is significantly reduced when using SAR technology.

As previously mentioned, this work focuses solely on the use of less-complex 1-D HRR profiles. The data and code utilized in the above studies were not easily obtained or utilized. Furthermore, the code used below was meant to resemble a robust, realistic system with minimal resources and maximal environmental stress (error/scenario difficulty). All previous research by Lincoln Lab Group 104 (Intelligence, Surveillance, Reconnaissance) in this discipline used the MSTAR data set for analysis. Conversely, all work analyzed in this report is original; new, stressful scenarios have been utilized in conjunction with the untested MTFP data set. The use and study of MTFP data will both verify previous performance evaluation and present unique opportunities for simple algorithm enhancement.

Initially, a MATLAB conversion of Duy Nguyen's original (HRR) code was obtained from Bill Coate [7] in Group 102 (Embedded Digital Systems) at Lincoln Lab. This code was only recently translated and verified for use in the Integrated Radar-Tracker Application for the DARPA/IPTO PCA Program. Due to familiarity and ease of compatibility, it was strongly desired to make this MATLAB code into the base for further research.

Numerous differences exist between the Group 102 MATLAB code and the code utilized by both Keith Sisterson and Duy Nguyen. Group 102 has aimed to design code that stresses

hardware, throughput requirements, and software engineering principles as opposed to the "robustness" of the tracker. For example, fake target HRR profiles are generated and used in combination with a non-moving radar platform and a 2-dimensional scenario environment to ease computations. Error statistics and parameters are perfectly adjusted to obtain the desired results. It is code explicitly used for "proof of concept". It utilizes parallelism ("MATLAB mpi") to maximize computational efficiency and will be released to a broader audience. Most of the findings below require significantly more exhaustive analysis. Again, the research below clearly does not focus on computational efficiency but more so on robustness and realism.

2.2 Code Changes

2.2.1 Minor Code Changes
There have been frequent adjustments and additions to the Group 102 MATLAB code in order to achieve the desired level of realism and robustness. These changes have been both minor and major in nature. Most importantly, there has been direct communication between Group 102 and Group 104 through the duration of this research. Essentially, Group 102's software has been tested with real (or more-realistic) data in a robust simulation tool during studies outlined within this document. Dialogue has been continuous as minor corrections and bug fixes are recommended.

One minor change is the parameterization of grazing angle (depression angle) of the radar platform for use with a larger database. HRR profiles are distinct across grazing angle in addition to aspect angle. During statistics training and CAT, profiles are extracted from the template database according to this parameter. Currently, grazing angle also geometrically restricts the simulated position of the radar platform.[*] Also of concern to FAT, the aspect angle threshold alluded to in Sections 1.5 and 1.6, which determines whether or not SAT can be used, was added to the MATLAB version of FAT. The authenticity of this system is thus significantly increased.

A final change for future versions of FAT would include a grazing that is calculated on every scan as radar platform position and target position varies. Ideally, the grazing angle calculated in this manner should be used to extract profiles available in the database from angles closest to that. Some of the other minor changes have already been mentioned, such as the adjustment to the HRR generation code and the GPS data conversion code.

2.2.2 GMTI Simulator
This is the most significant addition to the base MATLAB code. This function utilizes known radar principles to develop noisy radar detections based upon given parameters. The GMTI (Ground-Moving-Target-Indicator) radar simulator takes the aforementioned GPS truth data in Cartesian coordinates and outputs a radar detection (report) consisting of range, azimuth, Doppler, and HRR profile subject to sensor measurement error. A parameter exists in the current software to activate this error generation.

2.2.2.1 Radar Parameters Used
Recall that the fundamental motivation for this research was to provide a realistic simulation tool. Therefore, most of the radar parameters used in this simulation are based upon known parameters tuned to current military aircraft and radar systems. Specifically, this function

---

[*] This is due to the fact that the Database does not contain profiles from a large range of grazing angles

attempts to simulate the operating environment and capabilities of the U.S. Air Force JSTARS (Joint Surveillance Target Attack Radar System) surveillance aircraft. From *Jane's electronic aircraft*, the aircraft's primary sensor is the Northrop Grumman AN/APY-3 multimode, electronically/mechanically steered, side-looking, combined MTI and SAR. Currently, MTI radars are not capable of simultaneously detecting a moving target and forming an HRR profile. First, low-resolution GMTI radar is used to identify moving ground targets above a minimum detectable velocity (MDV). The bandwidth of these radars is typically on the order of 15 MHz. Subsequently, higher resolution radar is pointed in the direction of the apparent target and an HRR profile is formed. This study involves 1-meter resolution HRR profiles, requiring a bandwidth on the order of 150 MHz.[*] Most of the following parameters are used to compute measurement error and not HRR profiles, thus they are tuned to simulate the low-resolution GMTI radar. Some of the parameters obtained for JSTARS are classified. However, the numbers below are either unclassified known parameters or arbitrary nominal values. The true parameters will increase the performance of the MTI radar due to decreased theoretical values used to compute measurement error:

Figure 15. Air Force JSTARS Ground Target Surveillance Aircraft

Geometric Data:
1) Radar Platform Height = 10668 m. JSTARS operating altitude (35,000 ft). The combination in this simulator of a fixed platform height and grazing angle currently restrict the range at which the platform operates. A larger range increases the measurement error (the reason why specifications for the Global Hawk UAV were not used: operating altitude of 19,000 meters).
2) Grazing (Depression) Angle = 8°. Used because it is the angle at which the most MTFP HRR data was available.
3) Radar Platform Velocity. Given in Cartesian coordinates with no assumed z-direction component. For JSTARS, typical orbit speed is between 200 and 260 m/s (390 and 510 knots).

Bob Coury of Group 104 has developed MATLAB code that utilizes the following radar parameters to determine the expected SNR (Signal-to-Noise Ratio) needed for effective moving target indication [6, p. 146]. This SNR plays a large role in theoretical measurement error calculations:
4) P_d (probability of detection) = 0.90. This corresponds to a rate of detection of 90%. This is a typical value used to define the probability that a given target will be detected under given conditions at a given range on any one scan of the antenna. Duy Nguyen also uses this value in

---

[*] from $\Delta R(resolution) = \dfrac{c}{2B_w}$ where c = speed of light

36

similar studies. In addition to being used in SNR calculations, this principle is included in the code. It would correspond to 90% of the target reports generated being thrown away or "not detected". There is also a parameter to turn this feature on and off; for tests below this feature is off.

5) P_{fa} (probability of false alarm) = 1×10^{-5}. This is solely used in SNR calculations. A typical value for this parameter is between 1×10^{-6} and 1×10^{-4}. It represents the probability of an incorrect detection being recognized by a single target-detection threshold detector at the conclusion of any single integration time for the Doppler filter whose output the detector is processing [4]. This has been arbitrarily chosen.

6) # of CPI's (Coherent processing interval's) = 5. This number is largely arbitrary as well; any integer value could be used. As you decrease the number of CPI's, the SNR needed to detect targets with the same P_d and P_{fa} increases and you have less information about the target. This number can be tuned for use with any particular system and should be a function of system requirements.

7) Swerling Type = 1. This is a number representing a particular type of mathematical target model that can vary a probability of detection curve. This is a suggested number for ground moving targets.

The following radar parameters are later used to calculate measurement error variance:

8) β (Bandwidth) = 15 MHz. This is simply a nominal value chosen to represent the typical bandwidth for X-band MTI radars, the most commonly used tracking radars. This parameter has a large affect on range error.

9) f_c (center frequency) = 10 GHz. The JSTARS center frequency is typically between 8-10 GHz. A typical X-band tracking radar center frequency is 8-12 GHz. This is close to the center frequency for the DCS sensor used in obtaining MTFP data (9.6 GHz).

10) λ = c (speed of light) /f_c = 3 cm. Dependent upon f_c. Typical of an X-band radar (between 2.5 and 4 cm).

11) T = .1 s. This is the length of a CPI. This value is taken as a nominal value and can be changed to fit system requirements. The true value for JSTARS is known but classified. This has a large affect on Doppler error, the least influential of error sources.

12) D (radar aperture diameter) = 7.31 m. JSTARS value (24 ft). This has a large affect on azimuth error.

The most important step in the development of a sensor model for this simulation is accurately modeling error in each measurement. This measurement error is the reason that a Kalman filter is utilized and aspect angle estimation error occurs, strongly influencing system performance. From Section 1.3.3, the measurement equation is written as

$$z_k = H_k x_k + noise$$

It is assumed and has been proven [2] that these errors, or *noise*, are zero-mean white Gaussian processes. The theoretical standard deviations for these Gaussian processes can be set based on the above sensor and signal processing characteristics. The following equations are taken from [8, p. 47]:

$$\sigma_r = \frac{c}{4\beta\sqrt{SNR}} = 0.892 \text{ m} \qquad (28)$$

$$\sigma_\theta = \frac{\lambda}{2D\sqrt{SNR}} = .366 \text{ mrad} \qquad (29)$$

$$\sigma_{\&} = \frac{\lambda}{4T\sqrt{SNR}} = 0.0134 \text{ m/s} \qquad (30)$$

The MTI simulator uses this information to add Gaussian noise to the true values for Range, Range Rate (Doppler), and Azimuth. Below is a visual example of a straight-line constant velocity scenario with added noise according to the above parameters. The dots are the true target positions while the +'s are the detected target positions:
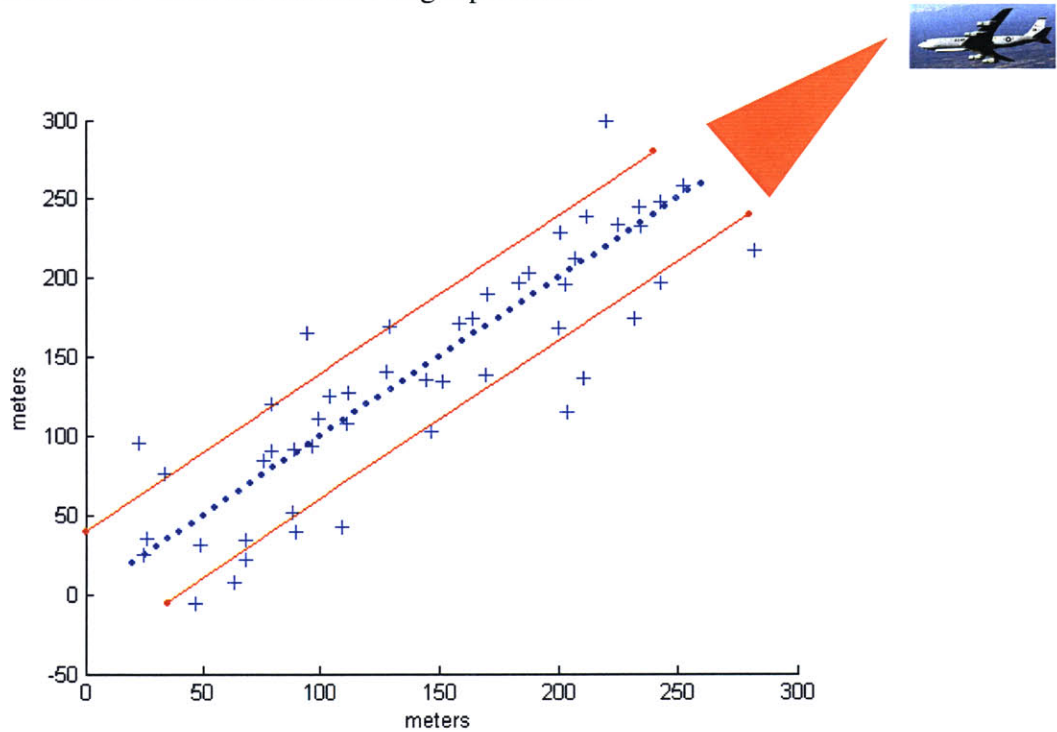
Figure 16. Example of added measurement error in Cartesian coordinate plane.

In this case the radar platform is located at [53 km, 53 km] as shown above, leading to a range of approximately $R = 76$ km. At this range, the σ_θ of .366 mrad translates to the expectation that 68% (1 standard deviation) of the measurements will have an error less than R x $\sigma_\theta = 28$ meters. The solid red line above indicates this threshold. By further examination, one can notice that there are the expected 34 detections (68%) within these bounds. Additionally, the error is about $1/10^{\text{th}}$ of the beamwidth $R \times \theta_{3dB} = R \times .88\frac{\lambda}{D} = 273 \text{ m}$. Once this measurement error has been validated, the Kalman filter is used to smooth this noise. All research and analysis below implements this MTI error simulator and utilized the parameters as the constants outlined above. More error (higher variances, lower P_d, higher MDV, longer R) places more stress on the tracker.

Again, the purpose of this tracking system is to be able to mitigate the effects of this noise in a realistic situation through the use of FAT.

2.2.3 Scenario Generation and Tracking Parameters

The scenario generating function is used to create the ground truth position and velocity data for all targets in the form of a pre-generated *Targets* matrix (# of scans × [x $\dot{x}$ y $\dot{y}$] × # of targets). The GPS data depicted in Section 1.2.2 forms a base for generating multiple kinematically challenging scenarios. As mentioned earlier, a text file is converted into MATLAB position and velocity data. Furthermore, scenarios may be manually created by cropping the GPS data or simply mathematically generating the *Targets* matrix.

Following the addition of measurement error, the complete formation of the detection occurs when the radar report is augmented with an HRR profile. Currently, the true aspect angle of each target is calculated and the corresponding profile is extracted from its template database. The use of this non-moving HRR profile as a moving-target profile is rationalized in Section 2.3. When data analysis and track-report association occurs, the following parameters essential components of the tracking system:

1) Number of Classes, Class ID #'s - Typically 1 or 2 but can range as high as 100. All analysis done below uses the most kinematically challenging two-target scenarios. Target type is specified by an identification number obtained from the detection augmentation function (*TestMeas* or *GetFakeHRR*). This ID # is used to extract the correct template database file.

2) Number of Other Classes, other ID # – Specify the number of "*other*" classes to be used in the Statistics training function (typically 4).

3) Scenario Total Time – Preset, or set during the Scenario Generation function as the length of the GPS history available.

4) GPS Scan Time – This is essentially the scan update time, dt. It will use this to extract the proper cells from the *Targets* matrix in the Scenario Generator and will also be used in the Kalman filter.

5) MaxSpeed = 30 m/s and MaxAccel = 10 m/s^2 – This is used to constrain association possibilities. It is the maximum expected speed and acceleration for the targets being analyzed. It is important to have correct values, especially for MaxAccel. If not, correct associations may be labeled as 'impossible' by the criterion in Section 1.3.2.2.

6) NewLimit =1, NoviceLimit = 2, Established Limit = 3 – This parameter describes the limit for the number of scans that may pass without a detection before the specified type of track is removed.

7) Grid Size – The total grid size and grid element size are important pre-set parameters. As previously mentioned, the tracker will only perform calculations on measurements with tracks in the same or adjacent grid elements.

8) Platform Position and Velocity – This is currently parameterized and should eventually be input to the system as a matrix similar to the *Targets* matrix with different information for every scan.

9) DeAlias Speed – As discussed in Section 1.3.2.1; defined as the velocity value of the PRF:

$$DeAlias(m/s) = \frac{PRF}{2 \cdot f_c} \cdot c$$. For efficient processing, it is recommended that the DeAlias value

be above the max speed. This is the case in most tracking simulation tools so as to avoid Doppler ambiguous situations.

10) CVHLimit = 9.82, LatHLimit = 7.83, ArcHLimit = 7.83. These are the limits of the χ^2 for the acceptance of constant velocity, Linear Acceleration, and Arc-of-Circle hypothesis. These values were taken from [1], but have not been verified for this research.

11) Cvsq = 9.82, latsq = 7.83, arcsq = 7.83. These are the vales for q, used in the formation of the plant noise matrix in the Kalman filter. These parameters will play a small role in hypothesis testing. They are taken from [1] but have not been verified.

2.2.4 Statistics Generation/Analysis Tools

The statistics necessary for proper functioning of CAT and SAT are generated prior to the operation of the tracker. This statistics generation function has been adjusted to return all necessary and available information from numerous HRR signature comparisons.

As explained in Section 1.5.1, the expected Match and Mismatch mean MSE score and their variances (μ_{match}, $\mu_{mismatch}$, σ^2_{match}, $\sigma^2_{mismatch}$) are calculated for use in SAT. A comparison is made between a "test" profile of one target and other template profiles of both the same (Match statistics) and different (Mismatch statistics) targets. CAT (explained in Section 1.4.1) necessitates the mean and variance of MSE scores used to form the MSE vectors. Again, this vector is formed by comparing a test profile of one target at a particular aspect angle against a group of profiles from the templates of all other targets within a parameterized aspect angle "error window".

An extensive test has been completed in which statistics were generated while testing every single available MTFP profile for a grazing angle of 8°. This is a total of approximately 2600 HRR profiles tested in order to generate the most accurate statistics possible. Specifically, the statistics generation function performs MSE comparisons using every one of these profiles as a test profile against all other profiles within 50 degrees of aspect angle of the test profile aspect angle. This produced over 6.5 million MSE comparisons. Every single comparison returned the following information:

(1) aspect angle of the test profile

(2) target class of the test profile

(3) aspect angle of the template profiles

(4) target class of the template profiles

(5) resulting MSE scores

(6) difference between the aspect angles of the test profile and template profile

(2), (4), (5), and (6) are used to compute Match and Mismatch statistics for SAT. Statistics are generated for all integer values of (6), which corresponds to 1-50°. Typically, match and mismatch statistics are computed disregarding the sector of the test profile but have included sector information in the tests below. Remember that the expected values for MSE Vectors used in CAT are generated by comparing each "test profile" from the database from one class in one sector against every template profile within 50 degrees of aspect angle in every class. The resulting MSE scores from this test are organized in a way such that knowledge of (5) and (6), will lead one to compute the expected MSE vectors for any error window between 0-50°. Lastly, the function used in CAT to compute the MSE score now returns all MSE scores and corresponding aspect angles to evaluate if the minimum MSE score came from the appropriate template profile aspect angle.

Multiple MATLAB Performance Analysis Tools are available to better evaluate every successive "run" of the tracker.* The functions *CATGenerate* and *SATGenerate* allow the user to form MSE Vectors and match/mismatch statistics while specifying a desired error window(s)/threshold(s). Moreover, it allows the user to select the ID # of the specific targets to

---

* one "run" is described as when targets are tracked from the beginning to the end of one scenario

be used in statistics generation. With CAT, these will be specific to the scenario. The user may also plot and view these results. The function *DisplayEndOfRun*, in multiple-run sessions, can analyze and/or average any type of information returned from any point in a session or run (i.e. the number of missassociations per run).

2.3 Data Usage (Concerns)

There is one main concern with the research below at this point. Section 2.2.3 briefly mentions how each "moving-target" MTI detection is augmented with an HRR profile. Currently this HRR profile is not a moving-target profile, but a profile from the non-moving template database formed from SAR images. Therefore, a problem arises when pattern matching is performed on a non-moving profile from a radar detection (should be a moving profile) and a group of non-moving profiles from the template database. If an exact match is found as expected in CAT, the log MSE score is negative. The results will not be similar to those expected in an entirely real system/scenario where radar detections are augmented with moving-target HRR profiles that should be noisy versions of the non-moving template profiles. This is a concern both within MSE Vector formation in CAT and similar "group" MSE comparisons in a SAT database (Section 5.3).

The temporary solution is that the minimum MSE score, which could be an exact match, is not used in these "group" comparisons. Instead, the second-lowest score is used, resulting in the guarantee that an exact match and thus a "too negative" MSE score will never occur. With this method, the resulting MSE scores are as expected and mimic those of a more realistic simulation, albeit the way in which they are obtained is unrealistic.

The only permanent solution would be to obtain real or simulated moving-target HRR profiles. I have explored these options extensively and there is no real unclassified moving-target HRR data that could have been easily acquired and/or utilized. However, contact has been made with the Submillimeter-Wave Technology Lab at UMass-Lowell, who has simulated moving-target HRR's in the past. They have radiated scaled target models provided by the National Ground Intelligence Center in order to obtain HRR and other radar signatures at 360° of aspect angle coverage. However, the bottom line is that the results from research on CAT and SAT available to this point, while not entirely accurate numerically, do reflect important trends and results that are expected to occur with real moving-target HRR profiles as well.

CHAPTER 3.

KINEMATIC TRACKING/ESTIMATION

3.1 Kalman Filter Performance

The noise inherent in radar detections is assumed to be Gaussian, hence legitimizing the use of the Kalman filter to dampen the effects of this noise and produce "smoothed" detections. This smoothing effect is demonstrated below.
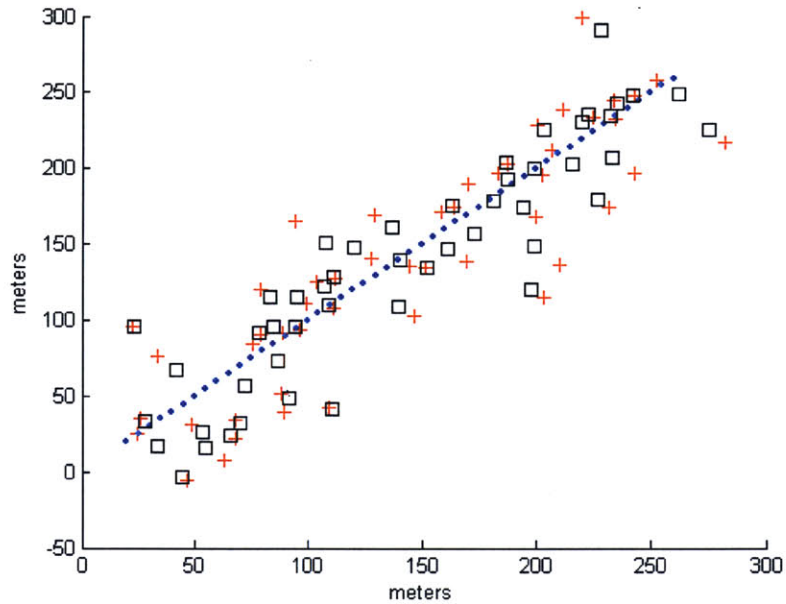
Figure 17. Kalman filter "smoothing" (• ground truth, + noisy detections, Kalman filter output) in Cartesian coordinate plane: x (meters) and y (meters)

As evidenced above in Figure 17 (and leftmost plot below), the majority of Kalman filter position estimates are closer to the ground truth position than are the radar detections. However, the intensity of this smoothing effect depends upon scan update time (*dt*) and the speed of the target. As you increase *dt* and/or target speed, the PDF associated with the expected target position in state space widens thus increasing the allowable position error. The Kalman filter then assumes that the noisy detections are closer to the position mean, eventually leading to the acceptance of the detection as true position. Consequently, the estimate is barely smoothed at all (see rightmost plots below).
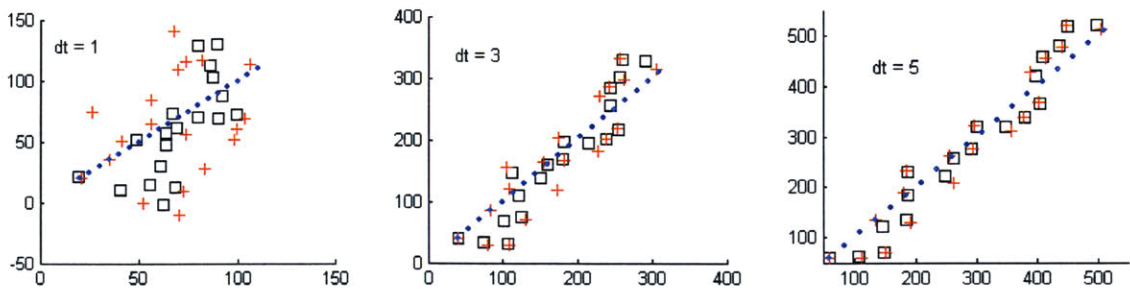
Figure 18. The effect of Kalman filter on various scan update times (dt) for a target traveling at 10 m/s in Cartesian coordinate plane: x (meters) and y (meters)
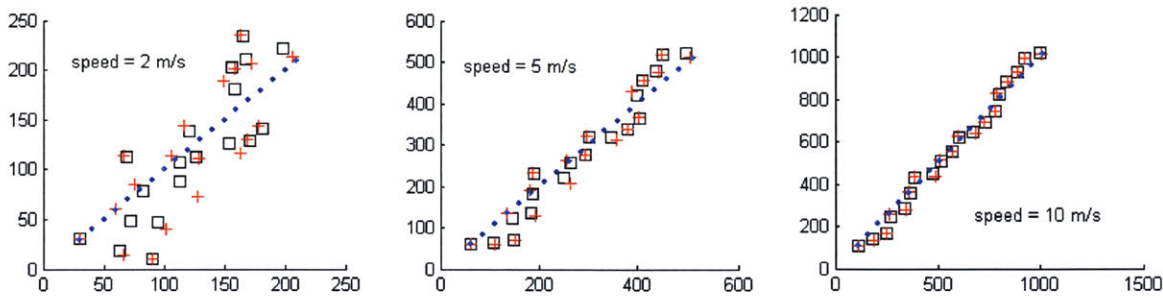
Figure 19. The effect of Kalman filter on various target speeds with a scan update time of 5 s in Cartesian coordinate plane: x (meters) and y (meters)

Figures 18 and 19 show that the Kalman filter is ineffective as both speed and scan update time increase. Current tracking systems typically operate at an optimal scan update time between 3-5 seconds. Additionally, the ground targets of interest typically have a cruising speed above 10 m/s. Therefore, the Kalman filter provides minimal mitigation of the noise inherent to radar measurements within some of the scenarios tested below. When target maneuvers are expected to occur, it is recommended that $dt < \tau_m$ where τ_m is the maneuver time constant (time to complete 66% of the maneuver). Typically, the τ_m used in the scenarios generated for this study are less than 5s, again proving that the effectiveness of the filter depends upon both the scenario and target dynamics, and forcing the use of a smaller dt for the purpose of analysis. Regardless, the Kalman filter will still minimize the mean squared error as long as the target dynamics and noise are modeled correctly. It additionally provides the following advantages [9]:

1) Different target types and environments can be modeled differently by simply changing a few key parameters. For example, in this code, the various target maneuvers are modeled using the parameter q in the plant noise matrix.
2) The Kalman filter also models range-dependent target dynamics well. Clearly, as target range increases, the target angular dynamics (expected error) changes. The Kalman filter is equipped to mitigate these situations.
3) The filter is highly adaptable: The sampling interval (scan update time) is easily adjustable and can handle missed detections.
4) It provides a measure of estimation accuracy through the covariance matrix, which is useful for maneuver detection.
5) Recursive estimation is used, meaning that only the target history and covariance matrices from the previous scan are used in state estimation.

3.2 Aspect Angle Estimation Enhancement

3.2.1 Filtering Options

The Kalman filter velocity output and thus aspect angle estimation is the most important calculation in this tracking system. Therefore, an improvement in Kalman filter performance would have a direct impact upon overall tracker performance. Much of the following is the summary of [6, p.193]; a comparison of a variety of filtering methods. This information was used to decide how research (track filtering, in particular) should proceed.

As stated in Section 1.3.3, this kinematic tracker uses a white noise constant velocity (CV) dynamic model. Random target dynamics (target acceleration, i.e. maneuvers) are taken to enter

the system as white noise. The Q matrix is where this uncertainty is modeled. The results from this form of modeling are no different than if a constant acceleration (CA) target model were used. The CA filter models the time-derivative of the target acceleration as white noise, resulting in a dissimilar Q matrix (size and cell values). The selection of q for the formation of this matrix is a process best performed by simulating expected target trajectories against the tracking filter and adjusting parameters to minimize some error criteria. This study has been performed in the past with this tracker and the q values used were determined in this manner.

Another alternative is the Singer Acceleration model, which assumes the target acceleration (used in addition to position and velocity as a state) to be a first-order process. The state transition matrix differs as does the Q matrix. The use of an acceleration state is only of value when a velocity measurement is available. With a measurement of position alone (as in this simulation environment), an accurate estimate of acceleration can only be provided when $10dt \gtrsim \tau_m$. The results comparing the CV and CA filters with the Singer model showed little difference despite the Singer model being matched to actual target dynamics.

Coordinated turn models are also available when velocity measurements are present. They model the rate of change of the acceleration vector in terms of turn rate, velocity vector, and white noise. This filter is typically used to model turning aircraft. One of these methods is the nearly constant speed horizontal turn (HT) model, which directly uses target speed as a filter state. The nearly constant speed constraint assumed for a coordinated turn is introduced using a small value for the process noise entering the system through the speed state.

The choice of which filter models to use in a tracking system depends upon the types of maneuvers expected. However, the various filters can be effectively used simultaneously in maneuver adaptive filtering. The most popular and promising of these is the Interacting Multiple Model (IMM) approach. The state estimates and covariance matrices from the multiple target maneuver models are combined for the transition between target maneuver states. This approach considers maneuver transition probabilities (probability that a target will transition to a maneuver or remain in its current state). Using the transition properties, state estimates and covariance matrices are computed by "mixing" the numerous filter outputs for the various maneuver possibilities. This process is similar to the classification inherent to CAT with its dependence upon Bayes' decision rule.

A comparative performance study on various filtering methods was executed and outlined in [6, p232]. Included in this analysis were the CV model, Singer model, adaptive Singer model, HT model, and IMM (using CV, Singer, and HT). The kinematic tracker error results were given by RMS (root mean squared) prediction error defined in terms of mean and variance of the error. The CV filter generally outperforms the Singer filter while the large speed error and slower recovery time hampered the Singer filter performance. The Maneuver Adaptive Singer filter has a large peak error despite having better smoothing and recovery effects. Meanwhile, the IMM filter gives the best overall performance, however recovery after maneuver may be slow at some points depending upon the scenario/maneuver tested. The ability of this method to maintain the correct velocity through turns was significantly better than other methods. While more complex, the IMM was consistently the superior performer in this study during both periods of maneuver and non-maneuver. However, for its level of complexity, the CV filter did not perform badly relative to its counterparts. Due to implementation and time constraints, the decision was made to continue analysis of the Lincoln Lab tracker using a CV filter. While the IMM filter did appear to provide an advantage, this advantage was not large enough to warrant the transition to an IMM approach, as this would basically be considered creating a new tracker.

44

3.2.2 Curve-Fitting

In addition to altering the type of filter used, an attempt was made to utilize the position outputs of the Kalman filter for curve fitting in an aspect angle estimation algorithm. A history of these positions (of length k) for each track was stored after each scan; k is a pre-set parameter. The MATLAB functions *polyfit* and *polyval* are used to perform these operations:

```
POLYFIT(X,Y,N) finds the coefficients of a polynomial P(X)
of degree N that fits the data, P(X(I))~=Y(I), in a least-
squares sense.

[P,S] = POLYFIT(X,Y,N) returns the polynomial coefficients
P and a structure S for use with POLYVAL to obtain error
estimates on predictions.
```

Polyfit was used twice to calculate Px, Sx and Py, Sy. Both times, the "X" used in the function call above was the sequence of integers from 1 to k. When Px and Sx are calculated, "Y" is the track history x-coordinates. When Py and Sy are calculated, "Y" is the track history y-coordinates. Next, *polyval* was used twice:

```
Y = POLYVAL(P,X), when P is a vector of length N+1 whose
elements are the coefficients of a polynomial, is the value
of the polynomial evaluated at X.
```

"x2" and "y2" were calculated to be "Y" in the above function definition. "P" was Px and Py respectively, while "X" was a number sequence from 1 to k, incremented by a small amount from above in both cases. The technique of using the number sequence twice within *polyfit* ensures that each set of position history coordinates (x, y) is followed by the resulting line chronologically. Finally, "x2" and "y2" are the x and y coordinates of the new best-fit curve.

The order, N, of each "x" and "y" calculation involving in the above curve-fitting was determined by visually evaluating the resulting curve fit for $k = 4$ data points meant to represent a turning target; the situation that line fitting is needed most for. This test is shown in Figure 20 below where the numbers in the legend refer to the order, N, of the "Px" calculations and the "Py" calculations, respectively. It was determined that a second order curve-fit for both coordinates (case 2,2) best represents a true target path and would therefore provide the most accurate estimation of aspect angle in this, and similar situations.

45
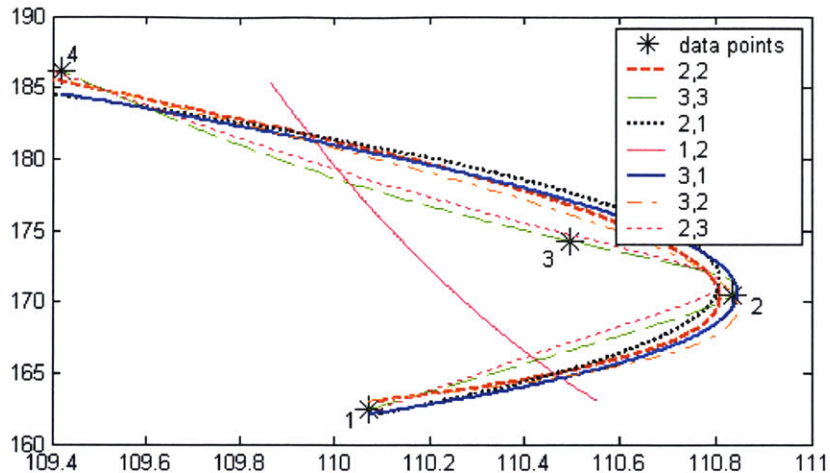
Figure 20. Test to determine order, N, of line fitting operations.
[Cartesian coordinate plane: x (meters) and y (meters)]

Once curve fitting is performed on k data points, an estimate of the aspect angle is calculated. As mentioned above, the final result of this fitting operation is a set of coordinates, "x2" and "y2" (incremented by .01), that represent the best fit curve. There are 100 points on this curve between each data point. Therefore, the slope of this line and thus a velocity vector in both directions is calculated using the difference in x and y position between points on this curve.

The point on the curve at which the velocity vector and aspect angle are calculated is a chief concern. Initially, calculations occurred at the point on the curve closest to the actual data point in question (current radar measurement). However, it was discovered that due to the method that MATLAB performs line-fitting operations, the velocity vector at this point is not close to what is expected. Therefore, tests have been performed that compute aspect angle at various "delay points" along this line. The "delay" number represents a point on this curve going back in time. For example, using scenario in Figure 20, if an aspect angle were calculated for a delay of 50, it would correspond to a calculation point halfway between point 4 and 3. If the delay were 0, the calculations would occur at point 4, if 100, point 3, if 200, point 2, etc.

A multitude of tests have occurred which evaluate the effectiveness of this curve-fitting aspect angle estimation algorithm. The history size, scenario type, and maneuver type have all been varied. The scan update time remains one second in order to evaluate more data points in a best-case scenario. A full run of the kinematic tracking algorithm is performed, with the track position history saved at each point. After each scan, the true aspect angle and Kalman filter estimated aspect angle are calculated and stored. Additionally, a curve-fitting estimate of aspect angle is calculated using the above algorithm. Both estimates (Kalman and curve-fitting) of aspect angle are compared with the true aspect angle and a mean and standard deviation of the resulting aspect angle estimation error throughout the scenario is plotted below. The x-axis represents the delay number. The Kalman filter aspect angle estimation error (red *) remains constant as delay differs. The curve-fitting error is represented by blue +'s.

3.2.2.1 Straight-Line Constant-Velocity Scenario

Figure 21 shows the results from a straight-line, constant velocity scenario involving 100 target detections with one target traveling at 10 m/s at a scan update time of 1 second with

46

varying *k*. In a constant velocity scenario, it is hypothesized that increasing history time, *k*, will improve the results (lower the mean aspect angle error) of curve fitting because more data points exist that lie closer to the target ground truth (straight line):
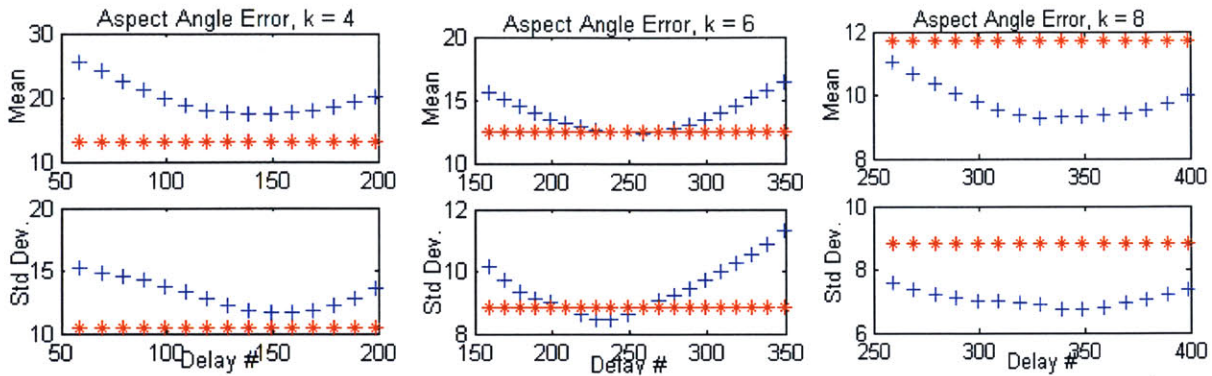
Figure 21. Aspect angle error estimate comparison while varying history size, k. (Red * – Kalman estimate, Blue + - curve-fitting)

Figure 22 shows the results from a straight-line, constant velocity scenario involving 100 target detections with one target traveling at 10 m/s with a history size of 6 with a varying *dt*. In a similar fashion, an increased scan update time should improve the results because the detections are more spread in space and thus better resemble a straight line:
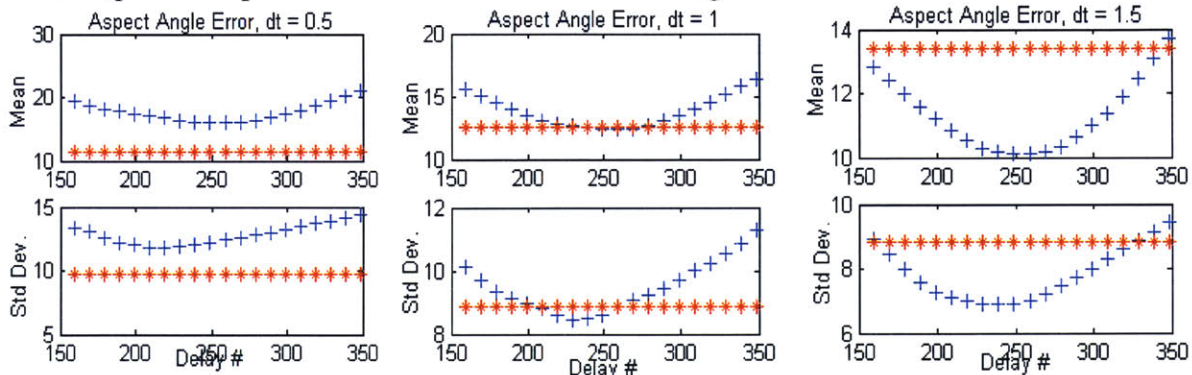
Figure 22. Aspect angle error estimate comparisons while varying scan update time, dt. (Red * – Kalman estimate, Blue + - curve-fitting)

A number of the above tests occurred. The velocity of the target was also varied as both 10 m/s and 5 m/s to form tables 1 and 2 below. Visually, the use of curve fitting starts to become advantageous when the minimum of the blue (+) curve initially reaches below the red (*) line as in the middle plot in Figures 21 and 22. Any *k* and *dt* above the values used at this point should push the minimum mean error from curve-fitting below the mean error from the Kalman filter:

Effective k>	Effective dt>	Optimal Delay	Optimal Delay/k
4	1.8	150	37.5
5	1.2	200	40
6	1.0	250	41.7
7	0.8	290	41.4
8	0.5	340	42.5

Table 1. Evaluation of minimum k and dt when curve-fitting aspect angle estimation becomes advantageous (target traveling at 10 m/s in a constant velocity, straight-line scenario).

47

Effective k>	Effective dt(s)>	Optimal Delay	Optimal Delay/k
4	1.8	150	37.5
5	1.2	200	40
6	1.0	250	41.7
7	0.8	290	41.4
8	0.5	340	42.5

Table 2. Evaluation of minimum *k* and *dt* where curve-fitting aspect angle estimation becomes advantageous with a target traveling at 5 m/s in a constant velocity, straight-line scenario.

The above results can be used to draw conclusions for the use of curve fitting as it applies to aspect angle estimation in a straight-line, constant velocity scenario. Evidently, the optimal delay point varies with history size. It can be assumed that

$$Optimal\ Delay \approx 41 \times k$$

Further testing below *dt* = 0.5 did not occur because a scan update time of 0.5 seconds is an extreme best-case scenario. In conclusion, curve fitting appears to be an effective method for such a scenario. According to the above table, with a *dt* of approximately 1.8, you must only have a track history of 4 for minimal effectiveness. As mentioned earlier, a typical scan update time is between 3 and 5 seconds; according to the above results an acceptable value for all lengths of track history above *k* = 4.

3.2.2.2 Maneuvering Target Scenario

The results of the previous section can only be used in particular scenarios. Implementation of curve fitting would have to occur when it is known that a target would be maneuvering in that way. This could be possible if a network of roads were known and it was assumed that targets would be following these paths. Additionally, if minimal radar measurement error existed the use of curve fitting might also be possible because of accurate detections. A more accurate and valuable maneuver detection algorithm would result. Currently, due to the level of noise, almost all detections are associated with either constant-velocity ('CVT') or unmodeled ('UNM') maneuvers. When either of these mitigating factors mentioned above is unavailable, it must be assumed that targets will undergo maneuvers that are most challenging to kinematic trackers. Therefore, further tests were completed using the Curve/Sharp Turn scenario outlined in Section 1.2.2 and shown again below with a scan update time of 1 second. Increased update times are achieved by down sampling this data:

Cartesian coordinate plane: x (meters) and y (meters)
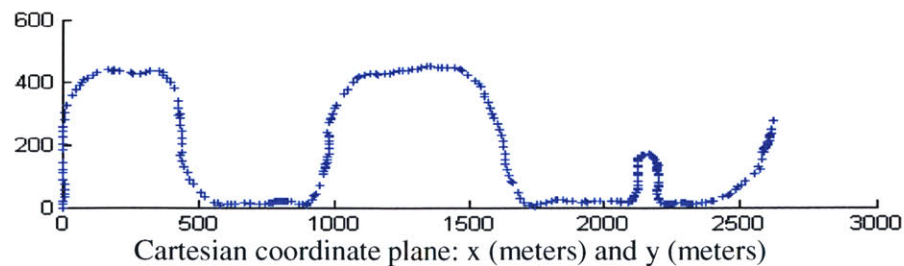
Of additional concern in maneuvering target scenarios is the overall amount of large aspect angle estimation errors (greater than 10°). This measure of effectiveness is also evaluated in the plots

48

below. Initially, the entire scenario was tested was tested; analysis was done at every position point for various scan update times (*dt*) and history sizes (*k*). Figure 23 analyzes this scenario with a history size of *k* = 6 while varying update time.
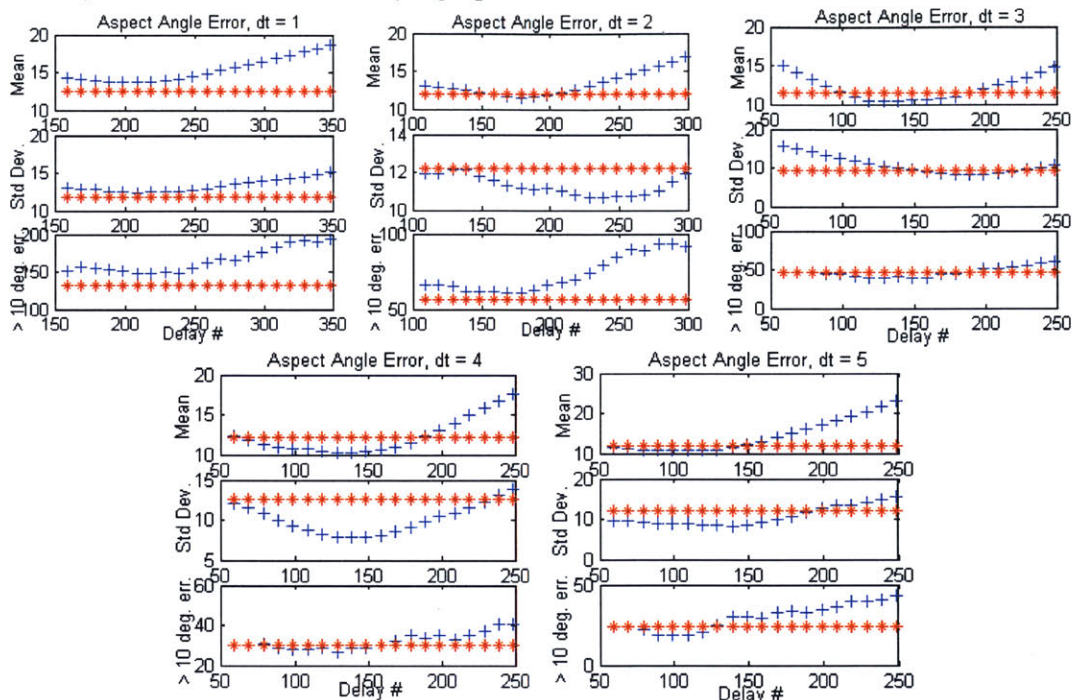
Figure 23. Aspect angle error estimation comparison for maneuver scenario while varying scan update time, *dt*. (Red * – Kalman estimate, Blue + - curve-fitting)

The next set of plots represent the entire scenario as well, keeping the scan update time at 3 while varying the history size:
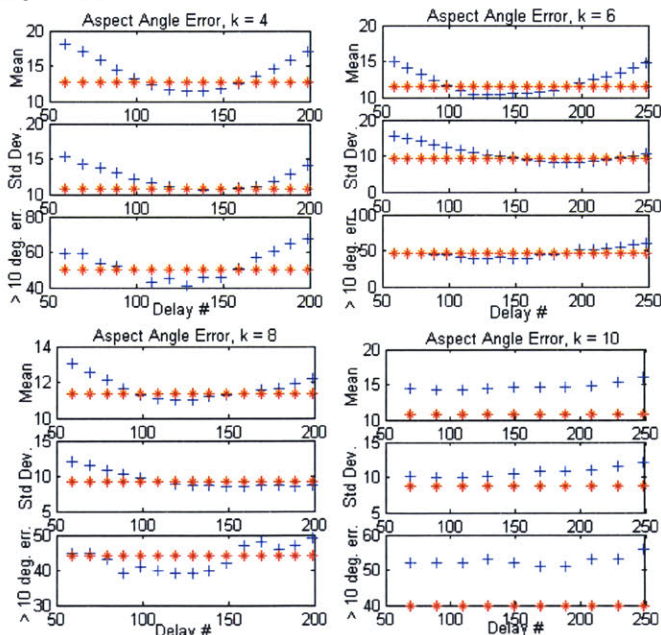
Figure 24. Aspect angle error estimate comparison for maneuver scenario while varying history size, *k*. (Red * – Kalman estimate, Blue + - curve-fitting)

49

The above results do not support the conclusions of the previous section. First, increasing history size is shown to be ineffective at lowering the minimum aspect angle error. This is most because as you increase history size, you risk an occurrence in which the data points used in aspect estimation are involved in multiple maneuvers. If so, aspect angle estimation error will increase. Similarly, as you increase scan update time, there is a greater chance that data points may be involved in different maneuvers, thus forcing the curve to fit to an incorrect maneuver. A small scan update time, coupled with a small history size, might lead to data points that are only undergoing a small part of the maneuver. For this reason it is again recommended that the distance traveled by the target in the data points, d, is greater than the τ_m distance.

The above tests also disprove the constant-velocity assumption that the optimal delay number is proportional to history size. Generally, the optimal history size from above would be between $k = 4$ to 8. A dt of approximately 3 seconds provides somewhat advantageous results. However, it is clear that this study is inconclusive because at no point is the use of curve fitting clearly advantageous in all situations. In part, this is because no clear relationship exists that leads to the selection of optimal delay number.

Most realistic scenarios will resemble the maneuvers taking place in this scenario. Therefore, further analysis was performed on aspect angle estimation during specific target maneuvers. The following figure shows this scenario at $dt = 2$ sec with 9 maneuvers labeled.
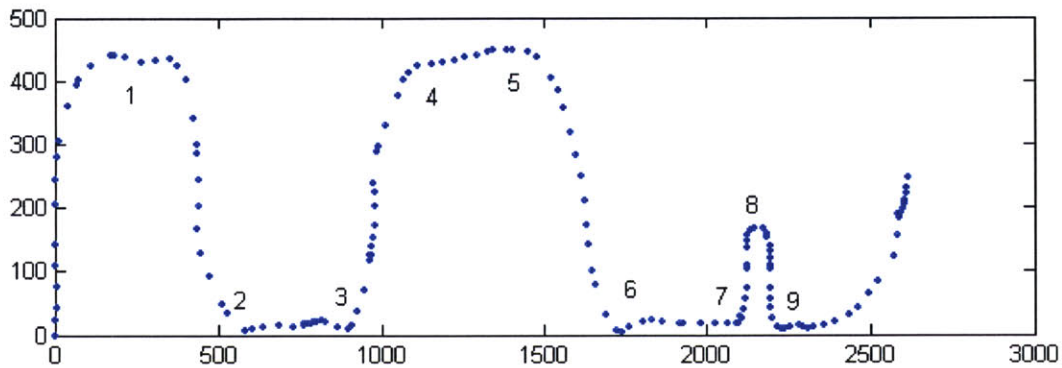
Figure 25. Curve/Sharp turn Scenario with maneuvers labeled
in Cartesian coordinate plane: x (meters) and y (meters)

These maneuvers were used to further analyze curve fitting as a method of aspect angle estimation during optimal performance when $k = 4$, 5, and 6:
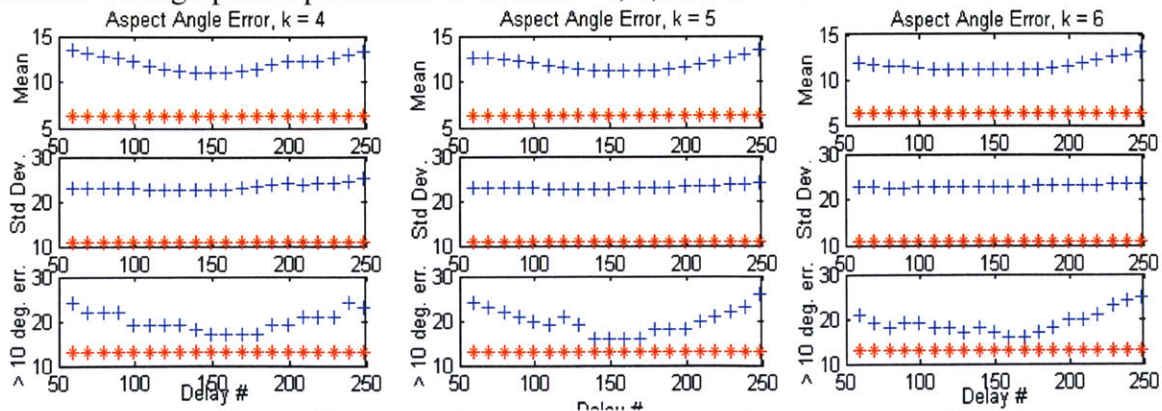
Figure 26. Aspect Angle error comparison for maneuvers only

50

The main objective of this section was to achieve improved aspect angle estimation during target maneuvers. Despite the parameters being set for optimal performance above, there is clearly no advantage gained. This method can provide improved estimation during constant-velocity scenarios. However, the level of measurement noise and the assumed scan update time of 5 seconds render the maneuver detector within the tracker ineffective (again, due to expected selection of only 'CVT' or 'UNM' as the maneuver hypothesis regardless of ground truth maneuver). If there is no accurate way to either determine when a target is maneuvering in a simple straight-line scenario or to select the optimal delay point, there can be no effective way to utilize the results of this section.

3.3 Aspect Angle Error Measurement

Improvement of aspect angle estimation would involve either major adjustments and/or changes to the Kalman filter or extensive research into other state estimation methods (such as the curve fitting method outlined above). In an effort to save time and maintain a low level of complexity, measurement and comprehension of the inherent aspect angle error is expected to be another, possibly more efficient, method of mitigating this problem. If we can model the tendencies of this error, then we can compensate for it throughout FAT.

Originally, it was assumed that the majority of aspect angle errors are less than 10°. This 10° assumption is used in the formation of the error window during CAT and as the "threshold" value in SAT. It is obvious that the radar range and measurement parameters directly affect the amount of error encountered. However, it will be shown that it is important and useful to be able to model and predict this error for the particular environmental geometry of any scenario because this 10° assumption is invalid and inaccurate. Aspect angle error will be measured here using the radar parameters outlined in Section 2.2.2.

3.3.1 Constant Velocity Scenario

The constant velocity scenario used above in Section 3.2.2.1 will be used to measure aspect angle error. In each run, 100 detections are simulated with the true aspect angle held constant for every detection. Thirty consecutive runs with random error in each were completed during which the speed of the target was equal to the run number in m/s. The scan update time was equal to 2 seconds and this test was performed twice: At constant aspect angles of 0° and 180° (target head-on and tail-on), representing the most geometrically challenging situations facing a radar tracking system. This is because with a target at broadside (90° and 270°), the overwhelming affect of azimuth measurement error will cause the detections of this target traveling in parallel to the radar to appear spread so that they (the detections) also appear parallel to the target, making for an estimated aspect angle that is always 90° or 270°. Overall, there are a total of 60 tests with 3000 independent aspect angle estimates. After each run, the Kalman filter track history and aspect angle estimates were saved for comparison with the true aspect angle. Figure 27 depicts the overall mean and standard deviation of the aspect angle errors for each speed tested.
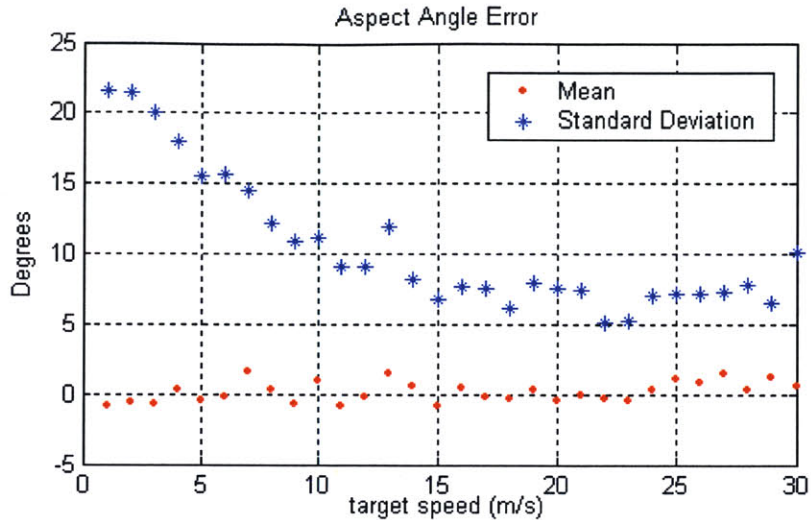
Figure 27. Aspect Angle Error from the Kalman filter for a constant velocity, straight-line scenario at aspect angles of 0° and 180°

Predictably, there appears to be a correlation between target speed and aspect angle estimation error. The true target speed as opposed to estimated target speed was used in the above tests because the estimate is extremely accurate in this simple scenario. This will not be the case in the following section. As speed decreases, the likelihood that a target is maneuvering increases thus the confidence of the Kalman filter decreases. This is not evident in studies of the covariance matrix of the Kalman filter, however, because the plant noise and measurement noise matrices remain the same regardless of speed (so long as 'CVT' is the hypothesized maneuver, which is typically the case).

3.3.2 Maneuvering Target Scenario

Because most realistic situations involve maneuvering targets, the maneuvering target scenario used above in Section 3.2.2.2 is also used to measure aspect angle error. The desired results are that the findings from this test mimic those of the constant velocity case so a relationship can be established between target speed and aspect angle error regardless of maneuver or scenario parameters.

The results below show the standard deviation of the aspect angle error for scan update times of 1, 2, 3, 4, and 5 seconds. Each scan update time was tested in twenty random runs of the maneuvering target scenario. Overall, there were 100 separate runs, with a total of approximately 14,000 independent aspect angle estimations. The table below shows the mean and standard deviation for all 5 tests. The radar platform was held constant.[*]

dt (s) =	1 (304 scans)	2 (152 scans)	3 (102 scans)	4 (76 scans)	5 (61 scans)
Mean (deg)	-1.22	-.91	-1.24	-.97	0.11
Std (deg)	16.30	16.58	16.55	17.46	15.88

Table 3. The mean and standard deviation of aspect angle error for the maneuvering target scenario with varying *dt*.

---

[*] If the platform is placed in the exact opposite position under the same conditions, the mean of the aspect angle error is opposite as well while the standard deviation remains the same.

52

The results in table 3 prove that the overall aspect angle error remains relatively constant for scan update times less than 5 seconds. As expected, the mean is approximately zero. Depending on the specific tracking environment, the aspect angle error could be well above 10º, disproving the assumptions of previous studies of this system.

Figure 28 plots the test data from above to illustrate possible correlation between aspect angle error and the Kalman filter estimate of target speed for this, more realistic, scenario. It shows the speed and aspect angle error of every test point (13338 random test points), regardless of target maneuver. This test will not be performed on specific maneuvering data points due to the aforementioned ineffectiveness of the maneuver detector. Regardless, the scenario tested in this case is generally more kinematically challenging than most real-life scenarios.
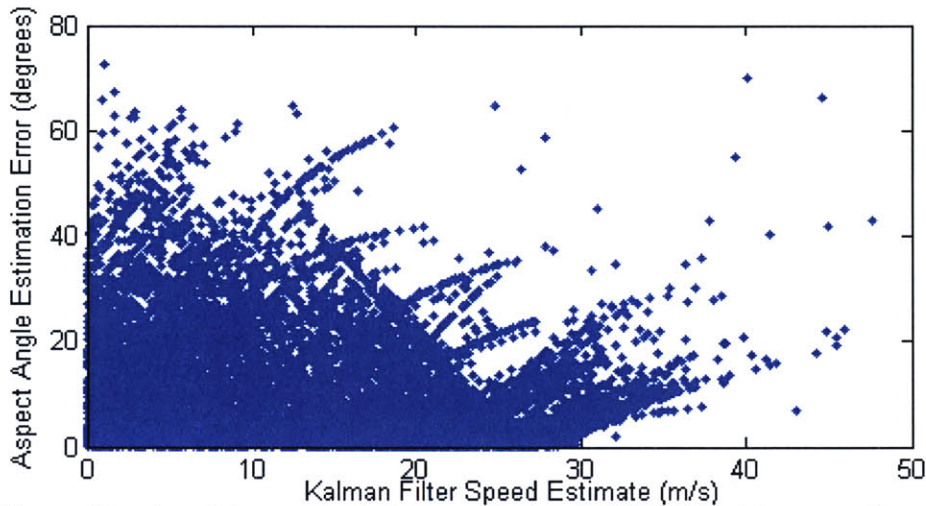
Figure 28. Plot of Aspect Angle Error v. Estimated Speed for Maneuver Scenario

There were no true target speeds above 30 m/s, so all data points above this are in error, but still must be considered. This plot shows a clear relationship between estimated speed and aspect angle error. Again, this test is only for the specific tracking environment outlined above and further tests must occur to validate this result. However, because of time constraints, the assumption will be made that aspect angle error follows such a relationship.

3.3.3   Error Prediction

Surprisingly, the results in the above figure mimic the trends noticed from the constant velocity test: that there appears to be a direct relationship between estimated target speed and expected aspect angle error. The above result will be utilized within the tracker to correctly determine both the CAT window size and SAT "threshold" value separately for each scan. The above data points are again used to compute the expected standard deviation of aspect angle error for specified speed intervals. Below is a table representing these computations for the above tests and scenario:

Speed(m/s)	0-1 (779)	1-2 (712)	2-3 (675)	3-4 (648)	4-5 (630)	5-6 (589)	6-7 (557)	7-8 (504)	8-9 (504)	9-10 (443)
Std (deg)	11.03	11.10	12.45	13.19	13.22	13.28	12.52	11.07	11.78	11.63
Speed(m/s)	10-11 (427)	11-12 (431)	12-13 (388)	13-14 (387)	14-15 (382)	15-16 (346)	16-17 (401)	17-18 (352)	18-19 (371)	19-20 (363)
Std (deg)	12.01	12.07	13.29	13.78	13.16	12.71	12.45	10.80	9.94	7.74
Speed(m/s)	20-21 (352)	21-22 (362)	22-23 (374)	23-24 (361)	24-25 (343)	25-26 (296)	26-27 (268)	27-28 (222)	28-29 (199)	29-30 (173)
Std (deg)	7.57	7.49	6.80	6.05	7.36	5.09	6.26	6.83	5.69	5.84

Table 4. Standard deviation of aspect angle error for specified intervals of estimated speed with the number of data points used in analysis in parenthesis

The above table shows that, approximately, 68% of aspect angle errors are less than 13 degrees for estimated target speeds from 0 to 17 m/s and less than 8 degrees for estimated target speeds from 17 to 30 m/s. Speeds can be grouped and analyzed with more or less detail, as desired.

Implementation: When FAT needs an aspect angle error prediction, the current Kalman filter estimate of target speed will be used in conjunction with the above table of standard deviations to determine error expectation. This occurs in window size determination in CAT (Section 1.4) as well as the determination of an aspect angle difference "threshold" used within SAT (Section 1.5). Specifically, the expected aspect angle error is computed as twice the standard deviation shown above, so as to include, by definition, 95% of all aspect angle estimation error. Such window "flexibility" requires that statistics be generated for "window" and "threshold" values other than the standard ten degrees. This has been done and the results will be discussed later.

Overall, the discovery of this apparent relationship leads the user to gain a great deal of comprehension of the probable performance of this tracking system. Again, it must be noted that every scenario will produce a slightly different relationship and therefore, an *a priori* simulation of the expected target maneuvers in the expected tracking environment must be performed. The above results will be used in the specific analysis below.

CHAPTER 4.

CLASSIFICATION-AIDED-TRACKING (CAT)

To study the performance of CAT, both the vehicle identification capability and track continuity capability must be evaluated. The assessments below will be similar to those used to test CAT in previous studies. In the past, all experimentation has used the MSTAR data set to supply HRR profiles processed with BHDI (Section 1.2.1.3). The tests below will use the MTFP data set and HRR profiles processed with the baseline weighted-FFT method to form the template database, augment the radar target detections, and subsequently analyze the performance of CAT.

4.1 Performance Analysis of Initial System

Detailed in Section 1.4, the operation of CAT basically involves using an ATR classifier to aid in data association by measuring class continuity from scan to scan. CAT is used when a multi-class database of HRR profiles is available *a priori*. Each report can be assigned a probability or likelihood that it is a member of a specific target class or type. A Bayesian classifier is then used to generate the class likelihood and is a function of both the ATR result and the previous track identification. An MSE vector is formed, consisting of the minimum MSE score from the comparison of the report HRR against a group of HRR templates from each target class. This "group" of templates is collected by taking all template profiles from aspect angles within ten degrees of the estimated aspect angle of the track/report pair in question. For the current (initial) system, this aspect angle "error window" is 10°. As noted in the previous section, this assumption of ten degrees of aspect angle error is incorrect; however, tests will be performed on such a system to use in comparative analysis with enhanced versions of CAT.

4.1.1 Vehicle Classification

In order to evaluate the vehicle identification capability of the tracker, we simulate the path of a Scud Launcher with no confuser vehicles using the maneuvering target scenario from above. The expected MSE vector for this Scud launcher was formed from the pre-generated statistics assuming a database of 1 target class and an *other* class. With this 10° error window, the statistics (in log-MSE score) from comparisons with all other classes in the database are:

$$\mu_{Scud} = [0.4970] \quad [0.5080] \quad [0.4547] \quad [0.4156] \quad [0.4872] \quad [0.4656] \quad \text{(sectors 1 – 6)}$$
$$\sigma^2_{Scud} = [0.0291] \quad [0.0194] \quad [0.0418] \quad [0.0570] \quad [0.0308] \quad [0.0265] \quad \text{(sectors 1 – 6)}$$
$$\mu_{other} = 1.1712 \qquad \sigma^2_{other} = 0.0695$$

It should be noticed that this initial version of CAT divides the target statistics according to aspect angle sector (0°-30°,30°-60°...180°) while the *other* statistics are not. This is inherently more inaccurate than if the *other* statistics were separated by sector as well. Also notice that as targets approach broadside (90° aspect angle, sectors 3 and 4), the variance of the MSE scores is higher than when they are head or tail-on (0° or 180°). This is because the target is only observed in range and more range bins with valuable information will appear in a head-on situation. The classifier will therefore have more trouble with targets at broadside.

Five runs (with random measurement noise) of the maneuvering target scenario were completed and evaluated. The true aspect angle, aspect angle error, estimated target speed, and

most importantly, and posterior probability (target classification) was saved after each scan.[*] A scan update time of 1 second was used to produce useable information from 302 scans per run. The Scud launcher is an exceptionally distinct target (in HRR) hence the following results will be considered a "best-case" scenario.

Figure 29 is a plot of the posterior probability: A function of the ATR classifier result and the prior knowledge of track class identification. It is a measure of the probability that the Scud launcher report HRR came from an actual Scud launcher according to the classifier, given past track history. Additionally, the blue •'s indicate that the ATR classifier has correctly identified a report. This is a function of the ATR result only. For example, if the classifier returns a value of 0.73, it means that there is a 73% chance that the report came from a Scud launcher, and a 27% chance that the target is of the *other* class of targets. If this percentage is below 50, then a red + indicates that the classifier made an incorrect decision:
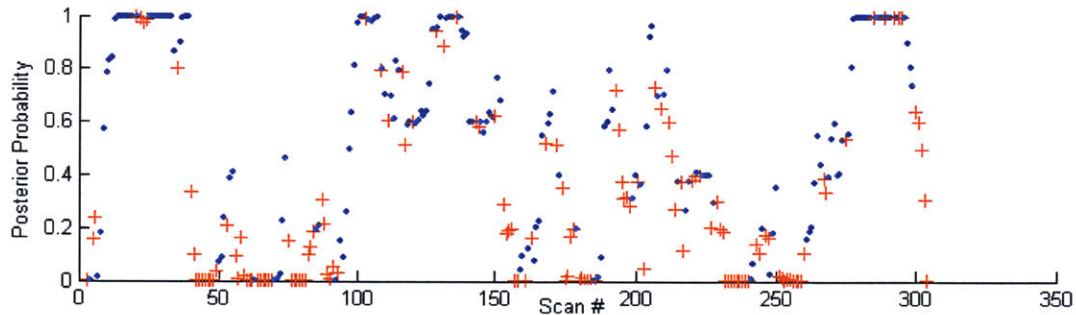
Figure 29. Poster probability accumulation for the Scud Launcher in the maneuvering target scenario. Blue • indicates correct classification by ATR classifier, while Red + indicates incorrect classification
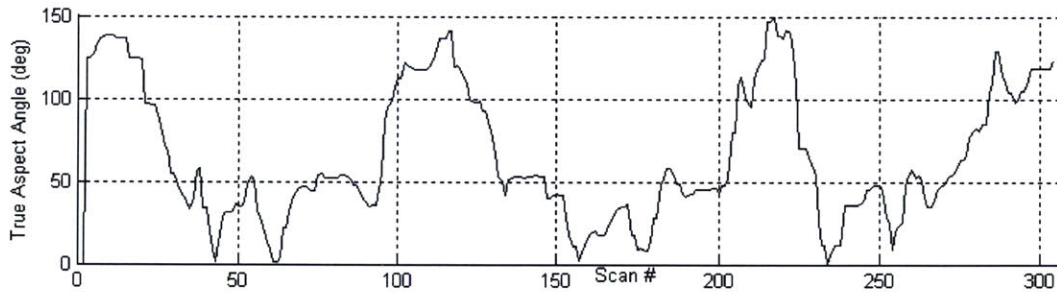
Figure 30. True Aspect Angle v. Scan # for the Scud Launcher in the maneuvering target scenario
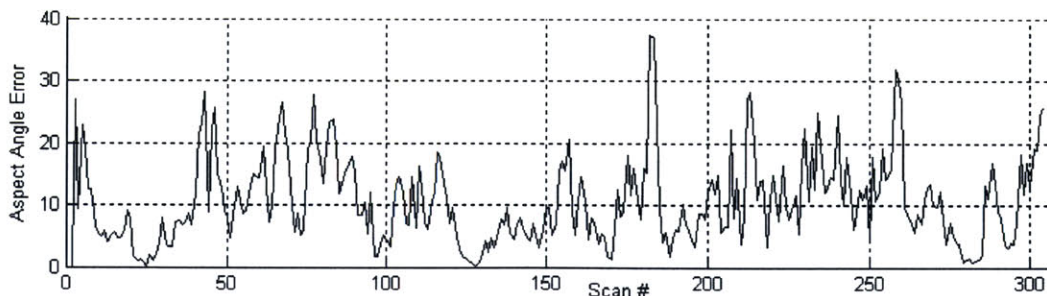
Figure 31. Aspect Angle Estimation Error v. Scan # for the Scud Launcher in the maneuvering target scenario

---

[*] A significantly smaller number of tests can be run on CAT due to the large amount of processing and thus time requirements
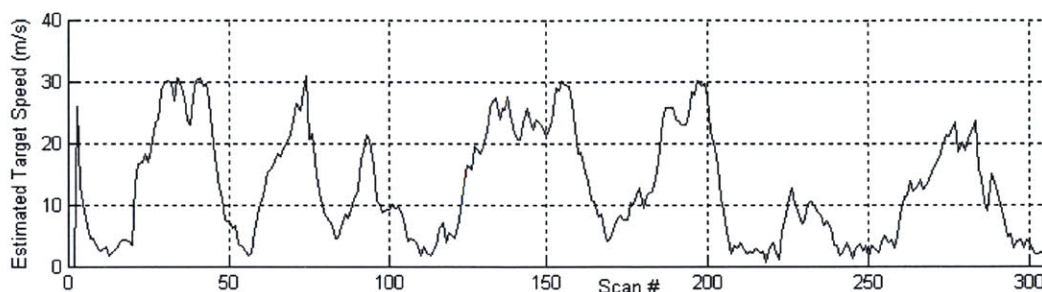
Figure 32. Estimated Target Speed v. Scan # for the Scud Launcher in the maneuvering target scenario

The probability that a correct posterior (P_{post}) decision being was made is 45.7% while the percentage of correct classification (P_{cc}) from the ATR algorithm was 54.0%. Overall, the ATR classifier returned an average value of 51.7%. This means that with no prior knowledge of track identification, the classifier thought that there was an average predicted 51.7% chance that the Scud Launcher report HRR profile actually came from a Scud Launcher. This means that there was basically a 50/50 chance that the classifier was correct. Additionally, it is possible for the posterior probability to converge to 99% despite an incorrect classification by the ATR. This would stem from a prior probability that is so high that it overrides the classifier results. The above results again reinforce the conclusion that as estimated target speed increases, aspect angle estimation error decreases (Figures 32 and 31). The true aspect angle plot is used to show how classification ability varies as aspect angle changes and targets approach broadside.

Five more runs of this scenario with the same random measurement noise were simulated while forcing perfect aspect angle estimation.
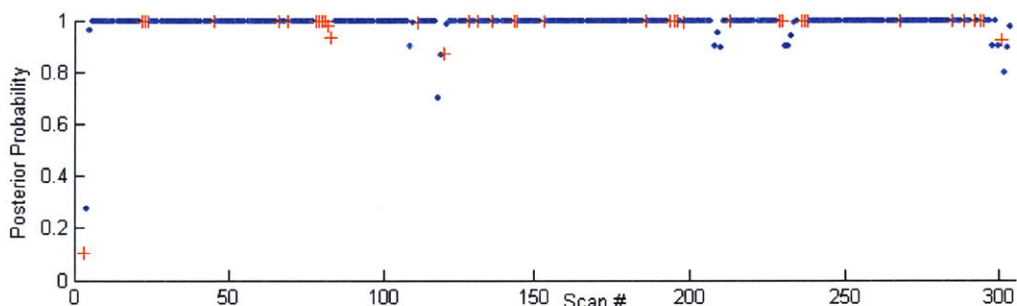
Figure 33. Poster probability accumulation for the Scud Launcher in the maneuvering target scenario with perfect aspect angle estimation. Blue • indicates correct classification by ATR classifier, while Red + indicates incorrect classification

In this case, the P_{post} is 99.3% while the P_{cc} is 87.1%. The average classifier value was 80.6%. This result reinforces the dependence of CAT upon accurate aspect angle estimation. With small estimation error, one can achieve near-perfect vehicle classification. It is therefore extremely important that the error window be large enough to include the true aspect angle, so that a "match" in HRR is found and this level of classification accuracy can be approached.

4.1.2 Track Continuity/Maneuvering Target Scenarios

For the purpose of the following tests, a "misassociation" must be clearly defined: It will be considered the case when, for a given scan, there is a change in the association matrix from

the previous scan. There is a change in the assigned track-to-report association (i.e. track 1-report 1, etc.) from one scan to the next. This tracking simulation software has perfect knowledge of the true identification of every report (report "1" is always from the same target; as is report "2" and so forth). Therefore, we can easily recognize when a report from one target is assigned to the track of another target. Once this incorrect assignment occurs, the track takes on the new identity of that report. All subsequent reports from that same target should be assigned to that track. Again, a misassociation is then considered a change in these expected assignments. Take a simple two-class, two-report test for example:

Scan 45: Track 1-Report 2; Track 2-Report 1
Scan 46: Track 2-Report 2; Track 1- Report 1

This would be considered a misassociation. It is true that most trackers have the ability to "correct" these missasociations, where the original association (track1-report2, track2-report1) is again assigned during the next few scans. This does occur for the simulation software used in this analysis, but there will still be at least one scan with such an inaccuracy to be counted. Moreover, all of the below scenarios will be measured according to the same standards.

4.1.2.1 X-non-crossing Scenario

CAT has the ability to drastically improve situations in which targets approach from different roads and then quickly diverge. Such scenarios are referred to as X-crossing or X-non-crossing scenarios (see Figure 1). The X non-crossing scenario explained in Section 1.2.2 is used to simulate a Scud launcher and a ZSU truck approaching an intersection and then quickly diverging. It will be assumed that the template database consists of five targets. The *other* class statistics will simply be comprised of the merged non-matching MSE scores from all targets in the MTFP data set.

Kinematically, the expectation is that the targets will cross as opposed to diverge. One hundred simulations (runs) of this scenario with a dt of 1 second show that the kinematic tracker chose the correct association only 67% of the time.[*] Twelve runs of this scenario with CAT implemented result in only 65.2% correct associations. This shows, with a limited amount of testing, that this version of CAT degrades data association accuracy. Perfect aspect angle estimation can improve this value considerably. Figure 34 plots the percent of missasociations versus scan number.
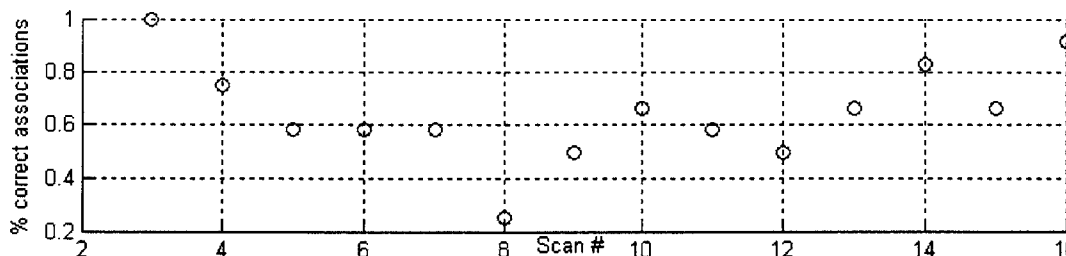
Figure 34. Percent of correct associations v. Scan # for X-non crossing scenario with CAT

---

[*] increasing the dt would further decrease the effectiveness of the tracker as there are less data points where the target would be turning and thus the tracker will be less likely to recognize the maneuver

58

Figure 35 represents the posterior probability for the Scud Launcher after each scan, averaged over the 12 random test runs. A blue dot indicates a correctly classified target while a red plus indicates the opposite.
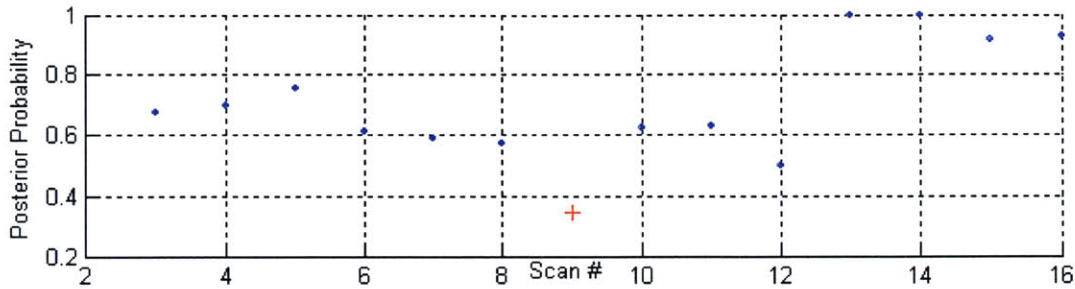
Figure 35. Averaged Posterior probability accumulation for the Scud Launcher in the X non-crossing target scenario.

As the target enters the maneuver (Scan 7), the posterior probability decreases, as does the ability to correctly classify and associate the target. As expected, after the maneuver (Scan 13), the posterior probability and thus confidence in track continuity increases.

Kinematic missasociations are corrected by the difference in the resulting incorrect and correct association χ^2-like score. This score will be directly related to the posterior probability. Therefore, as the prior probability increases, there will be less of an opportunity for misassociation. Information from the tests above has been used to quantify the level of prior knowledge within CAT needed to correctly associate the track/report pairs. This is done to illustrate the dependence of χ^2_{CAT} and correct track-report association on track priors. The figure below shows the *a priori* knowledge about the correct track identification on the x-axis. Therefore, if track 1 is a Scud Launcher and track 2 is a ZSU truck, a value of .3 is the *a priori* probability that track 1 is truly a Scud and track 2 is truly a ZSU. Again, the results of twelve separate runs of this scenario are averaged. The resulting posterior probability for the correct track-report association from the Bayesian classifier is indicated on the y-axis. As the percent prior probability increases for the correct association, there is a greater chance that the target will be correctly classified. This is true even for this less-effective version of CAT; the effect will be maximized for variants of CAT with improved aspect angle estimation.
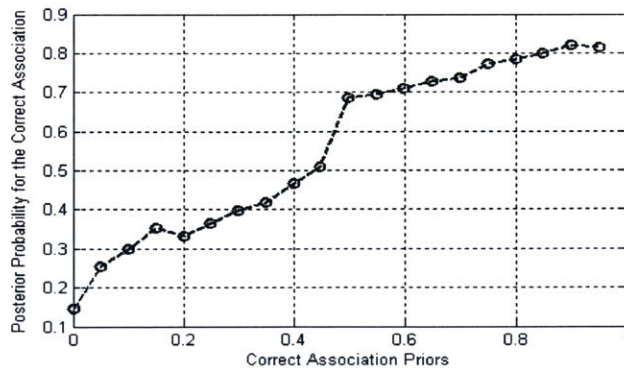
Figure 36. Posterior Probability as a function of the Prior Probability for the Correct Association for a scan update time of 1 second

4.1.2.2 Merging/Diverging Scenario

A second scenario will be tested which represents two targets, the Scud Launcher and ZSU truck, merging, following each other, and later diverging. This scenario is a descendent of the X-non crossing scenario and is shown below:
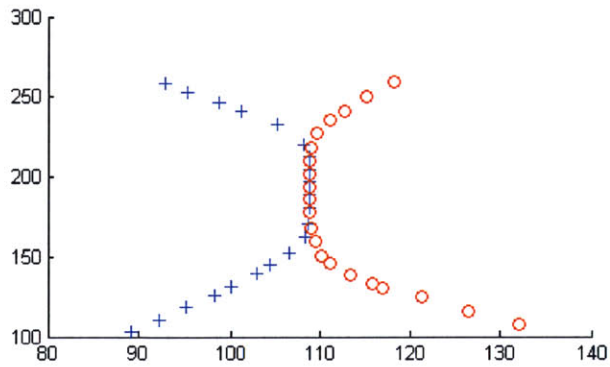
Cartesian coordinate plane: x (meters) and y (meters)

Again, a five-class template database is assumed. Ideally, at both the merge and diverge point, CAT should correct any misassociation by the kinematic tracker. With 50 runs, the Kinematic Tracker made the correct association 65% of the time while. Ten runs of CAT chose the correct association only 64% of the time. Figures 37 and 38 represent the averaged percent of missasociations and the posterior probability for the Scud Launcher after each scan. A blue dot indicates a correctly classified target (on average) while a red dot indicates the opposite in Figure 38.
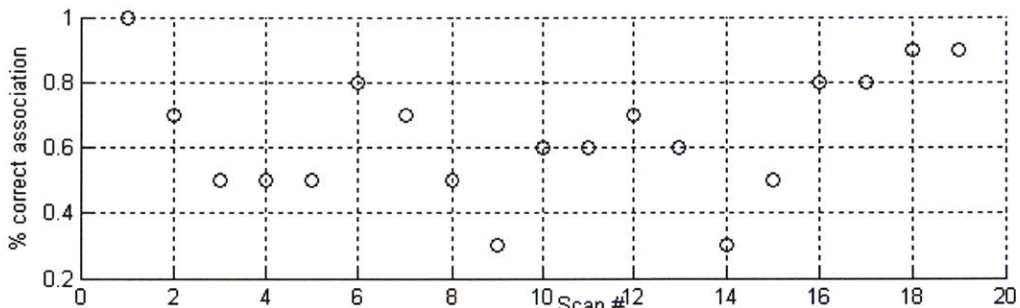
Figure 37. Percent of correct associations v. Scan # for merging/diverging scenario with CAT
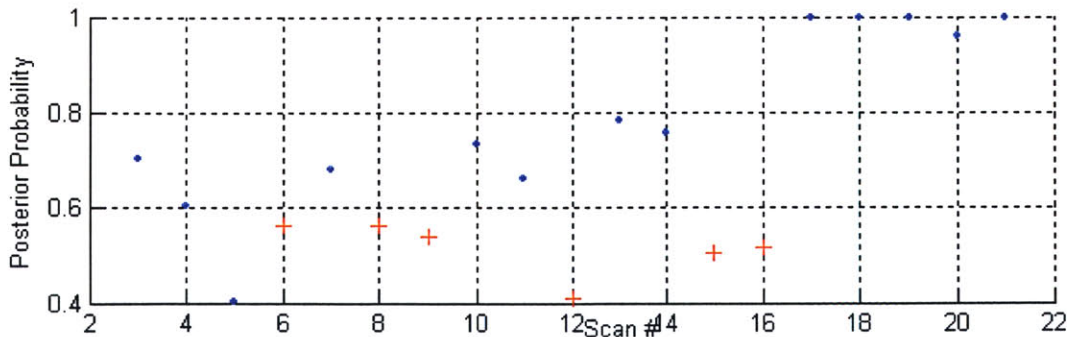
Figure 38. Averaged Posterior probability accumulation for the Scud Launcher in the merging target scenario.

60

As the target enters the maneuver (Scan 7), the posterior probability decreases, as does the ability to correctly classify and associate the target. The performance remains deteriorated throughout the "straightaway" and remains so until after the targets diverge. Again, CAT does not improve the performance of the kinematic tracker.

4.1.2.3 Passing Scenario

The same targets and template database used above were used to test a scenario in which two targets travel in parallel 5 meters apart with a constant velocity of 10 m/s in a straight line. One target is lagging behind the other by 3 meters; the scan update time is 5 seconds. With 50 runs, the Kinematic Tracker made the correct association 66.5% of the time while, while with 10 using CAT, the correct association percentage was only 61.5%. The figures below are similar in explanation to those above.
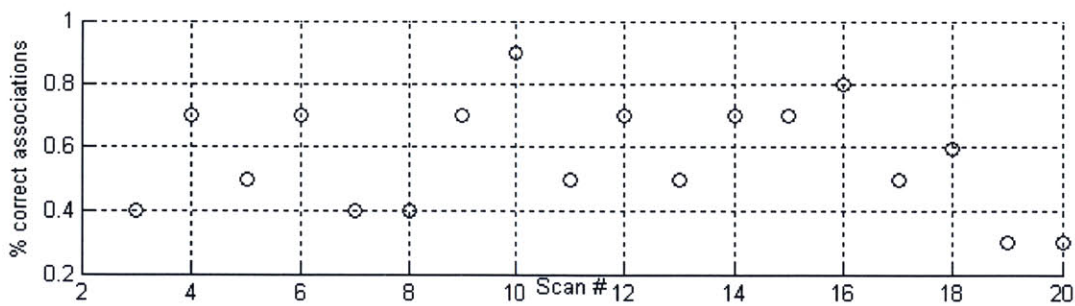
Figure 39. Percent of correct associations v. Scan # for passing scenario with CAT
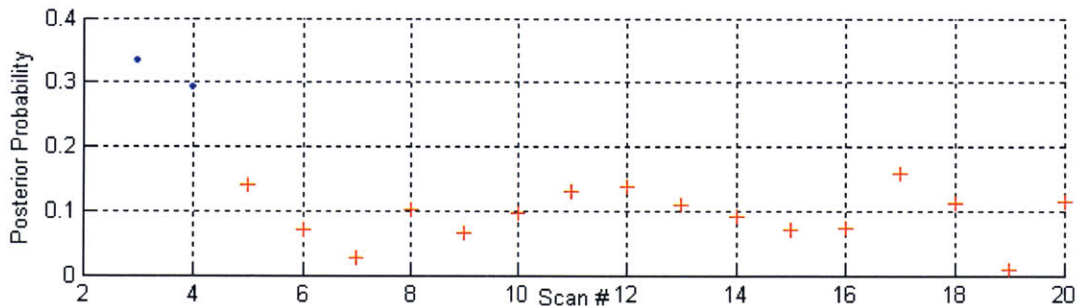
Figure 40. Averaged Posterior probability accumulation for the Scud Launcher in the passing scenario.

The percent of correct association shows no appreciable pattern related to scan number (as expected in this constant velocity, straight-line scenario). More noticeable is the inadequate performance of CAT. This was expected and can be attributed to the problem discussed below in Section 4.2.1.1. The enhanced version of CAT is not expected to provide any improvement in this situation. However, this scenario is a perfect candidate for SAT.

4.2 Error Window Optimization

The results of Section 4.1 clearly indicate that, given the proposed operating environment, CAT does not provide significant improvement over the use of the simple kinematic tracker alone. As mentioned earlier, it is hypothesized that this is due to error in aspect angle estimation. Moreover, Section 3.3 proved the assumption that the aspect angle error is consistently less than 10 degrees inaccurate. In fact, it was shown that for slower targets, *one*

standard deviation of expected aspect angle error was 13 degrees. In order to improve the performance of CAT, it was proposed that the aspect angle error estimation "window" be larger and thus more accurate. This section describes the process of window size selection and details the resulting statistical and performance changes.

4.2.1 Aspect Match Comparison

Specifically, the expected aspect angle error should be large enough so that most true aspect angle errors lie within this limiting value. Additionally, the computational and time requirements inherent to CAT should also be minimized. One goal was to ensure that at least 95% of all aspect angle errors should be included in this error estimate "window".

The findings of Section 3.3 were used in an attempt to meet this objective. As evidenced, the expected aspect angle error is strongly correlated with estimated target speed. Table 4, which quantifies the standard deviation of aspect angle errors in terms of estimated target speed, was used to determine the extent of this "error window". Recall that subsequent to Kalman filtering within FAT, a new aspect angle error widow is computed for each possible track-report association. Again, this will be equal to 2 standard deviations of the expected aspect angle error, given the estimated target speed for the current scan. 95% of all aspect angle errors should lie within this window. A corresponding "match" of report HRR and database HRR should then be found during CAT operations because this "error window" would ideally include the true aspect angle of the report target.

Figure 41 measures whether this does, in fact, occur. The maneuvering target scenario was used in this analysis to represent the most kinematically challenging scenario and to ensure that there are no data association conflicts. The scenario scan number is on the x-axis, while the aspect angle error is on the y-axis. The averaged aspect angle errors by scan are represented as black points while the optimized error window is plotted as a blue line and the old error window (10°) is plotted as a red line. A positive result occurs when, for any scan, the aspect angle error lies beneath this blue "error window" line. The amount of such occurrences is illustrated shown on the figure in terms of a percentage, called the aspect match %. Both the initial and enhanced CAT aspect match percentages are shown as 'Old %' and 'New %'.
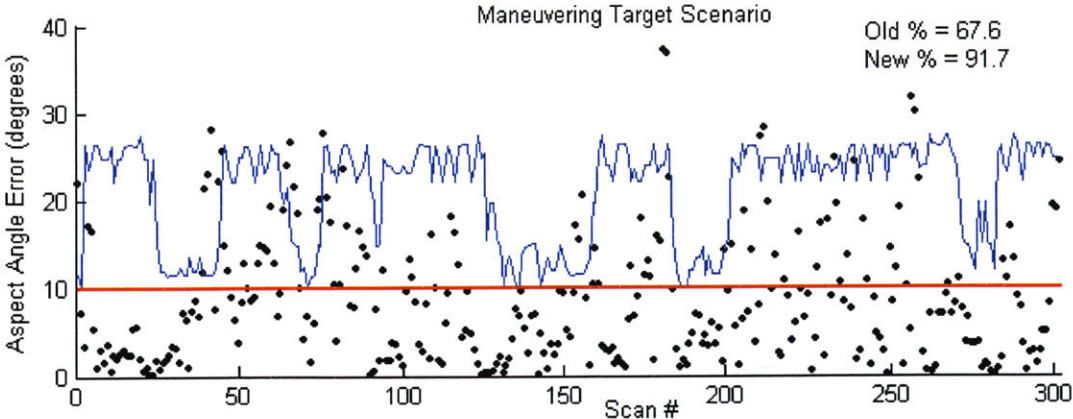
Figure 41. Aspect Angle Error and Error Windows v. Scan # for the maneuvering target scenario.

The plot shows that 91.7% of all aspect angle errors for this scenario lie within their corresponding error window. While this does not meet the pre-set goal of 95%, one must realize that this is a worst-case scenario. It still exhibits significant improvement over the initial version

of CAT by 35.6%. Furthermore, it proves that the tradeoff between error window size and computational requirements can be optimized under the assumption that estimated target speed correlates with expected aspect angle error.

4.2.1.1 Usability of CAT

While the above findings might prove valuable to CAT, a major concern arises due to the increase in error window. This occurs when the error widow is large enough so an aspect angle and HRR "match" is found in both the correct *and* incorrect associations. This problem is compounded when the aspect angle error window *only* leads to a match for the incorrectly associated report. This is explained in more detail below:

Assume a two-target, two-class scenario. The correct associations are track 1 - report 1 and track 2 - report 2:

True aspect angles:
Report 1 (target class 1): 90°   Report 2 (target class 2): 50°

Kalman filter estimated aspect angles for every possible association with an aspect angle error window of 25°:
track1-report1:   85° - class 1 "match" is found (85°+25° > 90°)
track2-report1:   68° - class 1 "match" is found (68°+25° > 90°)
track2-report2:   65° - class 2 "match" is found (65°-25° < 50°)
track1-report2:   74° - class 2 "match" is found (74°-25° < 50°)

In all cases, the estimated aspect angles lie within the error window, causing a "match" to be found.

This situation is entirely possible; in fact, it can be considered likely when targets are traveling in parallel or near-parallel situations. What the above example is trying to show is that the incorrect association (track2-report1 and track1-report2) will produce the same minimum log-MSE score as the correct associations due to an "HRR match" being found for all possible associations. Therefore the resulting χ^2_{CAT} matrix will include cells with similar scores and thus provide limited aid in ensuring accurate data association. This is especially prevalent in the results of Sections 4.1.2.3 and 4.3.2.3, where the tracker provides little to no added accuracy. The user of this tracking system must recognize this phenomenon in situations similar to above.

4.2.2 CAT Statistics Comparison

Another concern arising from the expansion of the aspect angle error window is the gradual merging of the matching and mismatching PDF's of the expected log-MSE scores for each class of target. Again, as you increase the "error window", there is a more extensive search through the database to include more HRR profiles from a larger number of aspect angles. It is hypothesized that there will be an increasing chance that an HRR profile from a non-matching target class will return a lower score than the matching score. This is simply due to the fact that more non-matching comparisons take place and the chance increases that a random non-matching template profile might match well with the report profile. Conversely, the increase in matching target comparisons should not affect the returned lowest log-MSE score. If an HRR

"match" was found at a given aspect angle, then testing profiles from the same target at other aspect angles will surely return a higher, and thus insignificant, unused score.

The clear advantage of using an expanded error window is that the likelihood that a match is found considerably escalates (Section 4.2.1). The statistical disadvantage is that the PDF's will merge and an MSE score returned from a correct HRR "match" might be closer to the mean MSE score for a non-matching target class. Statistics have been generated as explained in Section 2.2.4 for window sizes to include every integer between and including 1 and 50°. Figure 42 shows the expectation of the minimum log-MSE scores from CAT comparisons for sector 1 using a ZSU truck HRR as the "test" report profile. Again, the report profile signature is compared against a group of profiles from all classes in the template database. The minimum log-MSE score from these comparisons are used in these target classification procedures. This example is used to represent what will be seen with less detail in subsequent plots.
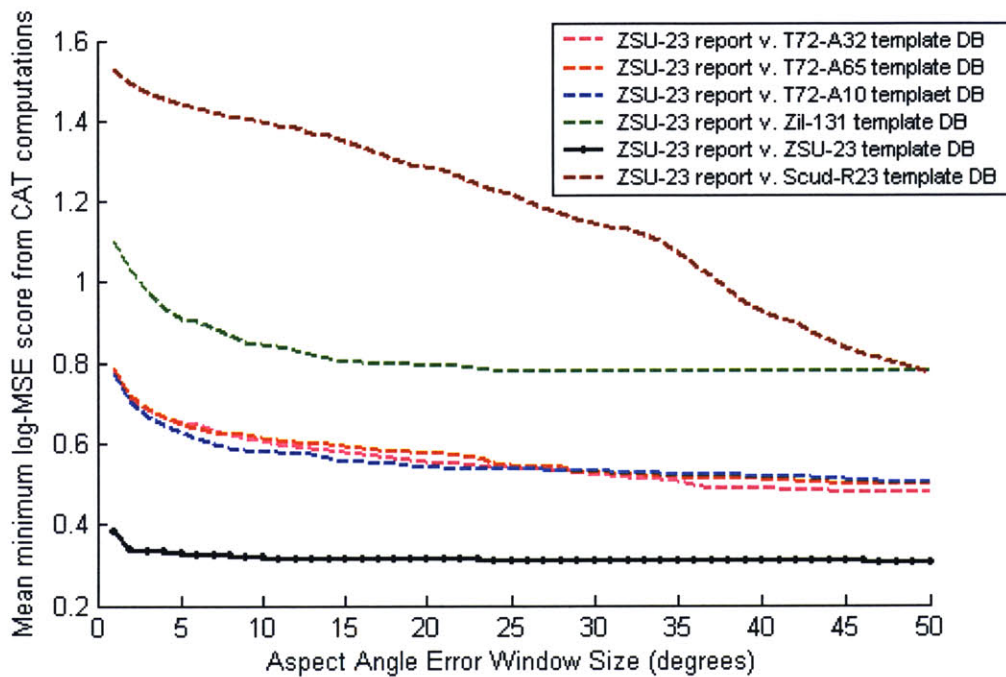
Figure 42. CAT Statistics for a ZSU-23 truck "test" profile in Sector 1 (0°-30°)

As expected, the lowest mean MSE scores above correspond to statistics for the comparison of the ZSU report profile against the database of ZSU HRR templates. Signature comparisons involving a ZSU report profile and templates from other target classes result in different behavior as the error window size is increased. Generally, the hypothesis that as aspect angle error window size is increased, the matching-class MSE mean remains relatively constant while the non-matching-class MSE mean gradually approaches the matching mean. It is at this point at which CAT would no longer provide accurate or influential aid in resolving data association conflicts. In Figure 42, the "merge point" does not occur for window sizes less than 50 degrees. Since the maximum error window used according to Section 4.1 would be 27.5 degrees, it can be declared that the disadvantages stated previously are not a concern. However, Figure 43 shows otherwise. Included in this figure are 36 of the above plots. Every target class is denoted by the same color line throughout every one of the plots below. The sector for each plot is denoted by the row of the plot, while the plot column denotes the target class of the "test" report profile.

64

The "merge point" occurs below for a number of comparisons. Specifically, the comparisons involving the three variants of T-72 tanks indicate that it is very difficult to tell the difference between these variants and the ZSU carrier. The merge point in most of these situations (columns 1-3) occurs before 10°. Additionally, the sector of the simulated report profile also plays a role in determining the advantage that CAT can provide. This again proves that targets at broadside (approximately 60-120°; sectors 3-4) are difficult to classify correctly because the mean MSE Score (and thus PDF's) are very similar for all target classes.

On the contrary, several advantageous situations are also presented below. The PDF's resulting from Scud report profile comparisons are extremely distinct across all aspect angles. It is therefore relatively easy to recognize and classify this target type. The same can be said, but to a lesser extent, for the ZSU carrier and Zil truck. In most meaningful comparisons (not columns 1-3), the "merge point" appears to occur near 25°, but this approximation differs depending on sector and target class. Overall, it can be concluded that increasing the aspect angle error window from 10° to even 27° results in very little, if any, detrimental effects to the separation of matching and non-matching class PDF's. Thus the confidence in the results from CAT should only heighten.

T72-A32: Blue   **T72-A65**: Green   **T72-A10**: Red   **Zil-131**: Cyan   **ZSU-23**: Purple   **Scud-R23**: Gold
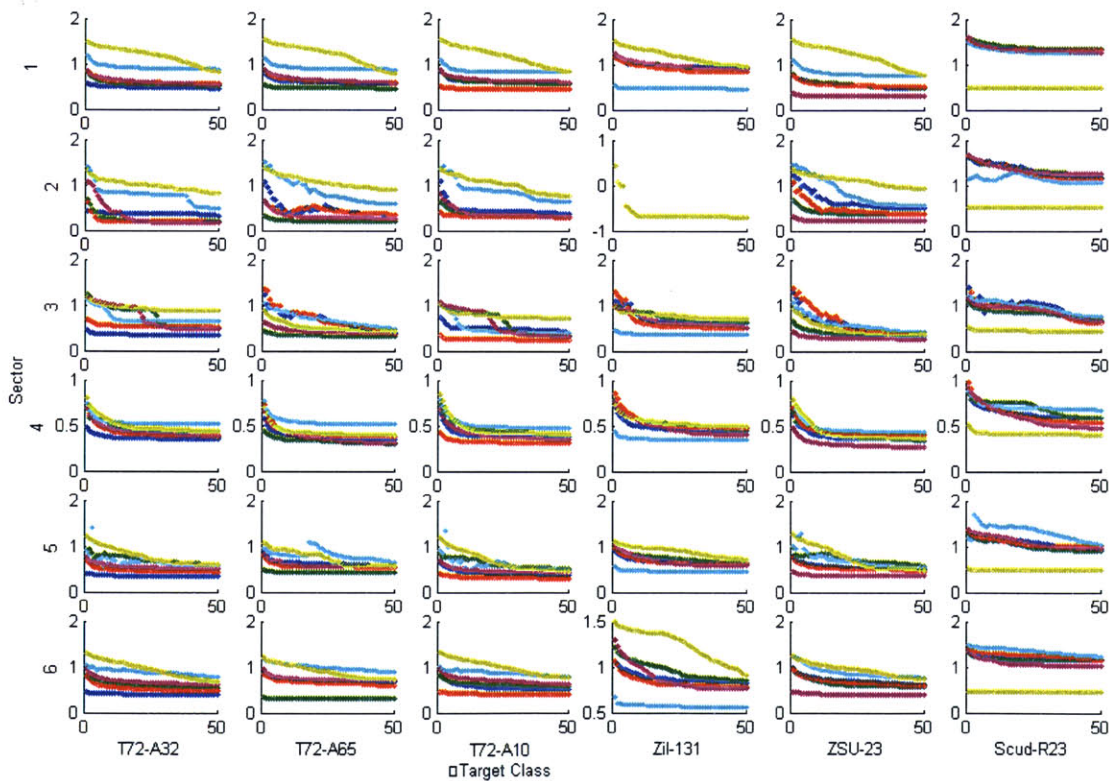
Figure 43. CAT Statistics for all Sectors and all Target Classes. The sector is indicated by row and the target class of the "test" report profile is indicated by column.

4.3 Performance Enhancement

This section will consist of assessments of CAT performance using the exact same scenarios, tests, and random runs as in Section 4.1. The initial system, with an assumed aspect

angle error window of ten degrees, will be compared with the enhanced system with the optimized error window size. Many of the same plots used above will be shown again for comparative purposes.

4.3.1 Vehicle Classification

Five runs (with the same exact random measurement noise applied to the initial test) of the maneuvering target scenario were completed with the new aspect angle error window applied. This experiment has the same true aspect angle, aspect angle error, and estimated target speed as above. However, the posterior probability and target classification should improve. A scan update time of 1 second was again used to produce useable information from 302 scans per run. Figure 44 compares the plot of posterior probability from the initial system with the plot from the enhanced system.
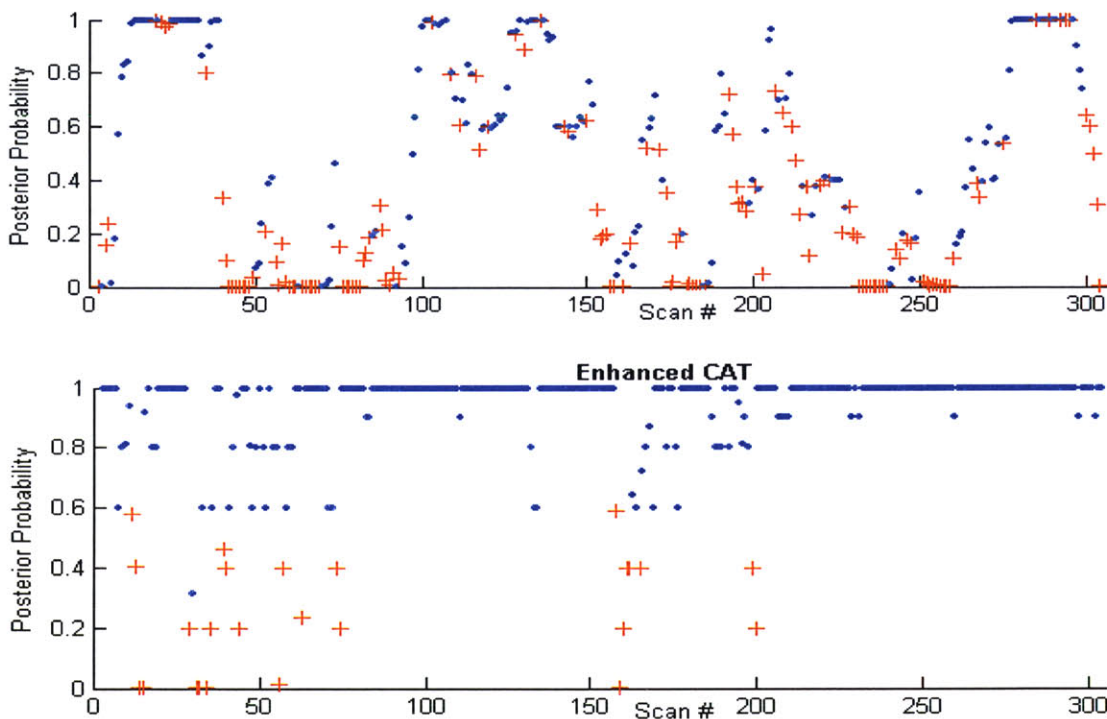
Figure 44. Poster probability accumulation for the Scud Launcher in the maneuvering target scenario for the initial system (top) and the enhanced system (bottom). Blue • indicates correct classification by ATR classifier, while Red + indicates incorrect classification

The percent probability that a correct posterior (P_{post}) decision is made was 89.8% while the percentage of correct classification (P_{cc}) from the ATR algorithm was 91.7%. Overall, the improved ATR classifier returned an average value of 88.9% for the correct association. The following table shows the statistical improvement over the previous system. The enhanced system almost doubles the effectiveness of the vehicle identification capability of the tracker. Since the overall goal is correct classification, it can be finally stated that aspect angle error window expansion provides 69.5% (approx. 70%) improvement in vehicle classification capabilities. Because data association is directly related to vehicle identification capability in CAT, improvements of this magnitude are also expected in track continuity evaluations.

	P_{post} (%)	P_{cc} (%)	ATR avg. (%)
Initial System (10° error window)	45.7	54.0	51.7
Enhanced System (variable error window)	89.8	91.7	88.9
% improvement	96.5	69.8	72.0

Table 5. Comparison of Vehicle Identification Capability

4.3.2 Track Continuity/Maneuvering Target Scenarios

4.3.2.1 X-non-crossing Scenario

The X non-crossing scenario explained in Section 1.2.2 is again used to simulate a Scud launcher and ZSU truck approaching an intersection then quickly diverging. The same test conditions used in Section 4.1.2.1 apply for this test. Again, the template database consists of five targets and the *other* statistics will be comprised of the merged non-matching MSE scores from all targets in the MTFP data set. Twenty runs of this scenario with the enhanced version of CAT implemented were completed. Table 6 shows the percent of correct associations for the KT, Initial CAT, and Enhanced CAT:

	% of Correct Associations
Kinematic Tracker	67.0
Initial System (10° error window)	64.8
Enhanced System (variable error window)	72.8
% improvement over Initial System	12.3

Table 6. Percent of Correct Associations for 3 variants of the tracker using the X-non-crossing Scenario

Figure 45 plots the percent of missasociations versus scan number for both the initial system (red squares) and the enhanced system (blue circles).
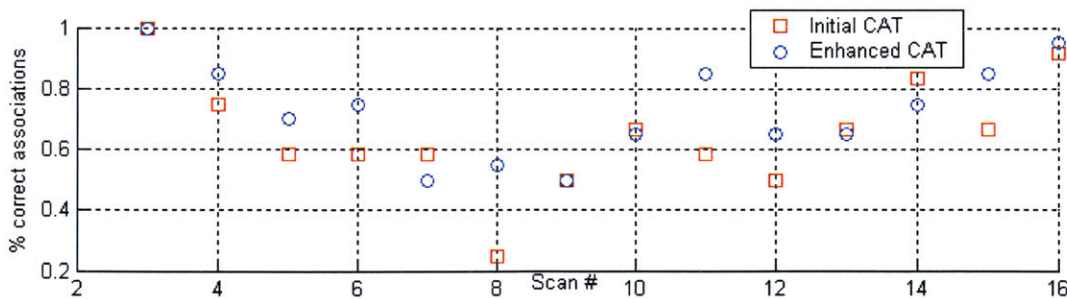
Figure 45. Percent of correct associations v. Scan # for X-non crossing scenario with Initial and Enhanced versions of CAT (initial – red square's, enhanced – blue circle's)

Finally, Figure 46 below compares the posterior probability for the Scud Launcher after each scan, averaged over the 20 random test runs for both variants of CAT. A blue dot indicates a correctly classified target while a red plus or indicates the opposite. The larger icons represent the data from the enhanced version of CAT.
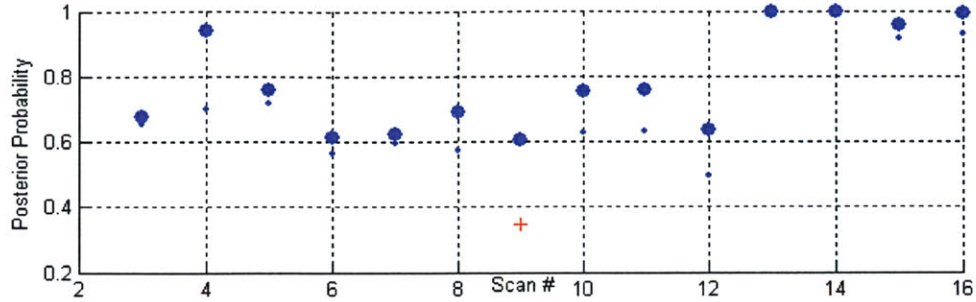
Figure 46. Averaged Posterior probability accumulation for the Scud Launcher in the X non-crossing target scenario (larger icons = enhanced CAT).

The above results support the conclusion that the enhanced version of CAT provides significant improvement in vehicle identification capability, which can be represented by the posterior probability plot (Figure 46 above). On average, all targets are correctly classified during each scan. In both this figure and the previous (% correct associations), improvements are greatest throughout the maneuver, between scans 5 thru 12; the desired effect.

4.3.2.2 Merging/Diverging Scenario

Again, the Scud Launcher and ZSU truck were used in analysis of the merging, following, then diverging scenario. The scenario environment is the same as in Section 4.1.2.2. There were 20 runs of this scenario completed with the enhanced version of CAT. Table 7 is used to compare the percentage of missasociations among CAT variants:

	% of Correct Associations
Kinematic Tracker	64.9
Initial System (10° error window)	64.0
Enhanced System (variable error window)	71.6
% improvement over Initial System	11.9

Table 7. Percent of Correct Associations for 3 variants of the tracker using the merge/diverge scenario

Figure 47 below plots the percent of missasociations versus scan number for both the initial system (red circles) and the enhanced system (blue +'s).
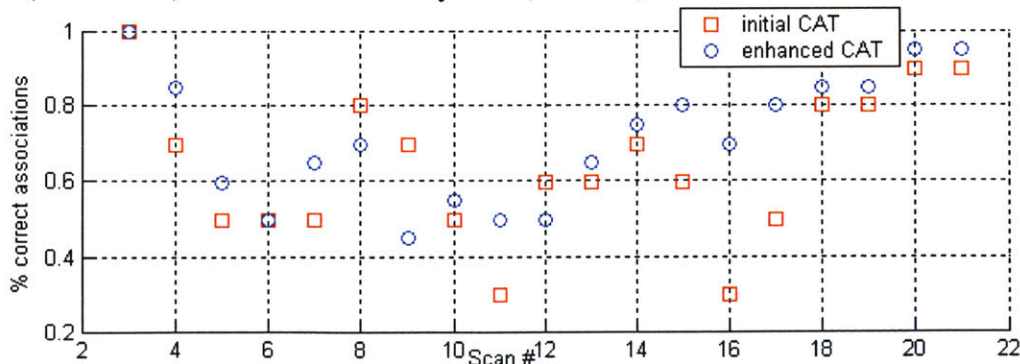
Figure 47. Percent of correct associations v. Scan # for merging/diverging scenario with Initial and Enhanced versions of CAT (initial – red squares, enhanced – blue circles)

68

Finally, Figure 48 compares the posterior probability for the Scud Launcher after each scan, averaged over the 20 random test runs for both variants of CAT. A blue dot indicates a correctly classified target while a red plus or indicates the opposite. The larger icons represent the data from the enhanced version of CAT.
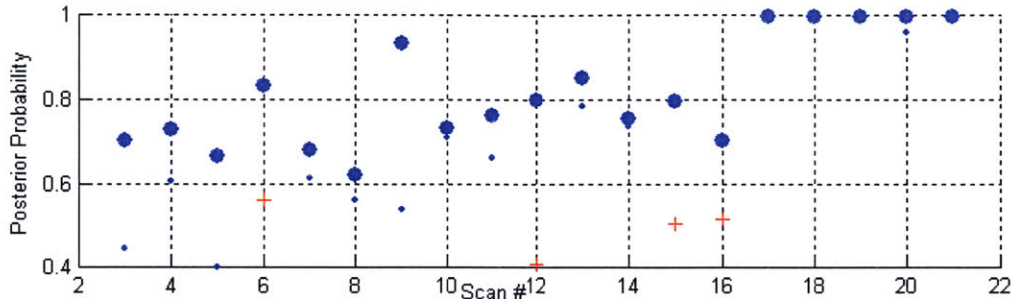
Figure 48. Averaged Posterior probability accumulation for the Scud Launcher in the merging/diverging target scenario (larger icons = enhanced CAT).

Again, on average, every target was correctly classified during each scan. During the merge and diverge point (Scans 5-9, Scans 16-19, respectively), general performance denigrates. However, this is when the enhanced CAT can provide the most aid. During the "straightaway", enhanced CAT denigrates because of the effect outlined in Section 4.2.1.1. Overall some improvement in this scenario still exists.

4.3.2.3 Passing Scenario

The same targets, template database, and scenario environment used above in section 4.1.2.3 was used to test the scenario in which two targets are traveling 5 meters apart in parallel in a constant velocity, straight line situation at 10 m/s. There were 10 runs of this scenario with the enhanced version of CAT implemented. The tables and figures below are similar in explanation to those above:

|	% of Correct Associations
Kinematic Tracker	66.5
Initial System (10° error window)	61.5
Enhanced System (variable error window)	62.5
% improvement over Initial System	1.6

Table 8. Percent of Correct Associations for 3 variants of the tracker using the passing scenario.
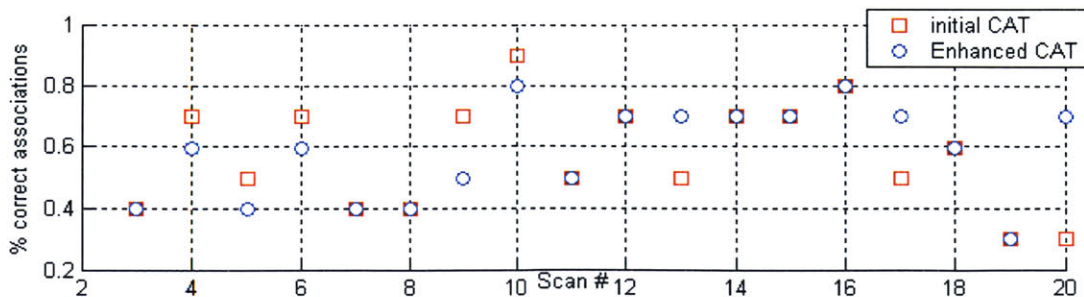
Figure 49. Percent of correct associations v. Scan # for the passing scenario with Initial and Enhanced versions of CAT (initial – red 0's, enhanced – blue +'s)

69
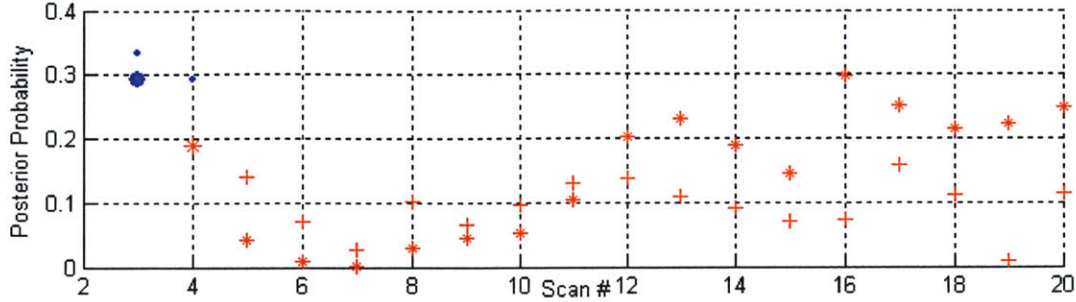
Figure 50. Averaged Posterior probability accumulation for the Scud Launcher in the passing scenario [larger icons (*'s denote enhanced incorrect classification) = enhanced CAT].

As hypothesized, there is little to no improvement over the initial CAT and strictly no improvement over using the kinematic tracker alone. It is not recommended that CAT be utilized in constant velocity, straight-line situations. However, the χ^2_{CAT} scores for all possible associations should be relatively similar and thus the intensity of the χ^2_{SAT} scores should force the tracker to choose the correct associations. Analytically, this is the case because the averaged difference in correct and incorrect association χ^2_{CAT} score from this test is 0.209. This is approximately only 1.5% of the overall range of returned χ^2_{CAT} scores, meaning that the χ^2 or χ^2_{SAT} scores would in almost all situations correct this poor performance.

4.4 Aspect Angle Return Accuracy

In other independent studies of FAT techniques (such as [10]), the concept of "back-estimating" aspect angle has been utilized. This refers to the use of the aspect angle of the best-fit template HRR found to "match" the report HRR in CAT (aspect angle producing the minimum MSE) as the actual aspect angle of the report. For example, if the initial Kalman filter estimate of the report target aspect angle is 68° and the search for a "match" in HRR via CAT (minimum MSE) returns a template from an aspect angle in the database of 75°, the latter would be stored and used as the true value for that report (used by future FAT operations).

The accuracy of this technique will be briefly studied using the maneuvering single-target scenario to again represent the most kinematically challenging scenario and to ensure that there are no data association conflicts. Five runs of this scenario with a scan update time of 1 second have been completed while returning the aspect angle of the template HRR that best matches (by MSE) the HRR of the target report. The average difference between true aspect angle and this CAT returned aspect angle is 3.80°. Comparatively, the average difference between the true aspect angle of the target and the Kalman filter estimated aspect angle is 8.03° (a difference in overall average error of 4.23°). Figure 51 compares the above errors by scan # in the maneuvering target scenario; only showing errors between 0° and 30°.
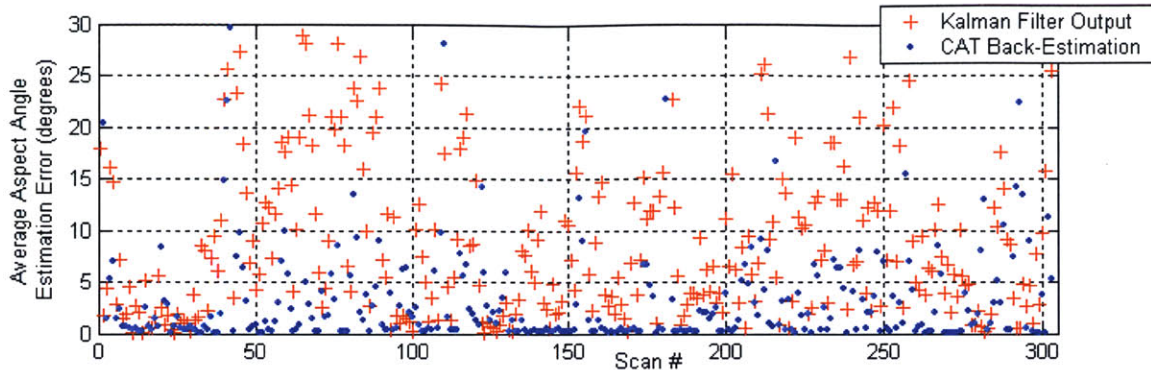
Figure 51. Plot of aspect angle Back-Estimation error and Kalman Filter aspect angle estimation error v. scan # for the maneuvering single-target scenario

Visually, it appears that this estimation method is much more affective than Kalman estimation. More importantly, the use of this method requires that CAT be in a useable situation (the target class is known and a database exists for that class), which is not always the case.

4.4.1 Correlation Adjustment for Back-Aspect-Estimation

An important detail not depicted above is that the average comparative difference of back-estimation error to Kalman estimation error per scan is 4.67°, slightly higher than the overall average difference of 4.23°, but still much less than the average error for the Kalman filter of 8.03°. The reason for this can be seen below in Figure 52 where back-aspect angle estimation error is shown for all magnitudes of error:
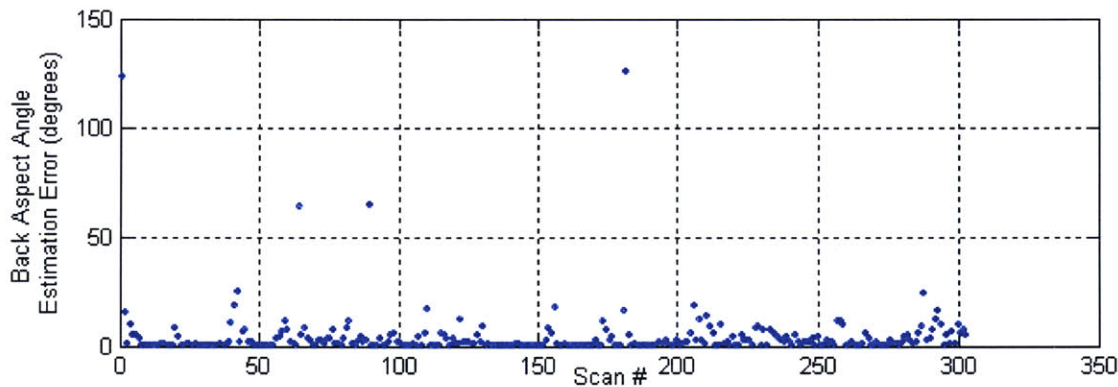
Figure 52. Plot of Aspect Angle Back-Estimation Error v. Scan # for the maneuvering single-target scenario

There are 3 scans (not counting the first) that have aspect angle errors greater than 30 degrees. This is most likely due to the fact that the best match template profile came from a profile that was "randomly similar" to the report profile. In order to fix this type of error, it was proposed that the back-estimate of the aspect angle be generated using all of the returned information from MSE comparisons as follows. The MSE score and corresponding template aspect angle for all of the comparisons are stored and used. A plot of this information will always be similar to Figure 53 below:

71
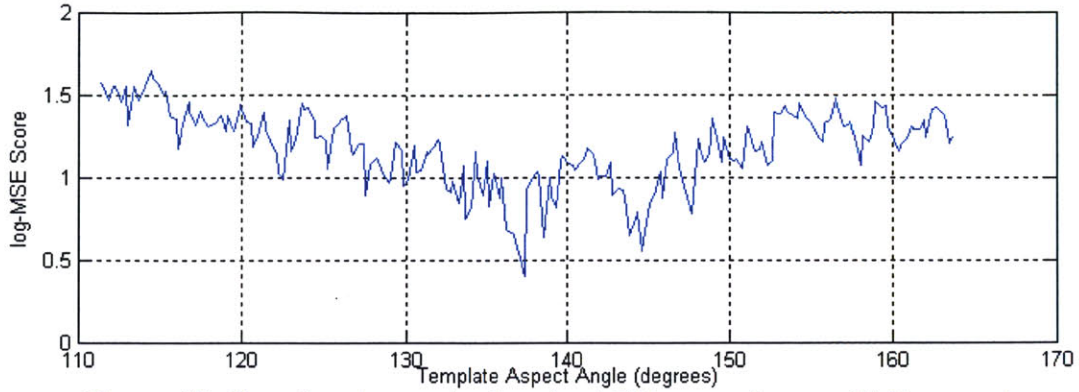
Figure 53. Template Aspect Angle v. log-MSE score after one CAT comparison

This figure would seem to indicate that the back-estimated aspect angle taken from the best-matching template HRR would correspond to approximately 138°. The "random similarity" referred to above, for example, might be visually represented by a random low spike in this figure at 123° causing a much larger error in aspect angle estimation:
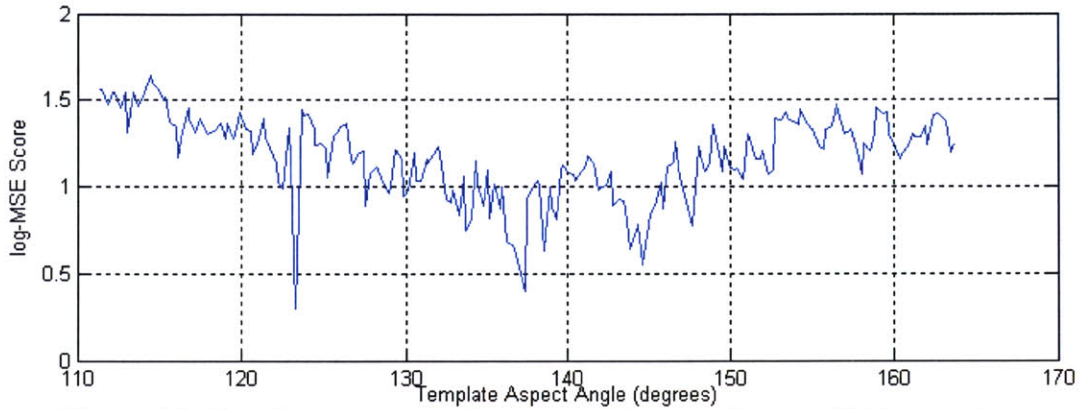
Figure 54. Template Aspect Angle v. log-MSE score after one CAT comparison showing "random HRR match" spike at 123° causing error

To mitigate these random circumstances, the MATLAB correlation function, *xcorr*, has been used to find an "averaged" minimum. The above data is correlated with a vector of zeros the that is the same size as the number of data points, except for a few consecutive cells with the value "1" of a specified parameterized length. This essentially averages every data point in the above figure using the specified number of surrounding data points. The minimum of the new, averaged set of data points is taken as the back-estimate of the aspect angle. Figure 55 shows the "smoothing" or "averaging" of the above data points for a variety of correlation "lengths" given the specific original return (jagged blue thin line on bottom):
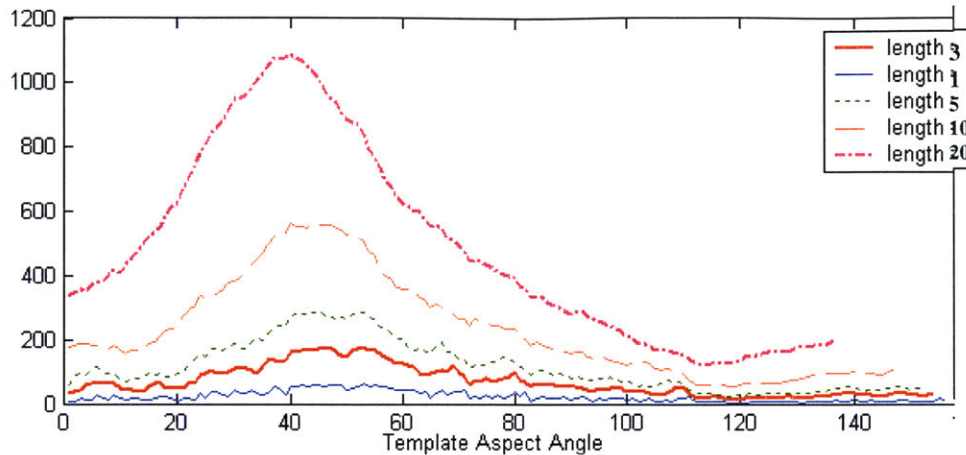
Figure 55. Correlation Results for specified of parameterized correlation lengths (intensity v. aspect angle)

As you can see, the longer the correlation "length" of 1's, the more smoothing takes place, thus alleviating the above problem. The maneuvering target scenario was again used and tested with a number of parameterized correlation lengths. The table below shows the resulting overall average back-aspect estimation error as well as the averaged difference in estimation error between the Kalman estimates and CAT Back-estimates (larger value is better). Additionally, the problem referred to above, the number of specific scans with large error (error over 30°), is also noted:

Correlation "length"	1	2	3	4	5	10	20	30
Average Overall Back Aspect Angle Estimation Error (degrees)	3.80	4.32	3.72	4.41	6.01	4.89	5.31	6.57
Average Difference between Kalman and Back Estimation per scan	4.67	4.70	4.73	5.09	3.71	3.84	3.36	1.63
# of scans where Back Estimation Error is greater than 30 degrees	3	3	2	3	8	8	4	6

Table 9. Back Aspect Angle Estimation performance for specified correlation lengths

The results indicate that the optimal correlation "length" is between 1 and 4. Using a correlation length of 3 provides a large advantage over Kalman Filter estimation per scan (4.73°) and the smallest overall average back aspect angle estimation error of 3.72°. There are only 2 problematic scans for a correlation length of 3 as opposed to 3 for lengths of 1, 2, and 4. Plans exist to harbor these findings in the future. Specifically, back-estimation will be useful in the accurate storage of HRR profiles in the SAT Database (Section 5.3) and as the track aspect angle used in report-to-track or report-to-database aspect angle difference comparisons. Remember that the above tests took place assuming the correct association. Therefore, the expected performance in a true system would not be as high due to incorrect associations. However, this should not have a major affect on performance because it is also expected that an incorrect association is recognized during SAT and the database would be reset in a more accurate fashion (see section 5.3.2 below).

CHAPTER 5.

SIGNATURE-AIDED-TRACKING (SAT)

Studying the performance of SAT involves the analysis of the match/mismatch decisions, which directly affect track continuity. The studies performed below will be similar to those used to test the version of SAT initially obtained, where it was determined that SAT was largely ineffective using only 1-D HRR profiles. This research will attempt to prove otherwise. Tests have been performed on the previous algorithm in the past, using the MSTAR data set and BHDI HRR processing. As stated in Section 1.5.1, the statistics and profiles evaluated in the tests below were generated using the MTFP data set.

5.1 Performance Analysis of Initial System

As detailed in Section 1.5, SAT aids data association by comparing the stored track HRR profile(s) to the HRR profile from the current radar detection. The most likely track-report pair is determined by a likelihood value representing the probability that the HRR profile's originated from the same "matching" target. This "match" is different from the "match" described CAT: It is considered a match in *target* as opposed to a match in target *class*. SAT requires no prior knowledge of target class and thus can only make decisions based upon the belief that the report target is the same as the stored track target. An MSE value for every possible track/report association is computed and an additional adjustment is made to the association matrix (χ^2_{SAT}).

One must recall that if the difference between the current report's estimated aspect angle and the track's stored aspect angle is less than a desired error threshold (typically ten degrees), then this signature comparison can be made. It was proven above that the standard aspect angle error is less than $10°$ only about 67% of the time. Therefore, the performance results from this "initial" version of SAT will resemble the performance of the kinematic tracker alone on 33% of the scans. When an MSE score is available, it is analyzed against the statistical expectations of MSE scores for both matching and mismatching target HRR's. Again, if an MSE score comes from comparing two profiles of the same class, it is expected to lie near the center of the match PDF; if not, it should lie near the center of the mismatch PDF. Therefore, greater separation in match and mismatch PDF's will result in more accurate and more valuable χ^2_{SAT} adjustments according to $\chi^2_{SAT} = -\log(MatchPDF/MismatchPDF)$. Section 1.5.1 details the statistics generation for the original system. The match and mismatch statistics are generated for a $10°$ threshold and are not distinguished by sector. These statistics and the resulting PDF's are as follows:

$$\mu_{match} = 1.0101 \quad \mu_{mismatch} = 1.2160 \quad \sigma^2_{match} = 0.1142 \quad \sigma^2_{mismatch} = .1384$$
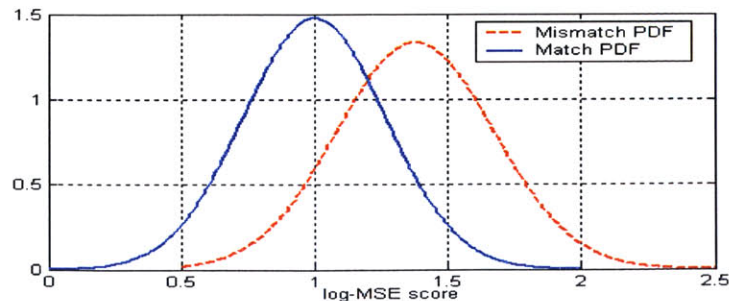
Figure 56. Match and Mismatch PDF's for initial SAT version

5.1.1 Constant Velocity/Parallel Following Targets

This scenario is exactly the same as the passing scenario tested during analysis of CAT. Twenty runs with 100 scans were generated and evaluated. A 20-scan section of this scenario (with a dt of 1 second instead of 5 seconds) with truth data and random measurement noise is depicted below. The •'s and 0's represent the target 1 truth data and detection, respectively, while the +'s and 's represent the same for target 2:
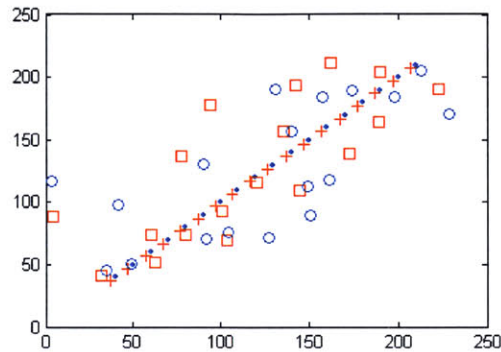
Cartesian coordinate plane: x (meters) and y (meters)

This scenario represents the situation in which SAT can best aid the data association conflict. During each scan, the following two hypotheses are evaluated:
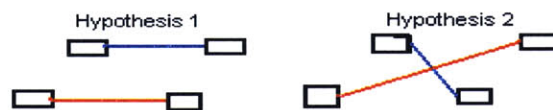
Hypothesis 1 is the true hypothesis. However, at many points, the noisy measurements are situated so that hypothesis 2 would seem correct. SAT is adept at fixing this problem because the HRR profiles from scan A and scan B are used to determine which report HRR (scan B) belongs to which track HRR (scan A). With the ground truth as hypothesis 1 above, the true aspect angle for either will not change throughout the entire run. Therefore, all HRR profiles from both targets should always be strikingly similar and SAT should correct most kinematic missasociations.[*] This scenario is used to evaluate SAT performance in a "best-case" scenario.

Twenty runs of this scenario only using the kinematic tracker reveal that the correct track-report association was chosen 50.4% of the time. Conversely, with the initial version of SAT in use (with a 10° aspect angle threshold), the correct association was chosen 95.2% of the time. If there were no aspect angle threshold in place, SAT would choose the correct association with probability 95.5%. The exceptional performance in this environment is expected.

5.1.2 X-non-crossing Scenario

The X-non-crossing scenario used to test CAT was used in testing SAT as well. It is hypothesized that only a very slight advantage will be gained by SAT in this case, if any. This is because as the target is maneuvering, aspect angle changes rapidly. The threshold will not allow

---

[*] for this same reason, CAT will be completely useless in this situation (Section 4.2.1.1)

SAT to be used while there will be very large errors in aspect angle estimation due to maneuver. If the SAT threshold were non-existent, the improvement would not be substantial because HRR profiles are extremely distinct over all aspect angles.

In 30 runs, the kinematic tracker alone chose the correct association with probability 69.5%. Overall, with SAT during the same 30 runs, there were 73.6% correct associations. Figure 56 shows the percent of correct associations for SAT in terms of scan #. All runs of this scenario were averaged to provide the below results:
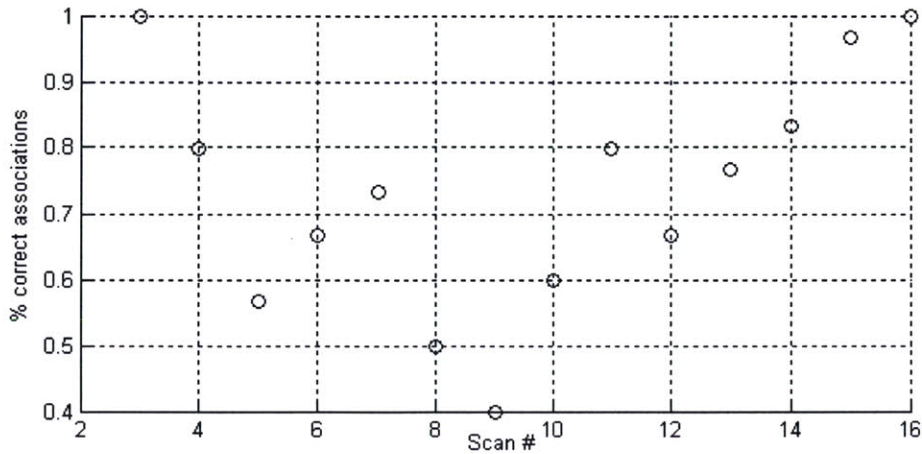
Figure 57. % correct association v. Scan # for the X-non-crossing scenario using the initial version of SAT

The following plot shows the average χ^2_{SAT} adjustment for both the correct associations (blue line) and incorrect associations (red dotted line) involving the Scud Launcher and the ZSU-carrier by scan #. Recall that a higher χ^2_{SAT} relates to a lower confidence in association (i.e. lower is better). Also recall that when a χ^2_{SAT} score is not available because of the threshold, the cell in the χ^2_{SAT} matrix is equal to zero; this is also averaged into the below results. In all situations, the difference between correct and incorrect association χ^2_{SAT} score is directly related to the probability of misassociation.
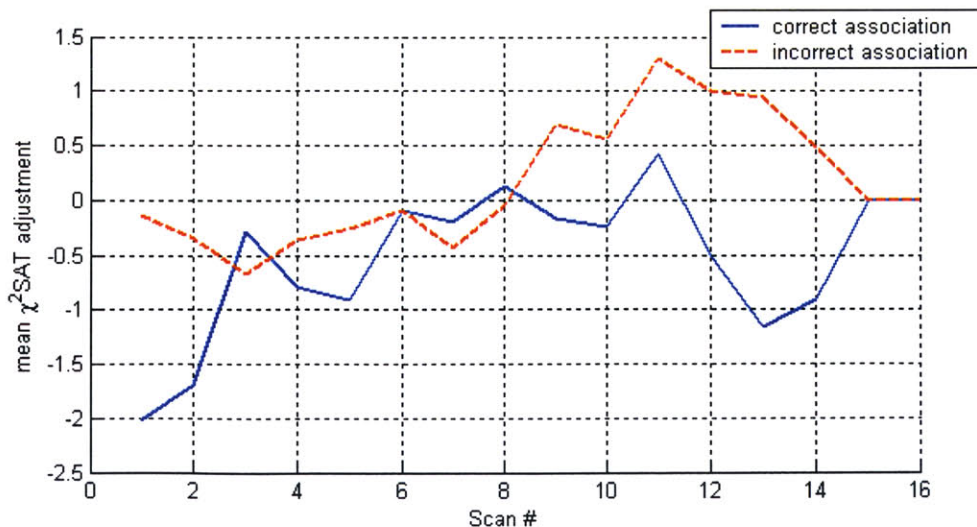
Figure 58. average χ^2_{SAT} adjustment for the correct (blue line) and incorrect (red dotted line) associations in the X-non-crossing scenario using the initial version of SAT

In scans 6-8 (the start of the maneuver), the χ^2_{SAT} adjustment leads to an incorrect association, however these mistakes are corrected soon after. Without the aspect angle threshold, the percentage of correct percentage increases to 86.0%, most likely due to an incorrect assumption for the aspect angle threshold.

5.1.3 Parallel Maneuvering Scenario

The parallel maneuvering scenario is made from the single-target maneuvering scenario used to test vehicle identification capability with CAT. All analysis will be done with respect to scan number. With a smaller dt such as the 1 second used in this testing, the performance will improve because there is less of a change in true and estimated aspect angle between scans. However, a large dt will cause the performance to degrade due to maneuvering, especially if $dt > \tau_m$.

Twenty runs using the kinematic tracker alone led to 50.0% correct associations. Through these 20 runs, SAT chose the correct association 81.3% of the time with an aspect angle threshold and 90.6% without an aspect angle threshold. Figures 59 and 60 evaluate the effectiveness of SAT during this scenario by scan #.

Figure 59. % correct association v. Scan # for the parallel maneuvering scenario using the initial version of SAT
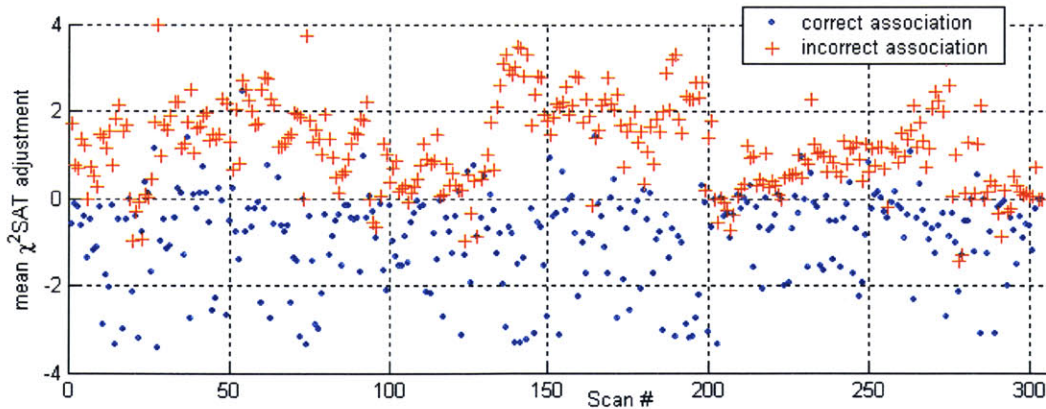
Figure 60. average χ^2_{SAT} adjustment for the correct (blue ·'s) and incorrect (red +'s) for the parallel maneuvering scenario using the initial version of SAT

There are only a handful of scans (all of which occur during maneuvers) in which the incorrect χ^2_{SAT} score is lower than the correct one. However, at no point is the incorrect score too low as to where it would not be corrected by an accurate χ^2_{CAT} or χ^2_{KT} adjustment. This proves that SAT

is extremely useful during constant velocity situations and provides little help or hindrance during difficult maneuvering situations.

5.1.4 Merging Target Scenario

The merging target scenario tested below is the same as is used to analyze CAT. SAT should be highly effect during the straightaway in the middle of each run and not as effective during the merge and diverge points. The following plots are similar in explanation to those above and are a result of 30 separate runs:

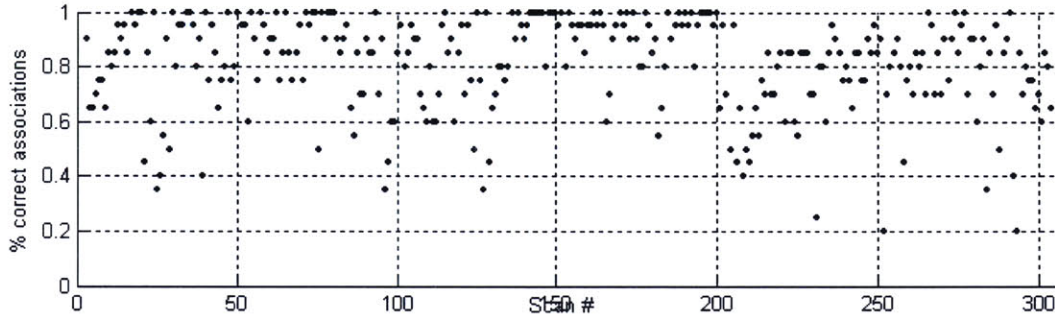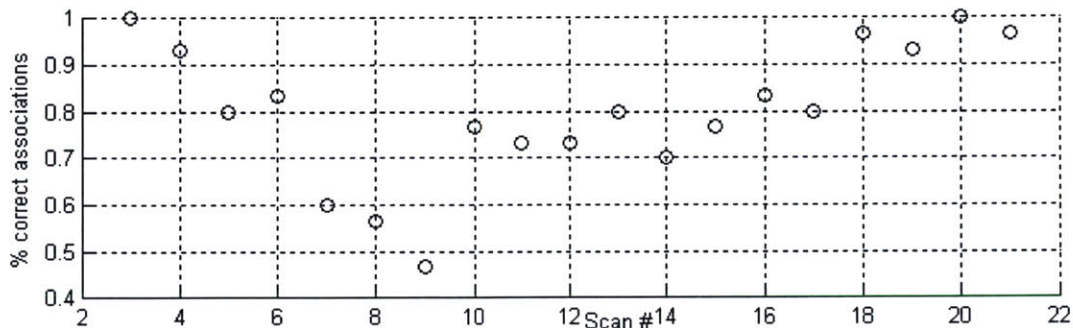**Figure 61.** % correct association v. Scan # for the merging target scenario using the initial version of SAT
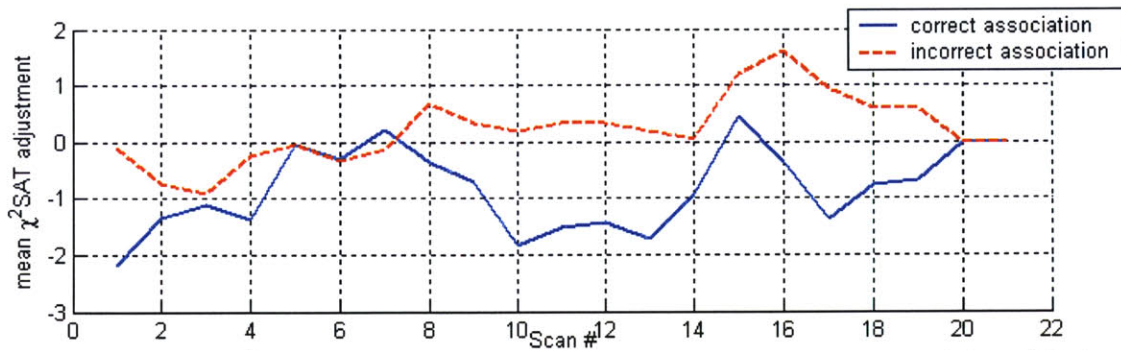
Figure 62. average χ^2_{SAT} adjustment for the correct (blue line) and incorrect (red dotted line) for the merging target scenario using the initial version of SAT

Thirty runs using the kinematic tracker alone led to 67.4% correct associations. SAT chose the correct association 80.0% of the time with an aspect angle threshold and 87.9% without an aspect angle threshold. As hypothesized, SAT performs exceptionally well during the straightaway (scans 9-15) and not as well during the merge (5-8) or diverge point (15-18). It appears that the merge point is a greater concern.

5.2 Enhanced SAT Statistics

As previously declared, the aid in data association that SAT provides is directly linked to the accuracy of, and separation in, match and mismatch PDF's. Additionally, the similarity between the method used to form these statistics and the actual comparisons performed during tracking is vitally important. Therefore, match and mismatch statistics have been evaluated while differentiating statistics by aspect angle sector and while varying the aspect angle threshold. This contrasts from the statistics used above in that no sector dependency existed and the aspect threshold was incorrectly assumed to be 10°.

78

The desired results are match and mismatch PDF's with greater separation and accuracy than in the above tests. PDF "separation" is measured by the difference between the lower (1 standard deviation) bound of the mismatch PDF and the upper bound of the match PDF. Using the statistics from the initial tests above, this corresponds to $\mu_{mismatch}$ - $\sigma_{mismatch}$ = 0.8440 and μ_{match} $_+$ σ_{match} = 1.3480 for a separation of –0.504. This is a measure of the PDF "overlap" with a larger separation value obviously desired. A large, random sample of the available MTFP HRR profiles have been used in the formulation of the below statistics. Specifically, there were 99485 matching target comparisons and 208193 mismatching target HRR comparisons used in statistics formation.

5.2.1 Use of Sectors

During analysis of the CAT statistics (Section 4.2.2), it was noted that the mean log-MSE scores are highly dependent upon aspect angle sector. Statistics were generated where, for each HRR signature comparison, the following was recorded:

    1) If the comparison originated from matching or mismatching target HRR profiles[*]
    2) The aspect angle of both profiles (and the aspect angle difference)

Figure 63 shows the mean of the match (blue line) and mismatch (red dotted line) SAT statistics. It is a plot of the log-MSE score versus aspect angle threshold where the plot row corresponds to the aspect angle sector. Subsequently, Figure 64 shows the PDF separation in terms of aspect angle threshold. Again, recall that the PDF separation in the initial version of SAT was approximately –0.5.
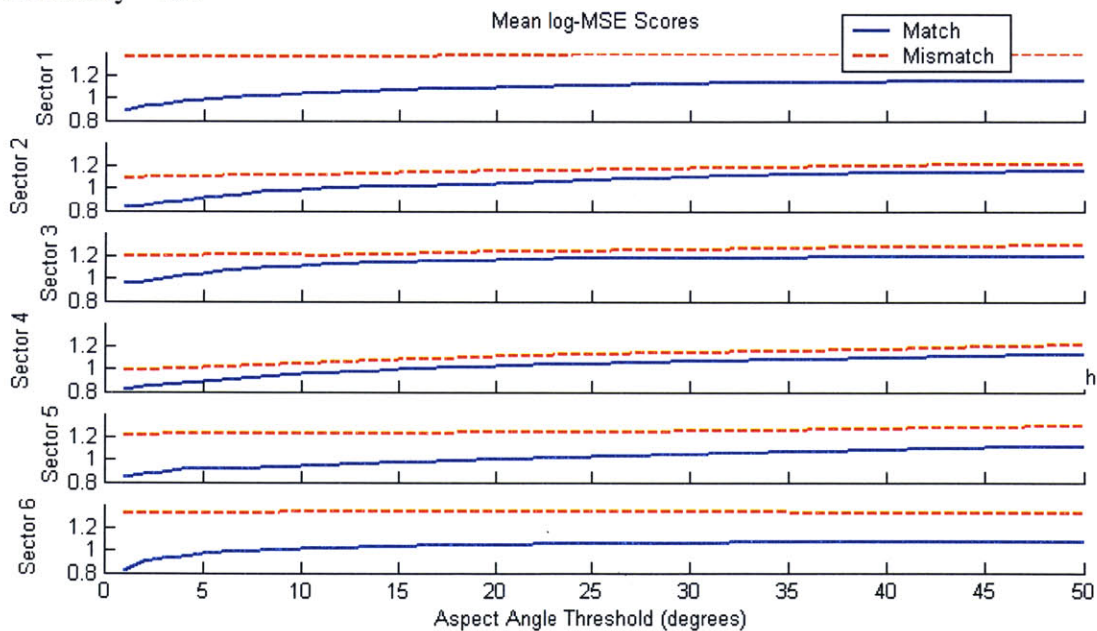
Figure 63. SAT Statistics (mean MSE score) for both matching and mismatching comparisons

---

[*] comparisons among the three variants of the T72 tanks were not used

79
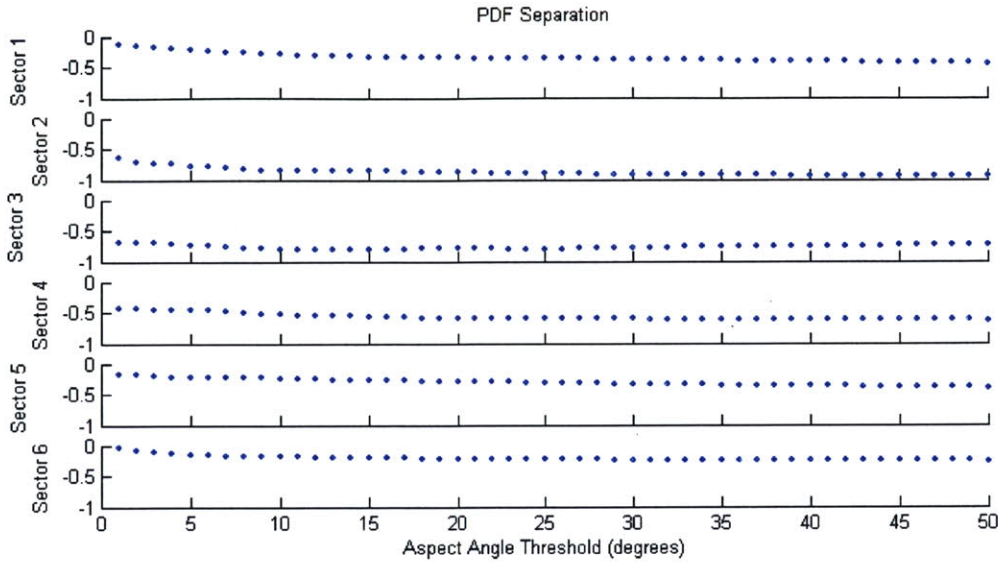
Figure 64. SAT Statistics (PDF separation) for both matching and mismatching comparisons

As with CAT, as targets approach broadside (90° aspect angle; sectors 3 and 4), the PDF separation decreases. It is therefore assumed that SAT will provide less assistance for targets at broadside. Only in sectors 1, 4, and 5 is the PDF separation generally above –0.5. Additionally, the mismatch mean from sector 4 is lower than the match mean from sector 3. This is most likely a product of the particular targets used in formation of these statistics. Regardless, this proves that the use of sectors in statistical comparisons and during FAT is inherently more accurate than when they are not; however, it remains to be seen if the performance of SAT improves in such a case.

It must be discerned that the PDF separation decreases as aspect angle threshold increases. However, there is still significant separation at the maximum error threshold point of 27.5 degrees (Section 4.1). This means that variable statistics and a variable aspect angle threshold should be used with confidence. In further tests, the threshold is determined using a method similar to error window size determination in CAT (Section 4.2.1). Figure 65 below is a plot of the SAT Statistics (mean MSE and PDF separation) with fused sectors information:
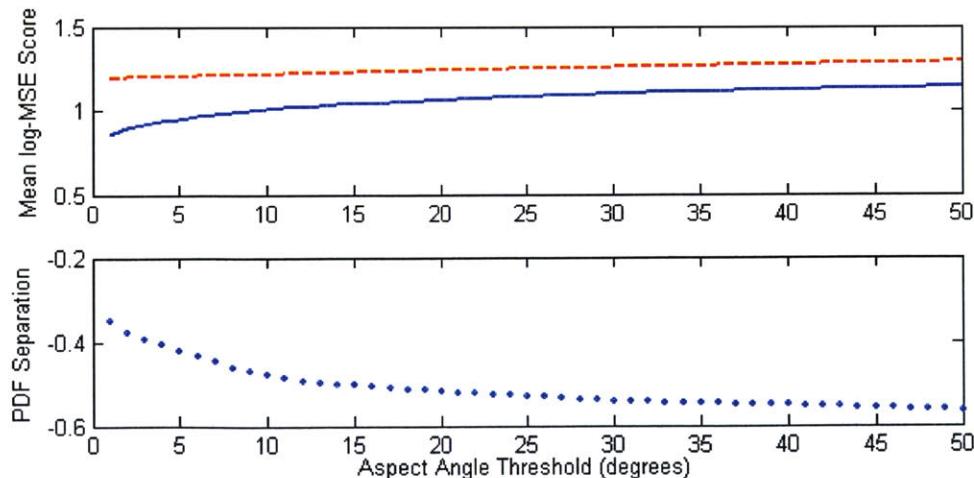
Figure 65. SAT Statistics (mean MSE score) for both matching and mismatching comparisons without the use of sectors

80

When the statistics are fused, as above, the PDF separation is higher than in sectors 2, 3, and 4, but lower than in sectors 1, 5, and 6. However, the main point is that PDF separation does not decrease severely after aspect angle thresholds between 10° and 25°. This means that there is flexibility when implementing a larger database search. The exponential decay seen above for the separation is due to a large increase in expected MSE variance when sectors are fused. Both methods will be compared in tests below.

5.3 On-The-Fly SAT HRR Database

Another proposed improvement to the existing FAT algorithm was to include the use of an "on-the-fly" SAT HRR database. Essentially, the report HRR profile, its corresponding estimated aspect angle, and its predicted aspect angle error window will be stored in the track history of its associated track after every scan. In future SAT HRR comparisons, the estimated aspect angle of the current track-report association would be used to extract these previously stored profiles from aspect angles within a calculated error threshold. Ideally this will eliminate problems related to situations where profiles in two sequential scans are not within 10° of aspect angle, thus rendering SAT useless. This error threshold takes into account the possible aspect angle error of both the stored profiles and the current report:

$$e_{total} = \max(e_{track\ Database\ profile} + e_{report})$$

All profiles in the SAT database within this total error threshold may be used as the "group" in MSE calculations. The error window used later to retrieve the appropriate statistics for χ^2_{SAT} generation is equal to the report error plus the mean of all $e_{track\ DB\ profile}$ used in comparison (template error from all available templates). Two proposed uses for the "group" of MSE calculations are 1) using the minimum log-MSE score, or 2) using the average log-MSE score.

5.3.1 SAT Database Statistics

A MATLAB function was generated to statistically analyze comparisons in the manner stated above. The maximum allowable error threshold is 50°. These statistics are 3-dimensional: the aspect angle error threshold, the number of database profiles, and the sector are all variables. One hypothesis is that as the number of profiles available for comparison increases, there is less of an opportunity for random error using an average of the scores and more of an opportunity for random error when using the minimum score. Therefore, before tests were done, it was assumed that a combination of these methods might lead to maximum effectiveness of an enhanced version of SAT.

Below are plots representing the mean, variance, and PDF separation of the log-MSE comparisons using both the average and minimum techniques. During these statistical evaluations, the matching and mismatching MSE scores were chosen at random from the overall set of matching and mismatching scores. There are 100 random trials at each threshold level between 1 and 50° and at each number of available profiles between 1 and 30. To ease visualization and analysis, the plots below have fused the results from each sector. However, it must be noted that the results for both of these techniques vary by sector in the same manner as above. In Figures 66 and 67, the aspect angle threshold is set constant at 20° while the number of available profiles is variable between 1 and 30.[*]

---

[*] Recall that the initial version of SAT uses a PDF separation of –0.5

81
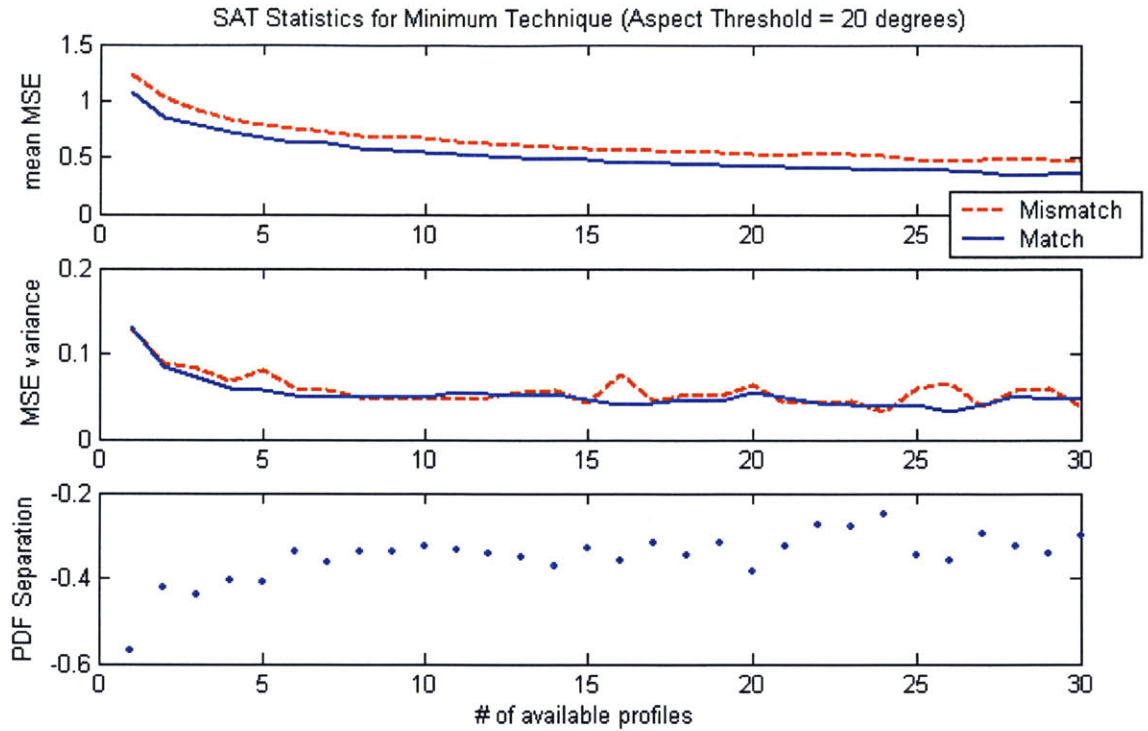
Figure 66. Merged SAT statistics for the minimum technique varying the # of profiles used (aspect angle threshold = 20°)
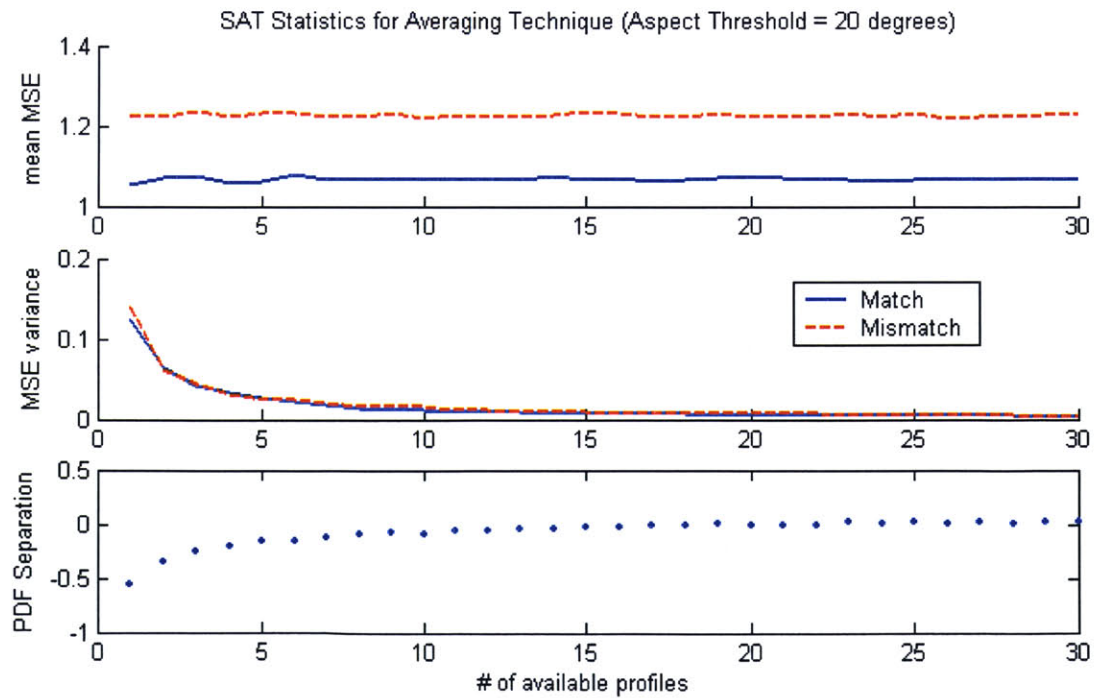
Figure 67. Merged SAT statistics for the averaging technique varying the # of profiles used (aspect angle threshold = 20°)

The next set of plots holds constant the number of database profiles available at 5 while varying the threshold value in order to demonstrate the affect of larger aspect angle error estimates:
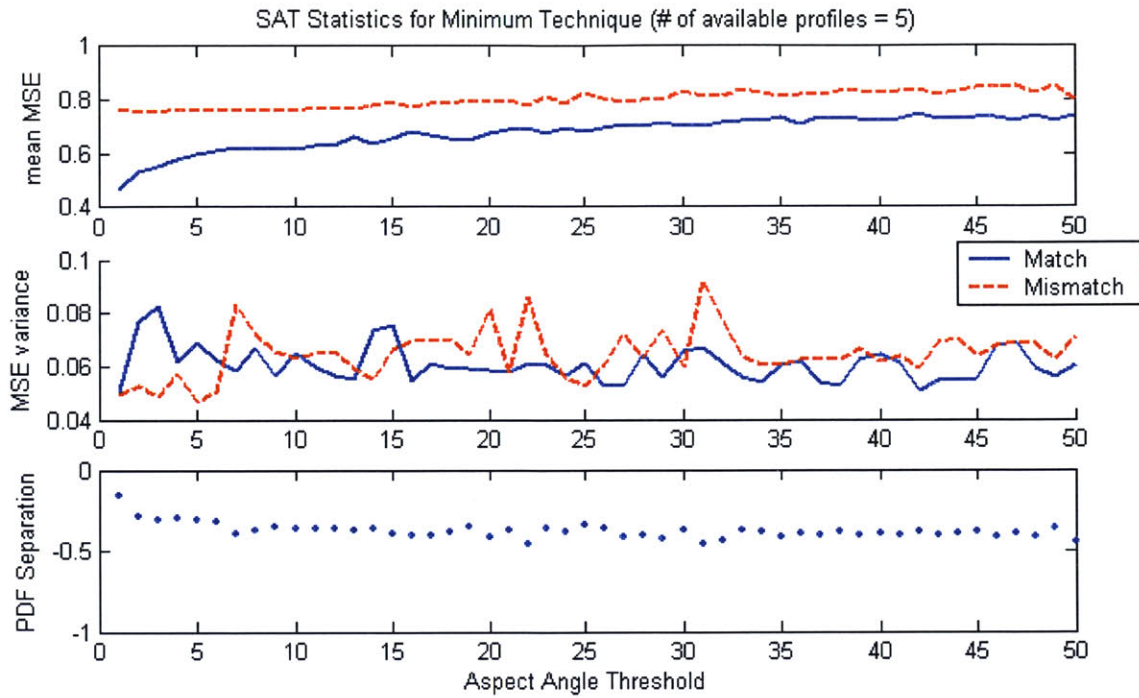
Figure 68. Merged SAT statistics for the minimum technique varying the aspect angle threshold (# of profiles used =5)
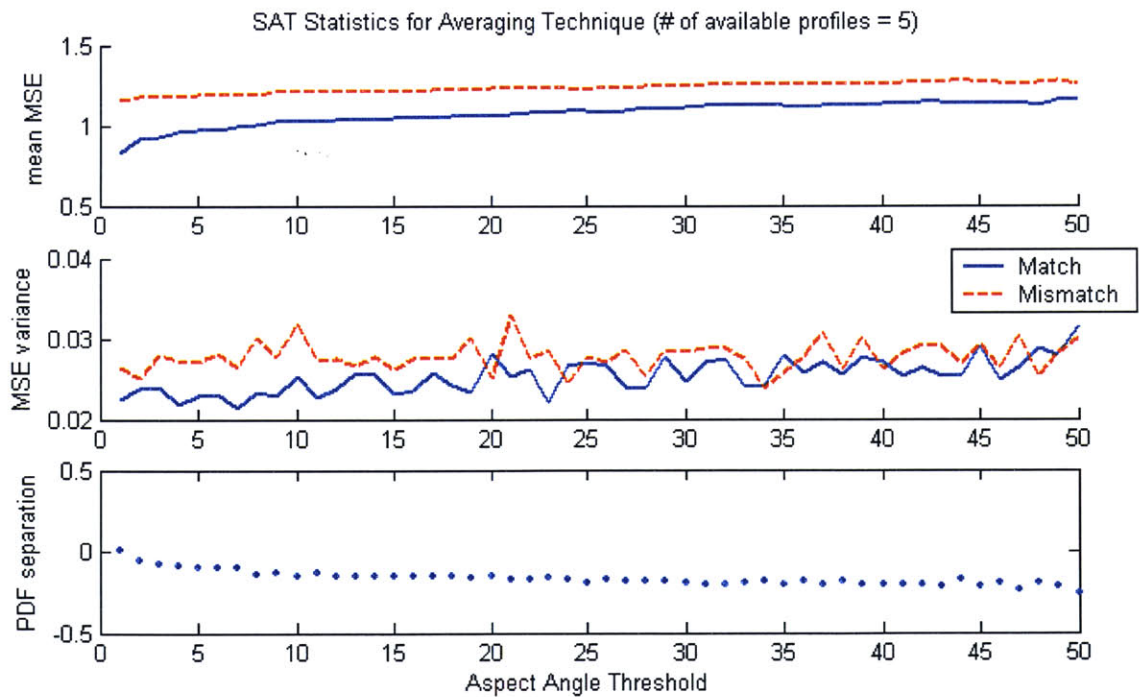
Figure 69. Merged SAT statistics for the averaging technique varying the aspect angle threshold (# of profiles used =5)

In both examples above, the averaging technique clearly provides greater PDF separation than the minimum technique, particularly as the number of available profiles increases. In all cases above, the PDF separation is greater than −0.5 at some point, leading to the conclusion that the use of a database will lead to more accurate data association under optimal conditions. Optimal conditions can be defined as when the aspect angle threshold is low and the number of profiles available is high. As aspect angle threshold increases, the PDF separation decreases. However, the PDF in the averaging technique is continually well above −0.5 with 5 profiles available while the minimum technique is not. This allows us to confidently use a larger (and more accurate) estimation of the aspect angle error. The combination of large PDF separation and low variance is important because it will increase the effectiveness of χ^2_{SAT} for MSE scores very close to the match PDF. Therefore, it is hypothesized that little advantage will be gained using the minimum SAT database technique, but a considerably larger advantage will be attained when using the averaging technique; specifically as the number of profiles grows large (greater than 5). Overall, at least minimal improvement is expected due to the simple concept of inherent accuracy in enhanced aspect angle error estimation and the ability to search a running database for closely matching profiles. While the use of sectors might improve performance, there is concern about incorrect sector estimation and the extreme discontinuity in statistics between consecutive sectors (2-3 or 4-5). Both techniques will be tested below.

5.3.2 Database Build-Up/Reset

One issue not addressed thus far is performance in the face of continually changing track-report associations. More specifically, recognizing when a track has a new target assigned to it. The answer is simple simulated environments yet remains the greatest challenge to a robust system. As mentioned in the analysis of CAT, the simulation tool used in this report always assigns the same number to the each target report (i.e. report 1 is always a Scud Launcher). It is therefore easy to use this knowledge and identify incorrect track-report associations and changing of track target class. When this occurs, the SAT database must be reset to begin to include HRR profile's from this new target. The results from this perfect knowledge case will be used as a control for the other, more realistic methods to reset the database. This represents a best case, or most-accurate situation, however, it is possible for other methods of resetting the database to produce better results.

Specifically, an HRR profile will be added to the database if it produces an MSE score within an expected "matching target" value. If a non-matching target HRR is added to the database mistakenly, it will be used as part of the "group" of HRR's in future analysis. Using the minimum technique, it will be harmful when the minimum MSE score from all comparisons results from this "mistake" database profile. For this reason, it is imperative to reset the database so that it does not contain such incorrect profiles. Using the averaging method, this incorrect database profile will serve to raise the average MSE score during future comparison's, thus leading to an eventual database reset when the average MSE score is above a specific limiting value. For this reason, there is less of an impact from these "mistake" profiles using the averaging method. Basically, this only affects the averaging method when the database is small, while it will persistently affect the minimum method. With the averaging technique, it is still possible that a "missed reset" will lead to a higher percentage of correct association because of the size and continual correct buildup of the database.

A realistic scenario does not have the luxury of perfect knowledge of target class-report assignments, or tracking would be unnecessary. Therefore, a decision must be made according

to a given standard as to when the target class of the track has changed and/or the database contains too many "mistake" profiles. One solution is to use the output of the classifier in CAT. However, one cannot rely upon the availability of this information because SAT, in contrast to CAT, by definition, was created to handle unknown target classes. This method will not be tested. A temporary solution to this problem is to use the actual SAT comparisons and statistics to decide when the target is different from those in its database or if database profiles themselves do not match well. There are several methods that can be used to perform these evaluations, many of which have been explored but not noted during the performance comparison phase below. Regardless, accurate resetting of the SAT database is imperative if one is to harbor the advantage gained by the apparent extreme separation in match and mismatch PDF outlined above.

The most effective method used to date forms the results below. Specifically, the SAT database will be reset when an MSE score from the hypothesized correct track-report association is greater than the expected mean matching MSE score plus 1 (or 2) standard deviation(s). A parameter used in conjunction with this method is called the "fail limit". It corresponds to the number of consecutive scans that the MSE score is permitted to be below the above limiting MSE value before the database is actually reset.* The SAT database of every track possibly associated with the radar detection in question is also reset; it is assumed that the other hypothesized association is also incorrect. This method is extremely dependent upon accuracy of the PDF's and statistics generation.

An additional tool used in database buildup is called "Database Cleansing". This feature can be easily turned on or off during initial parameter selection. If it is determined that the database should not be reset, cleansing occurs: The report HRR profile to be added to the database is tested against all other database HRR profiles within an appropriate error window. If any of the resulting MSE scores are higher than the limiting MSE value, then the next constraint is tested. An HRR profile is only added if the difference between the SAT MSE score from the hypothesized correct association and the MSE score from the hypothesized incorrect associations are all larger than a pre-determined limiting value. This limiting value is equal to the matching mean MSE score minus the mismatching mean MSE score. This constraint will correct instances in which all SAT MSE scores are below the high score limit yet the hypothesized correct association MSE score is higher than the incorrect association's MSE score. If all tests pass, the database of the track involved in the association in question is appended with this new profile.** The resulting system is somewhat complex, but has been created to mitigate situations found to be difficult for SAT to handle.

5.3.3 Performance Comparison

The following evaluations will utilize the aforementioned on-the-fly SAT database and database reset methods. Various methods of implementation are analyzed, including the original technique, minimum Technique, and averaging Technique. For all of the new tests, the aspect angle threshold value will be calculated as in section 5.3.*** There were 10 runs of each test using the same exact random number seeds (for measurement error) in each test. Some tests were run with the high MSE limit set using 2 standard deviations as opposed to 1.

---

* if no templates are available for analysis, one-half (.5) of a failure is added towards reaching the fail limit
** again, some tests are done using 2 standard deviations
*** the original technique test will only use an error threshold value equal to e_{report}

5.3.3.1 Enhanced SAT

The following table shows the percent of correct associations using the original SAT technique:

Scenario / Parameters	Constant Velocity (10 runs)	X-non Crossing (10 runs)	Merge/Diverge (10 runs)	Parallel Maneuvering (10 runs)
Kinematic Tracker	50.2	70.0	70.0	49.9
Initial SAT	84.1	74.3	76.3	66.8
Initial SAT (no threshold)	84.0	80.0	79.5	79.1
Enhanced SAT (sectors)	80.9	80.0	79.5	72.1
Enhanced SAT (fused sectors)	84.1	74.3	76.3	73.0

Table 10. % missasociations for the enhanced original technique

The improved performance of the initial SAT with no threshold is expected in scenarios where the ground truth is relatively straight-line motion; all of the tested scenarios have such periods. Slight improvement also occurs in the intersection scenarios (X-non-crossing and merge/diverge) because the bulk of improvement occurs on the constant-velocity scans. Generally, it would not be a bad idea to use the original version of SAT with no threshold, so long as the true target aspect angle is not expected to drastically change in one scan-update-interval (dt).

The above show that the use of sectors is inherently more accurate and helpful in maneuvering situations. However, performance is somewhat degraded in constant-velocity situations. This inference holds true during scan-by-scan analysis of the parallel maneuvering scenario, which includes scans of both constant velocity and target maneuvers. This can be explained by the prevalence of incorrect estimation of target aspect angle sector. For example, if a target has an aspect angle of 50° and a possible aspect angle error of 25°, the true sector would be 2 while the possible incorrectly estimated sector could be either 1 or 3.[*] Inexplicably, the larger advantage comes when sectors are used during intersection scenarios. While it is hopeful that SAT can be useful in all situations, more focus is placed upon the constant velocity and parallel target situations that CAT cannot resolve. Therefore, if using the enhanced original version of SAT, it is more advantageous to use a fused sector method.

Across all scenarios, the enhanced version of SAT using sectors provides an added 3.6% advantage over the initial version and a 2.1% advantage exists when fused sector information is utilized. Conversely, if a SAT threshold is not used with the initial system, an improvement in performance of 7.0% is attained. Again, the use of sectors significantly improves the performance and accuracy of SAT during the intersection scenarios.

5.3.3.2 Minimum SAT Database

Table 11 shows the percent of correct associations using the minimum SAT database technique:

---

[*] Because of sector prediction error, the fusion of sector information might also aid in CAT; this fact was not tested in this research

Scenario / Parameters	Constant Velocity (10 runs)	X-non Crossing (10 runs)	Merge/Diverge (10 runs)	Parallel Maneuvering (10 runs)
Kinematic Tracker	50.2	70.0	70.0	49.9
Initial SAT	84.1	74.3	76.3	66.8
Initial SAT (no threshold)	84.0	80.0	79.5	79.1
Minimum SATDB (Perfect Knowledge) - Sectors	73.8	80.0	78.4	69.3
Minimum SATDB (Perfect Knowledge) – Sectors/Std 2	38.6	80.7	81.1	71.0
Minimum SAT DB (Fail Limit 0) - Sectors	41.6	79.3	80.1	67.3
Minimum SAT DB (Fail Limit 0) – Sectors/Std 2	53.4	80.7	81.1	70.3
Minimum SAT DB (Fail Limit 1) - Sectors	46.7	80.0	81.6	68.3
Minimum SAT DB (Fail Limit 1) – Sectors/Std 2	53.7	79.3	81.1	68.6
Minimum SATDB (Perfect Knowledge) – No Sectors	80.8	81.4	78.4	75.0
Minimum SATDB (Perfect Knowledge) – No Sectors/Std 2	81.2	81.4	77.9	75.3
Minimum SAT DB (Fail Limit 0) – No Sectors	74.2	77.7	75.8	71.4
Minimum SAT DB (Fail Limit 0) – No Sectors/Std 2	73.5	80.0	77.9	75.3
Minimum SAT DB (Fail Limit 1) – No Sectors	73.0	80.0	76.3	71.8
Minimum SAT DB (Fail Limit 1) – No Sectors/Std 2	72.8	80.0	74.4	73.0

Table 11. % missasociations for the minimum SAT database technique

The minimum SAT database technique appears to provide little advantage over the initial SAT in all scenarios. However, there is a slight advantage (4.7%) when perfect knowledge of incorrect associations is used in evaluations with fused sector information. A severe degradation of performance exists when using the realistic methods to reset track databases, most likely due to the presence of the aforementioned "mistake" profiles in the database. Of note is the fact that in realistic situations (when fail limits are used), a high MSE limit using 2 standard deviations leads

to superior results. In most cases, the fusion of sector information improves performance. Again, there is potential for the use of this type of SAT database when perfect knowledge exists, however, better results are expected from the averaging technique.

5.3.3.3 Average SAT Database

The following table shows the percent of correct associations for the average SAT database technique:

Scenario / Parameters	Constant Velocity (10 runs)	X-non Crossing (10 runs)	Merge/Diverge (10 runs)	Parallel Maneuvering (10 runs)
Kinematic Tracker	50.2	70.0	70.0	49.9
Initial SAT	84.1	74.3	76.3	66.8
Initial SAT (no threshold)	84.0	80.0	79.5	79.1
Average SATDB (Perfect Knowledge) - Sectors	72.2	78.6	84.7	75.9
Average SATDB (Perfect Knowledge) – Sectors/Std 2	73.2	78.6	84.7	77.2
Average SAT DB (Fail Limit 0) - Sectors	66.5	80.0	84.7	76.2
Average SAT DB (Fail Limit 0) – Sectors/Std 2	61.4	77.9	85.8	75.9
Average SAT DB (Fail Limit 1) - Sectors	61.3	75.0	83.7	73.9
Average SAT DB (Fail Limit 1) – Sectors/Std 2	61.9	77.1	83.2	74.4
Average SATDB (Perfect Knowledge) – No Sectors	86.5	79.3	80.5	78.5
Average SATDB (Perfect Knowledge) – No Sectors/Std 2	86.6	80.0	81.1	80.6
Average SAT DB (Fail Limit 0) – No Sectors	76.5	79.3	83.2	79.3
Average SAT DB (Fail Limit 0) – No Sectors/Std 2	72.8	77.7	80.0	79.1
Average SAT DB (Fail Limit 1) – No Sectors	75.2	78.5	81.1	76.4
Average SAT DB (Fail Limit 1) – No Sectors/Std 2	72.3	78.6	80.5	77.4

Table 12. % missasociations for the averaged SAT database technique

Again, the use of sectors leads to inferior performance most likely because of incorrect sector estimation. Without sectors, the use of the average SAT database given perfect knowledge produces an impressive 7.7% advantage using 1 standard deviation to calculate the MSE limit and an 8.9% advantage using 2 standard deviations. In the more realistic case where a fail limit of 0 is used, an advantage of 5.6% is produced. Conversely, more attention should be paid to the latter three scenarios tested because the constant velocity, straight-line scenario includes exceptionally matching HRR profiles from scan-to-scan due to very little change in true aspect angle. In the latter three scenarios, the use of a fail limit produces slightly better results (1.5% better) than using perfect knowledge. A higher fail limit almost always degrades performance.

Regardless, the performance of the fused sector SAT database average method given perfect knowledge is significantly better than that of the initial SAT system with and without a threshold. This proves that if near-perfect knowledge of an incorrect association exists, than optimal performance will be attained using this method in all kinematic situations. There is strong potential for this technique in the future. Another observation to note is the percent of correct associations given a large # of available profiles. Figure 70 plots this knowledge for a variety of the better-performing SAT database methods up to the limiting case when 15 profiles are available (sufficient tests were not available for numbers higher than this):
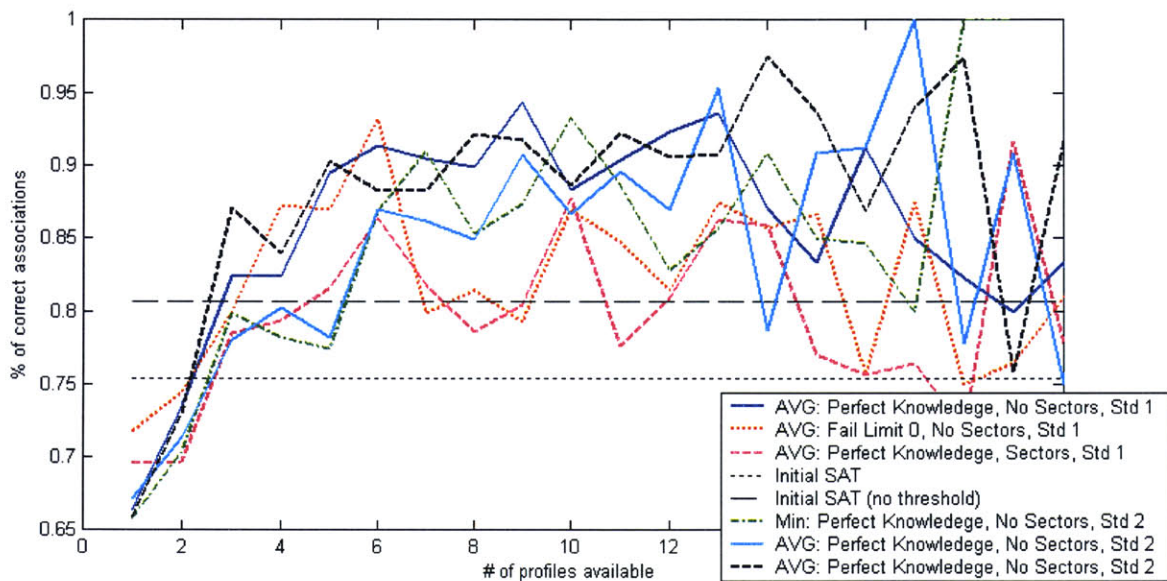
Figure 70. % of correct associations v. # of available database profiles

Again, the performance of the averaging technique is superior when perfect knowledge is attained and sectors are fused. However, in a realistic scenario using no sectors and 1 std, the performance is still always above the initial SAT once 3 profiles are available and, on average, still outperforms the initial version of SAT with no threshold. What must be taken from this observation is the point that if a sufficiently large SAT Database is available, it is possible to achieve near-perfect data association using the SAT averaging technique.

CHAPTER 6.

FINAL ANALYSIS AND CONCLUSION

6.1 Fusion of CAT and SAT

Recall from the above research that CAT is only useful during "intersection-like" target crossing situations. Conversely, SAT is particularly useful during parallel/following target situations. The simultaneous use of an enhanced version of both CAT and SAT should provide tracking performance that is far superior to both the kinematic tracker and the initial versions of CAT and SAT (FAT). The best-performing versions of these algorithms discovered above are used in this final analysis.

Specifically, the enhanced version of CAT with more accurate aspect angle error window estimation will be used. A five-target CAT database is also used. The average SAT database method will be used for SAT, testing both perfect knowledge and a fail limit of 0 using 1 standard deviation to calculate the high MSE limit. Additional tests will be performed using the aspect angle returned from CAT as described section 4.4.1 to represent the aspect angle of the report (as opposed to using the Kalman filter estimate) for later use with the SAT database. The resulting aspect angle error will then be analyzed while performance is not expected to drastically improve. Table 13 represents the percent of correct associations for the kinematic tracker, the initial version of FAT, and enhanced versions of FAT:

Scenario / Parameters	Constant Velocity (5 runs)	X-non Crossing (5 runs)	Merge/Diverge (5 runs)	Parallel Maneuvering (1 run)
Kinematic Tracker	51.2	67.1	68.4	50.0
Initial FAT	88.7	68.6	63.2	66.2
Enhanced FAT	79.8	71.4	70.5	83.1
Enhanced FAT (perfect knowledge SAT)	88.0	71.4	77.9	80.5

**Table 13.** % missasociations for specified tracking systems

Table 14 shows the average back-aspect angle estimation error per scan versus the Kalman filter estimation error for the above scenarios:

Scenario / Parameters	Constant Velocity (5 runs)	X-non Crossing (5 runs)	Merge/Diverge (5 runs)	Parallel Maneuvering (1 run)
Avg. Back Error (degrees)	4.1	14.4	11.9	17.2
Avg. Kalman Error (degrees)	0.8	17.9	16.4	10.8

**Table 14.** Evaluation of Back-estimation of Aspect Angle

In a multi-target environment, back estimation improves aspect angle estimation only during maneuvers. Again, an improved maneuver detector might be used in the future to take advantage of these findings. However, there was only limited testing done above with little attention paid to scan-by-scan evaluations.

90

The following four figures show the averaged χ^2_{CAT} and χ^2_{SAT} adjustments in addition to final χ^2_{fused} association matrix score by scan for the above four tests in order to analyze the origin of adjustments made throughout differing target maneuver models:
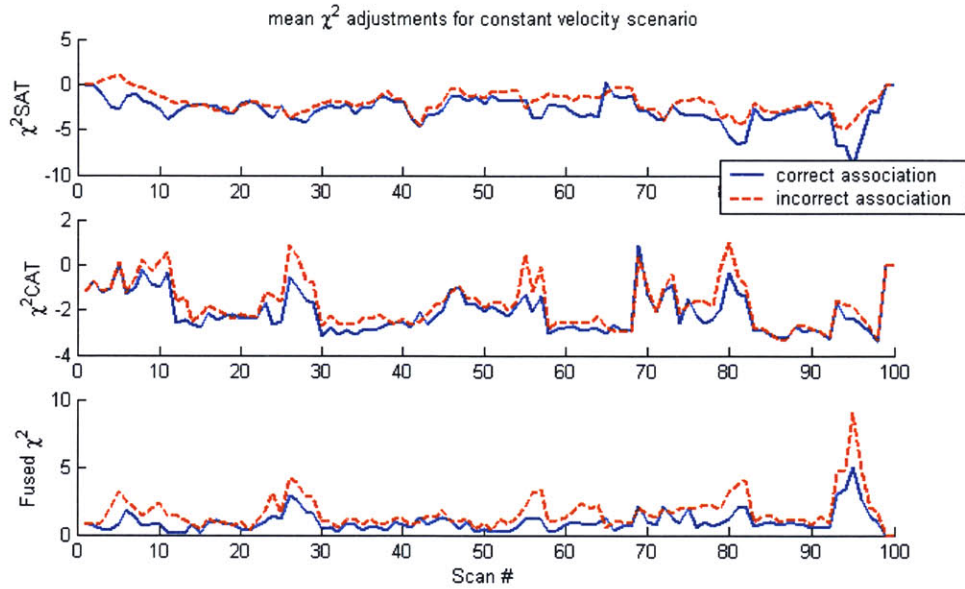

Figure 71. χ^2 scores by scan # for the Constant Velocity scenario

As expected, there is little difference between the correct and incorrect χ^2_{CAT} adjustment due to usability concerns (Section 4.2.1.1) in this straight-line scenario. Any assistance to data association originates from χ^2_{SAT}. Even so, SAT does not provide enough separation in scans 15 through 43. More statistical PDF separation would ensure separation for closer MSE score returns.
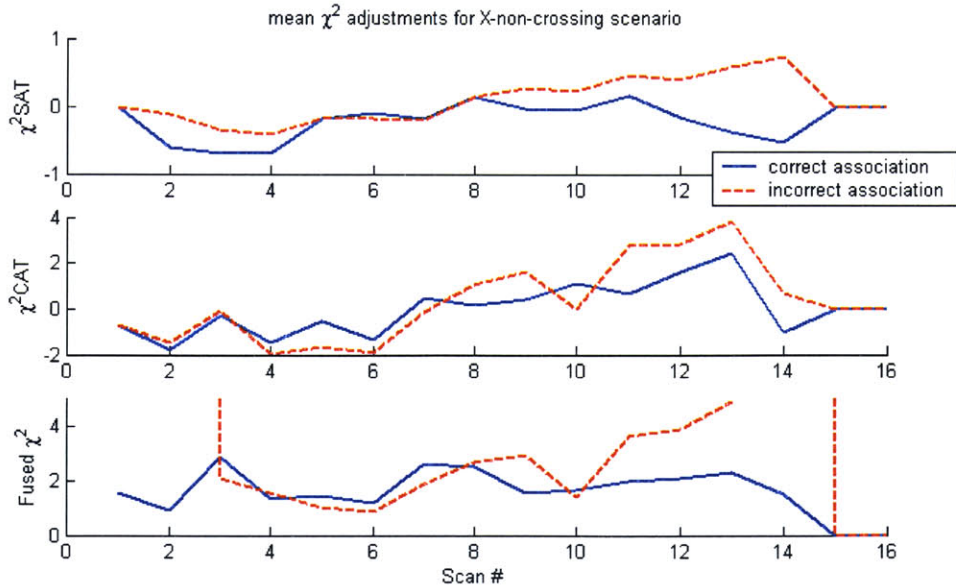

Figure 72. χ^2 scores by scan # for the X-non-crossing scenario

CAT appears to be a hindrance to data association until the targets meet in the intersection between scans 7 and 13. Additionally, SAT provides the greater advantage throughout the near-constant velocity points in the scenario at the beginning and end; especially when an opportunity for the buildup of the SAT database exists. Once the targets begin to meet and diverge, the χ^2_{fused} score ensures near-perfect data association. It will be interesting to see if these findings hold true during the merge/diverge scenario.[*]
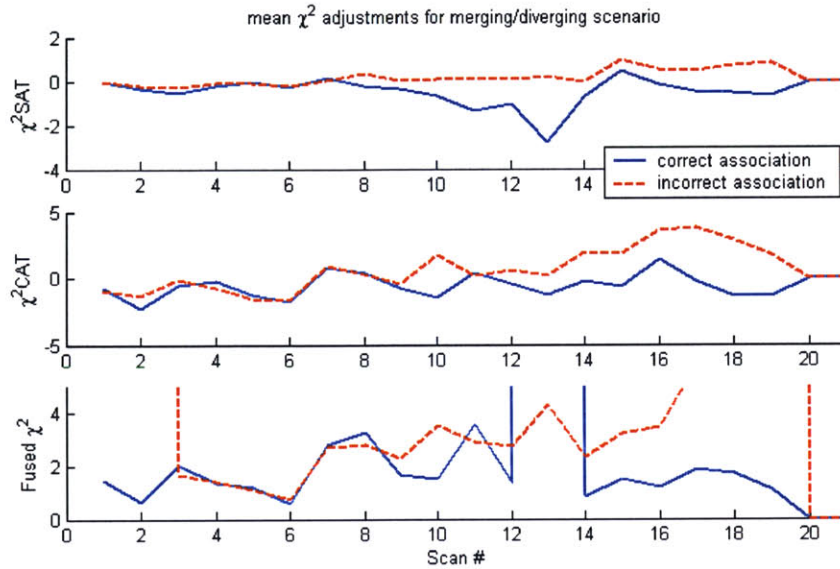
Figure 73. χ^2 scores by scan # for the Merge/Diverge scenario

Again, SAT begins to provide aid once there is sufficient time for database buildup and separation exists in the χ^2_{CAT} scores when the targets diverge and CAT becomes usable. Most likely, CAT does not provide sufficient assistance initially because of insufficient time to build up prior probability confidence.
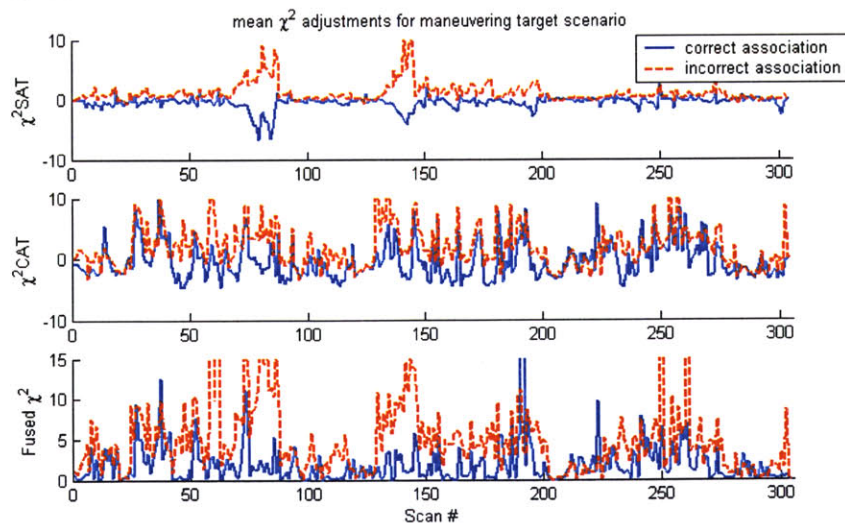
Figure 74. χ^2 scores by scan # for the parallel maneuvering target scenario

---

[*] The data points outside of the range of the χ^2_{fused} plot are due to an invalid score determined by the kinematic tracker

A number of "spikes" in difference between the χ^2_{SAT} scores exist above, again pointing to evidence of the advantages of a large database buildup. Also observable is the recognition of maneuvers when a similar difference exists between the χ^2_{CAT} scores. The above plots lead us to conclude that CAT should be effectively ignored when it is recognized that it might be unusable via predicted aspect angle error ranges. Moreover, SAT should be consistently used, with larger weight placed on χ^2_{SAT} scores emanating from comparisons involving a large amount of available database profiles. Regardless, performance is generally improved in all areas as a result of the implementation of the improved FAT system. However, more research and testing must be completed into the proper fusion of SAT and CAT.

6.2 Future Research / Conclusions

Plentiful suggestions for future research have arisen as a result of this study. First and foremost, a larger window of time would allow for an opportunity to adjust the kinematic tracker used above. As proven, measurement error and track filter performance are strongly correlated with aspect angle error. It is this error that drives the performance of the tracker and, if reduced, can lead to performance improvement and further optimization of computational requirements. Further exploration into maneuver detection (use of multiple, varying model types) might also lead to the ability to establish advantageous relationships between maneuver type and aspect angle error.

Additionally, as mentioned in chapter 1, SAR and ISAR technology has been used in SAT to this point. The use of a SAT database in conjunction with this technology will almost certainly lead to improved performance. The SAT database method should be analyzed in greater detail. Specifically, the method used to buildup and reset the average database should be optimized. Moreover, this same set of constraints and tests might also be used to aid in data association through the creation of a new χ^2_{SAT}-like value. Clearly, the possibility exists to harbor both the advantage presented by the PDF separation discovered in statistics generation and the data association accuracy when a large SAT database exists.

CAT presents a simple optimization problem where one needs to balance the advantage in finding a "match", with both usability and computational concerns. Varying statistical methods also exist and should be tested to evaluate the goodness-of-fit of the MSE vector. The use of back-estimation of aspect angle in conjunction with SAT should further be explored and quantified. In the absence of known targets, it still might be possible to classify the target as a particular type, as shown by the MSE separation exhibited between different vehicle types above.

Overall, this study cannot be validated or completed until real moving-target HRR profiles are used in the simulation. Recently, the simulated moving-target HRR profiles made available by UMass-Lowell have been obtained and future use of this data is imperative to confirm the conclusions and trends involved in the above conclusions. Regardless, the preceding results can be built upon at Lincoln Laboratory and elsewhere as the foundation of a robust, intuitive tracker that has been and can be vigilantly tested and evaluated in all phases.

REFERENCES

1. Nguyen, D. H., Kay, J. H., Orchard, B., Weatherwax, J. and Whiting, R. H., "Ground Moving Target Move-stop-move Mitigation with Feature-aided Tracking (DRAFT)," *MIT Lincoln Laboratory Journal*, 2002.

2. Sisterson, L.K., "UAV Radar Moving Target Tracker Description and User's Guide,", *MIT Lincoln Laboratory Project Report*, TT-29, July 1990.

3. Coate, W.G., "Preliminary Design Review: Kinematic Tracking for the PCA Integrated Radar-Tracker Application," *MIT Lincoln Laboratory Project Report*, PCA-IRT-4, 25 February 2003, issued 6 February 2004.

4. Stimson, G.W., *Introduction to Airborne Radar*, Hughes Aircraft Company, El Segundo, California, 1983.

5. Bourgeois, Francois and Jean-Claude Lassalle, "An Extension of the Munkres Algorithm for the Assignment Problem to Rectangular Matrices," *Communications of the ACM*, Vol 14, Dec. 1971, pp.802-806.

6. Blackman, Samuel and Robert Popoli, *Design and Analysis of Modern Tracking Systems*, Artech House, Norwood, MA, 1999.

7. Coate, W.G., "Preliminary Design Review: Feature-Aided Tracking for the PCA Integrated Radar-Tracker Application," *MIT Lincoln Laboratory Project Report*, PCA-IRT-5, issued 27 October 2004.

8. Bar-Shalom, Yaakov (Ed.), *Multitarget-Multisensor Tracking: Advanced Applications*, Artech House, Norwood, MA, 1990.

9. Ramachandra, K.V., *Kalman Filtering Techniques for Radar Tracking*, Marcel Dekker, Inc., New York, NY, 2000.

10. Sullivan, K.J, Ressler, M.B., Williams, R.L., "Signature-aided tracking using HRR profiles", *SPIE Proceedings of Aero Sense (In press).*, Toyon Research Corporation, SRI International, Air Force Research Laboratory, 2001.